

DRAFT VERSION JANUARY 17, 2025
 Typeset using L^AT_EX default style in AASTeX631

Exploring the Neutrino Mass Hierarchy from Isotopic Ratios of Supernova Nucleosynthesis Products in Presolar Grains

XINGQUN YAO,^{1, 2} TOSHIKAZU KAJINO,^{1, 2, 3} YUDONG LUO,⁴ TAKEHITO HAYAKAWA,^{5, 6} TOSHIO SUZUKI,^{7, 8} HEAMIN KO,⁹ MYUNG-KI CHEOUN,¹⁰ SEIYA HAYAKAWA,³ HIDETOSHI YAMAGUCHI,³ AND SILVIO CHERUBINI^{11, 12}

¹*School of Physics, Peng Huanwu Collaborative Center for Research and Education, and International Research Center for Big-Bang Cosmology and Element Genesis, Beihang University 37, Xueyuan Rd., Haidian-qu, Beijing 100191 China*

²*National Astronomical Observatory of Japan, 2-21-1 Osawa, Mitaka, Tokyo 181-8588, Japan*

³*Center for Nuclear Study, The University of Tokyo, RIKEN campus, 2-1 Hirosawa, Wako, Saitama 351-0198, Japan*

⁴*School of Physics, Peking University, and Kavli Institute for Astronomy and Astrophysics, Peking University, Beijing 100871, P. R. China*

⁵*Kansai Institute for Photon Science, National Institutes for Quantum Science and Technology, Kizugawa, Kyoto 619-0215, Japan*

⁶*Institute of Laser Engineering, Osaka University, Suita, Osaka 565-0871, Japan*

⁷*Department of Physics, College of Humanities and Sciences, Nihon University Sakurajosui 3-25-40, Setagaya-ku, Tokyo 156-8550, Japan*

⁸*NAT Research Center, NAT Corporation, 3129-45 Hibara Muramatsu, Tokai-mura, Naka-gun, Ibaraki 319-1112, Japan*

⁹*Institut für Kernphysik, Technische Universität Darmstadt, 64289 Darmstadt, Germany*

¹⁰*Department of Physics and OMEG institute, Soongsil University, Seoul 07040, Korea*

¹¹*Istituto Nazionale di Fisica Nucleare-Laboratori Nazionali del Sud, Via S. Sofia 62, I-95123 Catania, Italy*

¹²*Department of Physics and Astronomy, "Ettore Majorana" University of Catania, Via S. Sofia 64, I-95123 Catania, Italy*

(Dated: January 17, 2025)

ABSTRACT

We study the nucleosynthesis in a core-collapse supernova model including newly calculated neutrino-induced reaction rates with both collective and Mikheyev–Smirnov–Wolfenstein (MSW) neutrino-flavor oscillations considered. We show that the measurement of a pair of $^{11}\text{B}/^{10}\text{B}$ and $^{138}\text{La}/^{139}\text{La}$ or $^6\text{Li}/^7\text{Li}$ and $^{138}\text{La}/^{139}\text{La}$ in presolar grains that are inferred to have originated from core-collapse supernovae could constrain the neutrino mass hierarchy. The new shell-model and the model of quasi-particle random phase approximation in the estimate of three important neutrino-induced reactions, $\nu + ^{16}\text{O}$, $\nu + ^{20}\text{Ne}$, and $\nu + ^{138}\text{Ba}$ are applied in our reaction network. The new rates decrease the calculated $^7\text{Li}/^6\text{Li}$ ratio by a factor of five compared with the previous study. More interestingly, these new rates result in a clear separation of the isotopic ratio of $^{11}\text{B}/^{10}\text{B}$ between normal and inverted mass hierarchies in the O/Ne, O/C, and C/He layers where ^{138}La abundance depends strongly on the mass hierarchy. In these layers, the sensitivity of the calculated abundances of $^{10,11}\text{B}$ and $^{6,7}\text{Li}$ to the nuclear reaction uncertainties is also tiny. Therefore, we propose that the $^{11}\text{B}/^{10}\text{B}$ vs. $^{138}\text{La}/^{139}\text{La}$ and $^6\text{Li}/^7\text{Li}$ vs. $^{138}\text{La}/^{139}\text{La}$ in type X silicon carbide grains sampled material from C/He layer can be used as a new probe to constrain the neutrino mass hierarchy.

1. INTRODUCTION

Core-collapse supernova (CCSN) ejects a huge number ($\sim 10^{58}$) (Hirata et al. 1987) of three-flavor neutrinos and their anti-neutrinos which provide observational signals for the collective neutrino flavor oscillation (Sigl & Raffelt 1993) and the Mikheyev–Smirnov–Wolfenstein (MSW) effect (Wolfenstein 1978; Mikheyev & Smirnov 1985). Neutrinos launched from the surface of a proto-neutron star coherently scatter with one another and thereby change their flavors near the

sternyao@buaa.edu.cn

kajino@buaa.edu.cn

yudong.luo@pku.edu.cn

neutron-star atmosphere (collective oscillation). This effect induces an energy spectral split: the distribution at higher energies is swapped between ν_e and $\nu_{\mu,\tau}$ in the inverted hierarchy (Pehlivan et al. 2011). In contrast, in the normal hierarchy, the energy spectra of the three-flavor neutrinos do not change remarkably. After the collective oscillation occurs, neutrinos propagate through the O/Ne layer and reach the O/C or C/He layer in which the electron number-density satisfies the MSW high-density resonance condition for the flavor change again (Yoshida et al. 2006a, 2008). A substantial flavor conversion occurs between ν_e and $\nu_{\mu,\tau}$ for the normal hierarchy ($m_1 < m_2 < m_3$) and $\bar{\nu}_e$ and $\bar{\nu}_{\mu,\tau}$ for the inverted hierarchy ($m_3 < m_1 < m_2$), respectively, where m_i is the neutrino mass of each mass eigenstate (Wolfenstein 1978). In addition to these two effects of flavor conversions at high density, fast neutrino flavor conversion is also discussed in literature (Xiong et al. 2020; Wu et al. 2021; Nagakura & Zaizen 2022). Through these effects, the energy spectra of the three-flavor neutrinos exhibit specific variation at each position in the outer layers, contributing to the nucleosynthesis which depends on the neutrino mass hierarchy.

Experimentally, vacuum neutrino-oscillation project NO ν A reported a result in favor of normal hierarchy at 1.96σ C.L. (Acero et al. 2019; Acero et al. 2022), and combined Bayesian analysis of cosmological neutrino mass constraint prefers normal hierarchy (Jimenez et al. 2022). Further studies of neutrino flavor conversion in vacuum and high densities are necessary both experimentally and theoretically to reach the final result of still unknown neutrino mass hierarchy.

Woosley et al. (1990) proposed that during the SN ν -process neutrinos interact with abundant nuclei during propagation and lead to the synthesis of so-called ν -isotopes such as ${}^7\text{Li}$, ${}^{11}\text{B}$, ${}^{19}\text{F}$, ${}^{92}\text{Nb}$, ${}^{98}\text{Tc}$, ${}^{138}\text{La}$, and ${}^{180}\text{Ta}$. This process has been extensively studied by many authors (Heger et al. 2005; Hayakawa et al. 2010; Kobayashi et al. 2011; Hayakawa et al. 2013, 2018; Lahkar et al. 2017; Sieverding et al. 2018). These works were improved by taking account of the flavor conversions at high density. Although the flavor change does not affect the neutral-current (NC) reactions like ${}^{16}\text{O}(\nu, \nu' n){}^{15}\text{O}$, it impacts the final yields of ν -isotopes through the charged-current (CC) reactions like ${}^{16}\text{O}(\nu_e, e^- p){}^{15}\text{O}$, which depends strongly on the mass hierarchy (Yoshida et al. 2006b, 2008; Mathews et al. 2012; Kusakabe et al. 2019; Ko et al. 2020, 2022), where charged and neutral current reactions are induced by the exchange of charged W^\pm and neutral Z^0 bosons, respectively (Weinberg 2005). Therefore, the abundances of the synthesized isotopes at each layer reflect the neutrino mass hierarchy through both the effects of collective and MSW flavor conversion. The predicted isotopic abundances exhibit significant differences between normal and inverted hierarchies when the collective oscillation effect maximally operates (Ko et al. 2020, 2022). It is also pointed out that other nucleosynthesis processes such as νp and νi -process are affected by the collective neutrino oscillation (Sasaki et al. 2017; Balantekin et al. 2024).

Presolar type X silicon carbide (SiC) grains, X grains, were identified in primitive meteorites based on their exotic isotopic compositions (Amari et al. 1992; Nittler et al. 1996; Hoppe et al. 1996). It is a group of presolar SiC grains with robustly inferred CCSN origins (Liu et al. 2024). The nucleosynthesis of Li and B isotopes in CCSNe could be probed by examining their isotopic compositions of X grains in primitive meteorites (Hoppe et al. 2001). Possible main production sources of the solar-system B isotope are the galactic cosmic ray (GCR) spallation reactions in space, CCSN neutrino process, and AGB stars; most of ${}^{10}\text{B}$ originates from GCR, but ${}^{11}\text{B}$ originates mainly from both GCR and CCSN (Reeves 1994). X grains spent some time in the ISM before they were incorporated into the solar system so that their Li and B isotopic compositions could also have been additionally affected by GCR when they resided in the ISM. The previous theoretical studies (Woosley & Weaver 1995; Yoshida et al. 2006b; Austin et al. 2011; Prantzos 2012) show that part of ${}^{11}\text{B}$ in the solar system could arise from CCSNe nucleosynthesis. The boron and lithium isotopic ratios in the X grains have been measured, ${}^{11}\text{B}/{}^{10}\text{B}=4.68\pm0.31$ and ${}^7\text{Li}/{}^6\text{Li}=11.83\pm0.29$ with 1σ errors (Hoppe et al. 2001; Fujiya et al. 2011), but these values agree with the solar values within 1.5σ , $({}^{11}\text{B}/{}^{10}\text{B})_{\text{sol}}=4.04$ and $({}^7\text{Li}/{}^6\text{Li})_{\text{sol}}=12.06$ (Lodders et al. 2009). On the other hand, ${}^{139}\text{La}$ is mainly produced by s-process (Bisterzo et al. 2014), while ${}^{138}\text{La}$ is regarded to be mainly produced via ν -process (Woosley et al. 1990; Heger et al. 2005; Hayakawa et al. 2008). Therefore, if intrinsic ${}^{11}\text{B}/{}^{10}\text{B}$, ${}^7\text{Li}/{}^6\text{Li}$ and ${}^{138}\text{La}/{}^{139}\text{La}$ ratio can be obtained from X grains by suppressing asteroidal or terrestrial contamination, the data will provide valuable constraints on the astrophysical and physical parameters for the neutrino nucleosynthesis process.

In the present work, we propose that correlated, intrinsic isotope ratios of ${}^{11}\text{B}/{}^{10}\text{B}$ and ${}^7\text{Li}/{}^6\text{Li}$ vs. ${}^{138}\text{La}/{}^{139}\text{La}$ of presolar grains can directly constrain the neutrino mass hierarchy. We report here our theoretical study of the nucleosynthesis yields of ${}^6\text{Li}$, ${}^7\text{Li}$, ${}^{10}\text{B}$, ${}^{11}\text{B}$ and ${}^{138}\text{La}$ in a SN model by taking account of flavor conversions due to both collective and MSW effects. In addition to the $\nu + {}^4\text{He}$, $\nu + {}^{12}\text{C}$ and $\nu + {}^{138}\text{Ba}$ reaction rates, we use a series of newly calculated neutrino-induced reaction rates for $\nu + {}^{16}\text{O}$ and $\nu + {}^{20}\text{Ne}$, which change the ${}^{6,7}\text{Li}$ and ${}^{10,11}\text{B}$

abundances drastically in the present calculations. We show that the two-dimensional plot of these isotopic ratios are sensitive probes of the mass hierarchy.

2. METHOD

2.1. Supernova model and neutrinos

The pre-SN model calculation has been performed based on the model for SN 1987A with metallicity $Z = Z_\odot/4$, the initial mass of the progenitor star is $20 M_\odot$ (Kikuchi et al. 2015). The star evolves to a helium core of $6 M_\odot$ with the mass cut at $M_r = 1.6 M_\odot$, where M_r is the Lagrangian mass coordinate. We adopted the hydrodynamic calculation for the explosion from Kusakabe et al. (2019) and applied the resultant density and temperature profiles to the nucleosynthesis calculation. The hydrodynamic profile includes the region from $M_r = 1.6 M_\odot$ to $M_r = 6.0 M_\odot$ (helium core boundary), and is divided into 360 equal mass shells with $0.01224 M_\odot$.

The total neutrino energy is 3×10^{53} erg, and the exponential decay timescale of neutrino luminosity is set to be 3 s. We assumed that each neutrino flavor has the same luminosity (equal partition) and the energy spectra obey the Fermi-Dirac distributions with zero-chemical potentials. The initial temperatures are set to be 3.2, 5.0, and 6.0 MeV for ν_e , $\bar{\nu}_e$, and ν_x , respectively (Yoshida et al. 2008). We adopted the same method as Ko et al. (2022) to calculate the flavor change due to the collective and MSW effects.

2.2. Neutrino induced reactions

In addition to the theoretical $\nu + ^{12}\text{C}$ and $\nu + ^4\text{He}$ reaction rates in Yoshida et al. (2008), we also calculated $\nu + ^{16}\text{O}$ and $\nu + ^{20}\text{Ne}$ reaction rates for various modes of final states using the shell model (Suzuki et al. 2018). ^{138}La is almost purely produced by the neutrino process via the reaction $^{138}\text{Ba}(\nu_e, e^-)^{138}\text{La}$, although a small amount of ^{138}La comes from the γ -process $^{139}\text{La}(\gamma, n)^{138}\text{La}$ as well (Heger et al. 2005). We took the cross sections of this main reaction channel $^{138}\text{Ba}(\nu_e, e^-)^{138}\text{La}$ from the quasi-particle random phase approximation (QRPA) calculation (Cheoun et al. 2010a). After a ν -interaction populates excited states in a compound nucleus, the cross section leading to each final particle-emission channel is calculated using the branching ratios estimated in the Hauser-Feshbach statistical model (Hauser & Feshbach 1952) in the similar treatment as that in Suzuki et al. (2018) and Cheoun et al. (2010a). The other neutrino spallation reactions on $A \leq 70$ nuclei except for ^4He , ^{12}C , ^{16}O and ^{20}Ne are taken from Hoffmann & Woosley (1992). The cross sections used in our nucleosynthesis calculations (Cheoun et al. 2010a; Suzuki et al. 2018) depend on the incident neutrino energy, which arises from the nuclear structure and available phase space. This is critically important because the energy-spectral change from the initial Fermi-Dirac distribution due to the flavor conversions at high density affects the production yields of ν -nuclei via CC interactions, which depend on neutrino mass hierarchy. Hoffmann & Woosley (1992) provides only the cross sections averaged over a normalized Fermi-Dirac distribution for a given initial temperature. We calculated the reaction rate by folding their averaged cross section multiplied by our modified neutrino-energy spectra after flavor conversion instead of Fermi-Dirac distribution. To clarify the effect of the updated $\nu + ^{16}\text{O}$ and $\nu + ^{20}\text{Ne}$ reaction rates, we compared the abundances calculated using both the reaction rates derived based on Suzuki et al. (2018) (hereafter “Su18”) and Hoffmann & Woosley (1992) (hereafter “HW92”) in the present study.

2.3. Uncertainties of Reaction Rates

The flux-averaged measured $^{12}\text{C}(\nu_e, e^-)^{12}\text{N}_{g.s.}$ and $^{12}\text{C}(\nu, \nu')^{12}\text{C}^*$ reaction cross sections have $\pm 10\%$ and $\pm 20\%$ uncertainties for the CC and NC reaction channels, respectively (Bodmann et al. 1994). The difference between the theoretical calculations of nuclear shell model (Suzuki et al. 2006, 2018) and QRPA (Cheoun et al. 2010a,b) is less than the experimental uncertainties. Thus, the uncertainties of the reaction rates for ^{12}C and other target nuclei such as ^4He , ^{16}O , ^{20}Ne and ^{138}Ba are assumed to be $\pm 10\%$ and $\pm 20\%$ for the CC and NC reactions, respectively. We mentioned that the $^{11}\text{C}(\alpha, p)^{14}\text{N}$ reaction rate has the largest uncertainty among all 91 nuclear reactions related to ^7Li and ^{11}B in the present calculations because this rate exhibits roughly one order of magnitude variation depending on poorly known resonance parameters at Gamow-window energy of $E_G = 0.25\text{--}1.09$ MeV for effective temperature $T = 0.2\text{--}0.8$ GK of the SN ν -process. This leads to the biggest uncertainty in the final ^{11}B abundance.

3. RESULT AND DISCUSSIONS

3.1. Nuclear abundances and neutrino flavor conversions

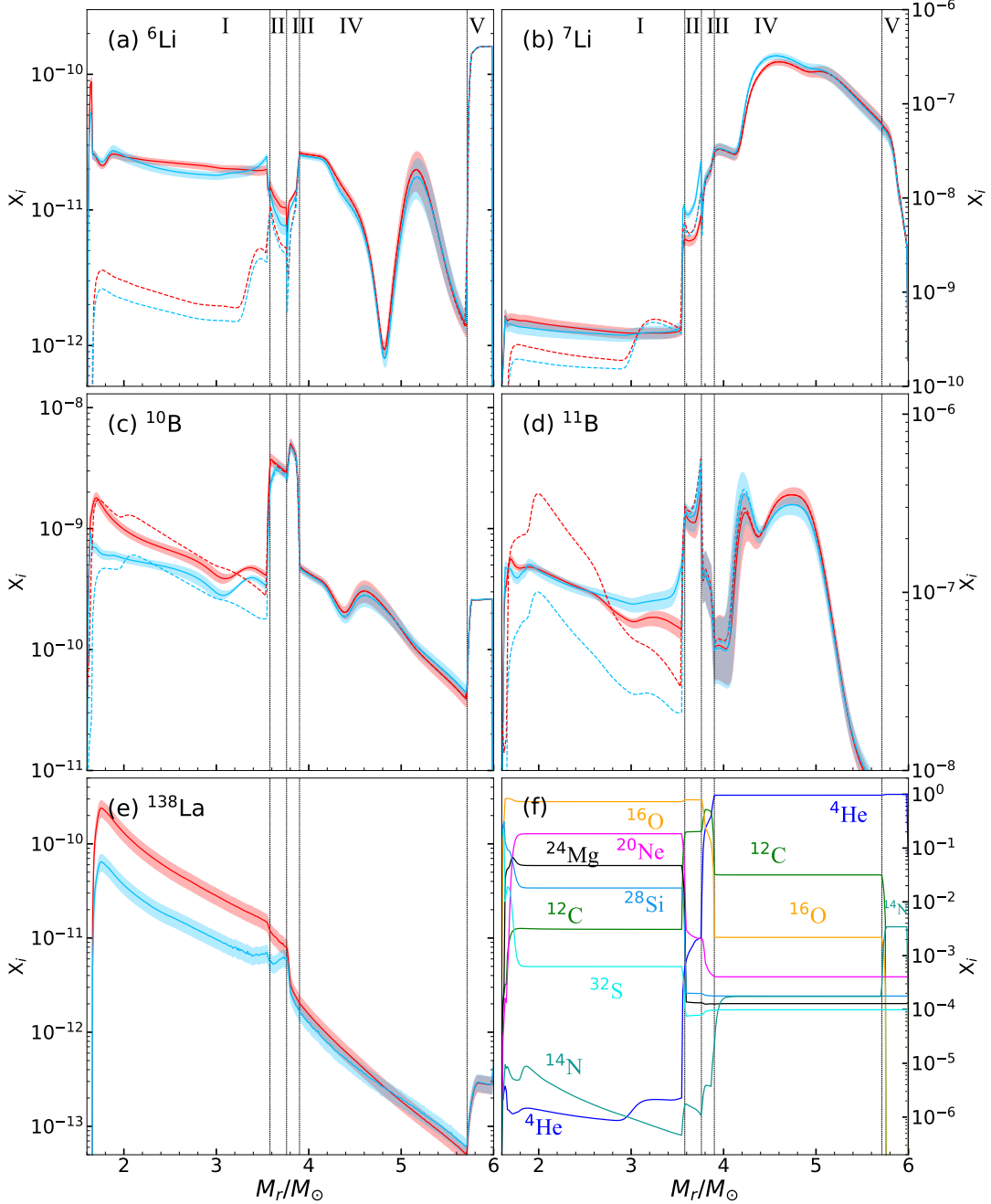


Figure 1. Mass fractions of (a) ${}^6\text{Li}$, (b) ${}^7\text{Be}+{}^7\text{Li}$, (c) ${}^{10}\text{B}+{}^{10}\text{C}$, (d) ${}^{11}\text{B}+{}^{11}\text{C}$, (e) ${}^{138}\text{La}$ and (f) most abundant nuclei at 50 secs after the SN core-bounce as a function of the Lagrangian mass M_r in the unit of M_\odot . The red and blue colors in panels (a) to (e) represent the calculated results of the inverted and normal hierarchy cases, respectively. Colored bands correspond to the uncertainties arising from those of ν -A reaction rates and ${}^{11}\text{C}(\alpha, p){}^{14}\text{N}$ reaction rate. The dashed lines show the results by using the ${}^{16}\text{O}+\nu$ and ${}^{20}\text{Ne}+\nu$ rates from Hoffmann & Woosley (1992) (HW92) instead of Suzuki et al. (2018) (Su18). ${}^{138}\text{La}$ is mainly produced via ${}^{138}\text{Ba}(\nu_e, e^-){}^{138}\text{La}$. We divide the star into five regions marked I - V of O/Ne, O/C, C/He, He/C, and He/N layers, respectively. The C/He layer is the transitional zone between the O/C and He/C layers. Note that the scales of the vertical axis are different for each panel.

Figure 1 shows the mass fractions of (a) ${}^6\text{Li}$, (b) ${}^7\text{Li}+{}^7\text{Be}$ (decay to ${}^7\text{Li}$ with $t_{1/2}=53$ days), (c) ${}^{10}\text{B}+{}^{10}\text{C}$ (decay to ${}^{10}\text{B}$ with $t_{1/2}=19.3$ secs)¹, (d) ${}^{11}\text{B}+{}^{11}\text{C}$ (decay to ${}^{11}\text{B}$ with $t_{1/2}=20$ mins), (e) ${}^{138}\text{La}$ and (f) several abundant nuclei after the explosion as a function of M_r , where only the stable nuclei are marked in each panel, e.g. (b) ${}^7\text{Li}$ represents ${}^7\text{Li}+{}^7\text{Be}$, etc. The red and blue solid lines with bands represent the calculated results in the inverted and normal hierarchies, respectively. The band width arises from the $\nu\text{-A}$ and ${}^{11}\text{C}(\alpha, p){}^{14}\text{N}$ reaction rate uncertainties discussed above. The calculated abundances with HW92 calculation are plotted as dashed lines.

We divide the star into five regions marked I - V of O/Ne, O/C, C/He, He/C, and He/N layers, respectively, following the scheme for $25 M_\odot$ SN model (Meyer et al. 1995), although region III is a transitional layer between the O/C and He/C layers. In Fig. 1 (a), the Su18 calculated results are significantly higher than the HW92 calculations by one order of magnitude in the O/Ne layer (region I). This is due to the production of ${}^6\text{Li}$ via the $\nu+{}^{16}\text{O}$ reaction, which was not considered in the previous nucleosynthesis calculations (Ko et al. (2022) and references therein), although ${}^{16}\text{O}$ is the most abundant nucleus in this region, as displayed in Fig. 1 (f). The ${}^6\text{Li}$ abundance in the inverted case (red) is slightly higher than in the normal case (blue). Similarly, the additional ${}^7\text{Li}$ is produced via the $\nu+{}^{16}\text{O}$ reaction in O/Ne layer of Fig. 1 (b). However, in the C/He (region III) and He/C layers (region IV), the ${}^6,{}^7\text{Li}$ are mainly produced by other reactions such as ${}^3\text{H}(\alpha, \gamma){}^7\text{Li}$, so that the solid lines and dashed lines are identical.

In Fig. 1 (c) and (d), most of ${}^{10,11}\text{B}$ are produced in the O/C layer (region II) by the $\nu+{}^{12}\text{C}$ reaction because there are plenty of ${}^{12}\text{C}$ (see Fig. 1 (f)). However, in C/He and He/C layers (region III and IV), ${}^{11}\text{B}$ is not particularly enhanced because of the secondary destruction reaction of ${}^{11}\text{C}(\alpha, p){}^{14}\text{N}$ induced by abundant ${}^4\text{He}$. In the O/Ne layer (region I) of Fig. 1 (d), there is a difference in the ${}^{11}\text{B}$ abundances between the solid and dashed lines using the two different sets of reaction cross sections for $\nu+{}^{16}\text{O}$ and $\nu+{}^{20}\text{Ne}$, as described in subsection 2.2. ${}^{11}\text{B}$ abundances by using the previous cross section data (red and blue dashed lines) decrease as M_r increases because the neutrino-flux is a decreasing function of M_r (Kusakabe et al. 2019). Moreover, the abundance of ${}^{11}\text{B}$ in the inverted hierarchy using the previous data (red dashed line) mostly comes from the ${}^{11}\text{C}$ produced by the ${}^{12}\text{C}(\nu_e, e^-p){}^{11}\text{C}$ reaction (Ko et al. 2022) because the high-energy parts of the spectra of ν_e and $\nu_{\mu,\tau}$ are exchanged due to the collective oscillation (Pehlivan et al. 2011), namely the ν_e spectrum is much enhanced than $\bar{\nu}_e$ (see blue line in Fig. 2). After adding the energy dependent $\nu+{}^{16}\text{O}$ and $\nu+{}^{20}\text{Ne}$ cross sections (solid lines), the final ${}^{11}\text{B}$ abundance changes drastically such that the large difference of the dashed lines between the two hierarchies almost disappears. This is because the $\nu+{}^{16}\text{O}$ reaction produces additional α particles that destroy ${}^{11}\text{C}$ by the ${}^{11}\text{C}(\alpha, p){}^{14}\text{N}$ reaction, where ${}^{11}\text{C}$ was produced from the ${}^{12}\text{C}(\nu_e, e^-p){}^{11}\text{C}$ reaction. The resultant M_r -dependence of ${}^{11}\text{B}$ is smoothed out as shown in Fig. 1(d).

The neutrino flavor-conversion due to the MSW resonance effect near C/He and He/C layers almost offsets the spectral change of the neutrino energy-distributions arising from the collective oscillation. In He-rich layers, spallation products of the $\nu+{}^4\text{He}$ reaction, i.e. p, n, d, ${}^3\text{H}$ and ${}^3\text{He}$, and the abundant α particles enhance both production and destruction of A=7 and 11 nuclei via ${}^3\text{H}(\alpha, \gamma){}^7\text{Li}(\alpha, \gamma){}^{11}\text{B}(\alpha, n){}^{14}\text{N}$ and ${}^3\text{He}(\alpha, \gamma){}^7\text{Be}(\alpha, \gamma){}^{11}\text{C}(\alpha, p){}^{14}\text{N}$. Therefore, one cannot find any appreciable difference in any nuclei between the two hierarchies within the reaction uncertainties in He/C layer, especially in the outermost region $M_r \geq 5M_\odot$.

As for ${}^{138}\text{La}$ in Fig. 1 (e), there is a noticeable disparity between the normal and inverted hierarchies in O/Ne layer (region I). The mechanism is similar to that for ${}^{11}\text{B}$ in Fig. 1 (d), except that ${}^{138}\text{La}$ production is negligible from the $\nu+{}^{16}\text{O}$ and $\nu+{}^{20}\text{Ne}$ reactions because ${}^{138}\text{La}$ is so heavy that the light-mass charged particles have tiny cross sections due to the Coulomb barrier in the secondary destruction process, except for neutron-induced reactions which have already been included in our network calculations. As shown in Fig. 2, the modified ν_e energy spectrum (blue solid line $4\pi r^2 \frac{d\phi_{\nu_e}}{dE}$) is larger than the initial one (blue dotted line) above 18 MeV due to the collective oscillation. Therefore, the production rate of ${}^{138}\text{La} \propto 4\pi r^2 \frac{d\phi_{\nu_e}}{dE} \times \sigma$ (red solid line) is much larger than the initial value. In the outer regions of the C/He and He/C layers (region III and IV), the MSW effect almost offsets the collective effect, leaving only a tiny difference between the two hierarchies, similar to ${}^6,{}^7\text{Li}$ and ${}^{10,11}\text{B}$. The difference of ${}^{138}\text{La}$ is sensitive to the neutrino mass hierarchy only in O/Ne layer and O/C layer (region I and II). These mechanisms are valid under the condition $T_{\nu_e} < T_{\nu_x}$ and $T_{\bar{\nu}_e} < T_{\bar{\nu}_x}$, and the result of relative abundance ratios is less sensitive to the adopted SN model.

To summarize, the most important reactions in O/Ne layer (region I) for B and Li production are neutrino-induced spallation reactions $\nu+{}^{12}\text{C}$ and ${}^{16}\text{O}$. While in C/He and He/C layers (region III and IV), the most significant reactions are (α, γ) and $(\alpha, p/n)$ reactions, for the production and destruction, respectively. As for ${}^{138}\text{La}$, it is mainly produced

¹ Notice that, in principle, we should consider ${}^{10}\text{Be}$ contribution here since it has a lifetime $t_{1/2} = 1.5 \times 10^6$ yrs. However, the yield of ${}^{10}\text{Be}$ in our calculation is 15 orders of magnitude lower than ${}^{10}\text{B}$ (see Table 1), and we can ignore this yield contribution.

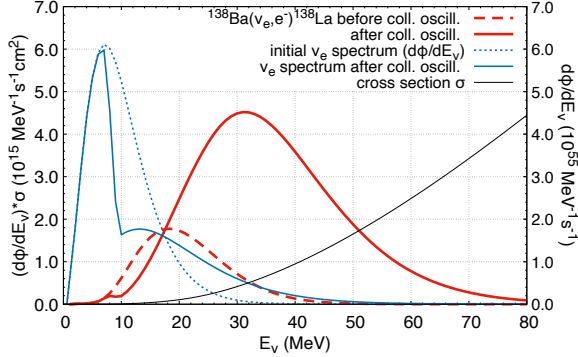


Figure 2. The dotted and solid blue lines are the electron-neutrino differential energy-spectra, $4\pi r^2 d\phi_\nu/dE_\nu$, at 10 km and 1000 km which are respectively before and after the collective oscillation. The black thin line shows the cross section of the $^{138}\text{Ba}(\nu_e, e^-)^{138}\text{La}$ reaction from Cheoun et al. (2010a). Note that the cross-section is shown such that the end-point at 80 MeV is set to be $8.894 \times 10^{-39} \text{ cm}^2$. The dashed and solid red lines present the electron neutrino-spectra multiplied by the $^{138}\text{Ba}(\nu_e, e^-)^{138}\text{La}$ reaction cross section, $4\pi r^2 d\phi_\nu/dE_\nu \times \sigma$, before and after the collective oscillation.

from the $^{138}\text{Ba}(\nu_e, e^-)^{138}\text{La}$ reaction in the O/Ne layer. Photo-induced reactions do not operate efficiently because photon number density above the threshold energy for the production of these isotopes is extremely small with the Planck distribution of photons at the effective temperature $T \simeq 0.1 - 1 \text{ GK}$ for explosive SN nucleosynthesis.

Based on these nucleosynthesis calculations, the isotopic productions $\Delta M(^A\text{Z})$ and overproduction factor $\Theta(^A\text{Z})$ are listed in the appendix Table 1 in the same tabular format of Meyer et al. (1995). In this table, all values are taken from our CCSN model 50 secs after the explosion, therefore, some radioactive nuclei appear in the table. As mentioned above, we divided the model into five major layers: O/Ne, O/C, C/He, He/C and He/N layers. To show the very inner structure of our model, we also divided the inner part ($M_r < 1.71M_\odot$) into three zones as Fe/Ni, Si/S, and O/Si zones, depending on the most abundant nuclei of each zone. The overproduction factor $\Theta(^A\text{Z})$ is the ratio of ^AZ abundance to the corresponding solar abundance, which is the same as in Meyer et al. (1995). For the radioactive nuclei, $\Theta(^A\text{Z})$ was calculated with the corresponding final stable daughter nucleus in solar system.

3.2. Isotopic ratios and X grains

Ko et al. (2020) have shown that the $^{138}\text{La}/^{11}\text{B}$ ratio is sensitive to the mass hierarchy. We here extend this idea to measurements of $^{11}\text{B}/^{10}\text{B}$ or $^7\text{Li}/^6\text{Li}$ vs. $^{138}\text{La}/^{139}\text{La}$ ratios in presolar grains originating from SNe. Type X SiC grains are robustly inferred to have condensed out of CCSN ejecta based on their multielement isotopic compositions (Amari et al. 1992; Nittler et al. 1996; Hoppe et al. 1996; Liu et al. 2024). Because SiC grains are condensed in the environment on condition $\text{C}/\text{O} > 1$, they are formed by mixed materials from C-rich and Si-rich layers (Lodders & Fegley 1995; Hoppe et al. 2001). ^{138}La is mainly produced in the inner regions of the O/Ne layer through the C/He layers (region I, II, III), whereas ^{10}B and ^{11}B are produced in entire regions, particularly in the O/C and C/He layers (region II and III for ^{10}B) and in the O/C and He/C layers (region II and IV for ^{11}B). ^7Li and ^6Li are mainly produced in the He/C and C/He layers (region IV and III), respectively (see Fig. 1). To show the effects of neutrino mass hierarchies imprinted in nucleosynthetic observable, we take the isotopic abundance ratios of $^7\text{Li}/^6\text{Li}$, $^{11}\text{B}/^{10}\text{B}$, and $^{138}\text{La}/^{139}\text{La}$ and display their correlations in Figs. 3 and 4, where $^7\text{Li}/^6\text{Li}$ and $^{11}\text{B}/^{10}\text{B}$ stand for $(^7\text{Li} + ^7\text{Be})/^6\text{Li}$ and $(^{11}\text{B} + ^{11}\text{C})/(^{10}\text{B} + ^{10}\text{C})$ in nucleosynthesis calculations. Figure 3 shows the $^7\text{Li}/^6\text{Li}$ vs. $^{138}\text{La}/^{139}\text{La}$ (panel (a)) and $^{11}\text{B}/^{10}\text{B}$ vs. $^{138}\text{La}/^{139}\text{La}$ (panel (b)) for the normal (blue solid lines) and inverted (red solid lines) hierarchies, respectively. Each point indicates the mass-fraction ratio averaged in a mass coordinate range of $\Delta M_r = 0.1224M_\odot$. The points with circles indicate the particular locations in this model, i.e. the inner-most mass-coordinate at $1.65 M_\odot$, the boundaries between the O/Ne and O/C, O/C and C/He, C/He and He/C, He/C and He/N layers at $3.58 M_\odot$, $3.77 M_\odot$, $3.90 M_\odot$, and $5.71 M_\odot$ respectively, and the outermost mass coordinate at $5.93 M_\odot$.

The difference between the two neutrino hierarchies in $^7\text{Li}/^6\text{Li}$ vs. $^{138}\text{La}/^{139}\text{La}$ (Fig. 3(a)) and $^{11}\text{B}/^{10}\text{B}$ vs. $^{138}\text{La}/^{139}\text{La}$ (Fig. 3(b)) appears in the mass region between 3.58 and $3.90 M_\odot$ which corresponds to the O/C and C/He layers. This is because ^7Li and ^{11}B abundances under the normal hierarchy are higher between 3.58 and $3.90 M_\odot$ than those under the inverted hierarchy, while ^6Li and ^{10}B abundances under the normal hierarchy are lower than those

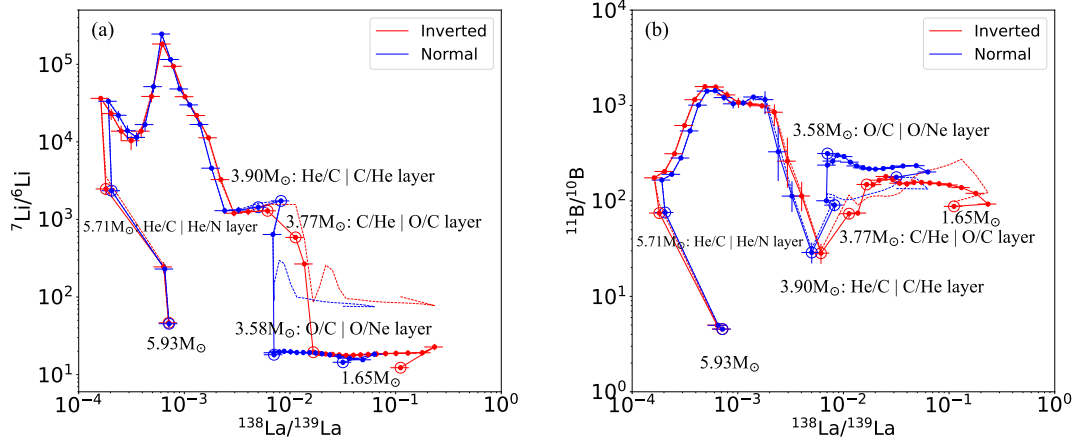


Figure 3. Calculated mass ratios (a) ${}^7\text{Li}/{}^6\text{Li}$ vs. ${}^{138}\text{La}/{}^{139}\text{La}$ and (b) ${}^{11}\text{B}/{}^{10}\text{B}$ vs. ${}^{138}\text{La}/{}^{139}\text{La}$. The red and blue dots represent the results for the inverted and normal hierarchies at each position in the present SN model. Each dot means a corresponding position of M_r in Fig. 1. The error bars represent the uncertainties of the abundance ratios arising from the uncertainties of ν -induced reaction rates and ${}^{11}\text{C}(\alpha, p){}^{14}\text{N}$ reaction rate. The points with circles indicate the particular locations in this SN model, i.e. the inner-most mass-coordinate at $1.65 M_\odot$, the boundaries between the O/Ne and O/C, O/C and C/He, C/He and He/C, He/C and He/N layers at $3.58 M_\odot$, $3.77 M_\odot$, $3.90 M_\odot$, $5.71 M_\odot$, respectively, and the outermost mass coordinate at $5.93 M_\odot$. The dashed lines are the results using HW92.

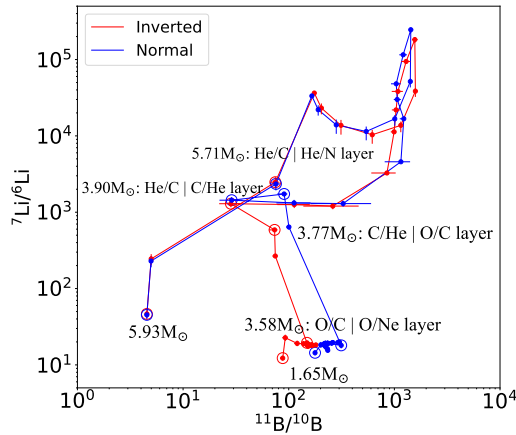


Figure 4. The same as Fig. 3 but for $({}^7\text{Li} + {}^7\text{Be})/{}^6\text{Li}$ vs. $({}^{11}\text{B} + {}^{11}\text{C})/({}^{10}\text{B} + {}^{10}\text{C})$.

under the inverted hierarchy (Figs. 1(b)-(d)). In Fig. 3(a), the two lines almost overlap in the inner layer at $1.63\text{-}3.58 M_\odot$ for ${}^7\text{Li}/{}^6\text{Li}$ vs. ${}^{138}\text{La}/{}^{139}\text{La}$. In contrast, for ${}^{11}\text{B}/{}^{10}\text{B}$ vs. ${}^{138}\text{La}/{}^{139}\text{La}$ in Fig. 3(b), the separation between the two lines is wider than that for ${}^7\text{Li}/{}^6\text{Li}$. This result suggests that combining boron and lanthanum may substantially constrain the neutrino mass hierarchy rather than the combination of lithium and lanthanum. This separation arises from the remarkable difference of ${}^{138}\text{La}$ at $M_r \leq 3.77 M_\odot$ in Fig. 1(e) between the two hierarchies. The ${}^{138}\text{La}/{}^{139}\text{La}$ ratio is sensitive to the ν -process because ${}^{138}\text{La}$ is mainly produced in the ν -induced reaction ${}^{138}\text{Ba}(\nu_e, e^-){}^{138}\text{La}$ (Heger et al. 2005). On the other hand, the newer $\nu+{}^{16}\text{O}$ rate from Su18 provides additional ${}^4\text{He}$ in the nucleosynthesis at $M_r \leq 3.77 M_\odot$, which separate the ${}^{11}\text{B}/{}^{10}\text{B}$ ratio more significantly compared to the result using HW92 (dashed lines in Fig. 3(b)). Such a result is valid even considering the uncertainties arising from nuclear cross sections in the model, as shown in the error bar in Fig. 3.

X SiC grains were found in the Murchison meteorite (Amari et al. 1992; Nittler et al. 1996; Hoppe et al. 2000). Hoppe et al. (2001) measured ${}^{11}\text{B}/{}^{10}\text{B}$ in these X grains. The ratio is almost identical to the solar ratio within

the uncertainty but a few orders of magnitude lower than the SN model prediction (Woosley & Weaver 1995). To explain this fact, Hoppe et al. (2001) suggested three possible solutions: 1) changing initial neutrino temperature, 2) mixing of layers with inhomogeneous isotopic abundance distribution, and 3) mixing of materials of C/O < 1. As for 1), we mention that the lower neutrino temperature $T_{\nu_x} = 6$ MeV rather than the temperature $T_{\nu_x} = 8$ MeV (Woosley & Weaver 1995), which Hoppe et al. (2001) referred to, has been adopted in the present calculation. The acceptable temperature range was found to be $4.8 \text{ MeV} \lesssim T_{\nu_x} \lesssim 6.6 \text{ MeV}$ to reproduce the SN contribution to ^{11}B in the framework of Galactic chemical evolution (Yoshida et al. 2005). As for 2) and 3), recent studies show that X grains form in CCSN ejecta at least after a few years but within thirty years (Liu et al. 2018; den Hartogh et al. 2022; Liu et al. 2024). Therefore, there is a possibility that the CCSN ejecta from different layers could be mixed due to several hydrodynamic instabilities, micro-turbulence, or frictional ejection dynamics of materials in some stage before, during, or after the grain formation. Although clear evidence for such a mixing has not been observed in X grains, there is an indirect observational fact for the co-condensation of oxygen- and carbon-rich meteoritic stardust from nova outbursts (Haenecour et al. 2019), which suggests that the mixing process could operate in ejection process.

The average $^7\text{Li}/^6\text{Li}$ ratio 11.83 ± 0.29 and $^{11}\text{B}/^{10}\text{B}$ ratio 4.68 ± 0.31 in the twelve X grains were precisely measured by Fujiya et al. (2011). In Fig. 4, we present $^7\text{Li}/^6\text{Li}$ vs. $^{11}\text{B}/^{10}\text{B}$ with the same setting as Fig. 3. Fujiya et al. (2011) discussed the difference between their measurements and previous theoretical SN model calculations, e.g., Rauscher et al. (2002). Since X grains are known to form a few years after the supernova ejection (Liu et al. 2018; Hoppe et al. 2018; Ott et al. 2019; Niculescu-Duvaz et al. 2022), significant effects could be caused by asteroidal or terrestrial contamination including the admixture of GCR components (Liu et al. 2021; Gyngard et al. 2009). By considering the Li/Si ratio and subtracting the GCR contribution, the measured ratio $^{11}\text{B}/^{10}\text{B}=4.68 \pm 0.31$ shows slight excess of ^{11}B from the solar-system value $^{11}\text{B}/^{10}\text{B}=4.03^{+0.07}_{-0.02}$ (Zhai et al. 1996). This suggests an admixture of other components such as the SN ν -process product in these X grains. Figure. 4 shows that none of the calculated $^7\text{Li}/^6\text{Li}$ and $^{11}\text{B}/^{10}\text{B}$ ratios for any SN layers can reproduce the values reported by Fujiya et al. (2011). This result supports the possibility that the observed lithium and boron may be subject to the mixing of a supernova ejecta and interstellar media whose composition is close to the solar materials or other terrestrial contamination.

In Fig. 3 & 4, clear separation of the isotopic ratio divergence between normal and inverted hierarchies appears in the inner region $M_r \leq 3.90 M_\odot$. Thermodynamic calculations have shown that formation of SiC dust requires a condition with C/O > 1 (Lodders & Fegley 1995). In our calculation, the C/He layer between 3.77 to 3.90 M_\odot satisfies this condition of forming X grains. Therefore, further search of X SiC presolar grains, especially of Li, B, and La isotopes is highly desirable in constraining the neutrino process and neutrino mass hierarchy. If other supernova presolar grains such as graphite, silicates, and oxides sampled materials from O-rich layers are found, our results would provide possible constraint on the neutrino mass hierarchy.

4. CONCLUSION

We adopted new $\nu + ^{16}\text{O}$ and $\nu + ^{20}\text{Ne}$ reaction rates from a new shell-model and $\nu + ^{138}\text{Ba}$ rates from QRPA calculations in the neutrino-induced CCNS nucleosynthesis, including both collective and MSW oscillation effects. The newly added $\nu + ^{16}\text{O}$ and $\nu + ^{20}\text{Ne}$ reactions provide additional $^{6,7}\text{Li}$ and ^4He production. The ^4He further modifies ^{11}B abundance by $^{11}\text{C}(\alpha, p)^{14}\text{N}$ reaction in the O/Ne and O/C and even C/He layers in Fig. 1. The collective oscillation effect enhances the high-energy tail of the ν_e spectrum in the inner layer under the inverted neutrino mass hierarchy by a factor of three. These two effects enlarge dramatically the separation of $^{138}\text{La}/^{139}\text{La}$ and $^{11}\text{B}/^{10}\text{B}$ ratios between the two hierarchies in $M_r < 3.90 M_\odot$ as shown in Fig. 3 (b). We also found the uncertainties of nuclear reactions and neutrino-induced reactions mostly come from $^{11}\text{C}(\alpha, p)^{14}\text{N}$, which affects the final yield of ^{11}B in outer layer by a factor of two, but the uncertainty is negligible in the O/Ne through C/He layers ($1.7 \sim 3.9 M_\odot$). In our model, C/He layer (3.77 to 3.90 M_\odot) has C/O > 1, satisfies the X grains formation condition. We propose that the isotopic ratios of $^{11}\text{B}/^{10}\text{B}$ vs. $^{138}\text{La}/^{139}\text{La}$ and $^7\text{Li}/^6\text{Li}$ vs. $^{138}\text{La}/^{139}\text{La}$ in X grains could be a probe to the neutrino mass hierarchy and clarify the effect of neutrino flavor conversion on the SN nucleosynthesis.

5. ACKNOWLEDGMENT

We gratefully acknowledge the referee of this paper for the kind and valuable suggestions. We also appreciate Hirokazu Sasaki and Motohiko Kusakabe for their in-depth discussions throughout this work. Yao was under the support of CSC scholarship from the Ministry of Education of China during his stay at the National Astronomical Observatory of Japan (NAOJ), where most of the numerical calculations for this paper were performed in the Center

for Computational Astrophysics of NAOJ. This work was supported in part by the National Key R&D Program of China (2022YFA1602401) and the National Natural Science Foundation of China (No. 12335009 & 12435010). The work of M.K.C. is supported by the National Research Foundation of Korea (Grants No. NRF-2021R1A6A1A03043957 and No. NRF-2020R1A2C3006177).

6. APPENDIX

We show the isotope table, similar to Meyer et al. (1995), of our $20 M_{\odot}$ supernova model. The masses are in units of M_{\odot} for three cases without and with neutrino oscillation for normal and inverted mass hierarchies. These isotopic abundances are taken from our CCSN model calculation at 50 secs after the core-bounce.

Table 1. Isotope source table for a $20M_{\odot}$ core-collapse supernova.

| | shell $M(r)$ ΔM | Fe/Ni | Si/S | O/Si | O/Ne | O/C | C/He | He/C | He/N | Total |
|-------------------------|-------------------------------|----------------|----------------|----------------|----------------|----------------|----------------|----------------|----------------|----------|
| | 1.600 0.012 | 1.624 0.024 | 1.710 0.086 | 3.583 1.873 | 3.767 0.184 | 3.901 0.134 | 5.713 1.812 | 6.000 0.287 | 6.000 6.000 | |
| $\Delta M(^1\text{H})$ | No-osci | 3.93E-08 | 1.57E-10 | 1.11E-10 | 3.64E-10 | 2.67E-11 | 1.43E-11 | 9.98E-09 | 2.18E-03 | 2.18E-03 |
| | normal | 3.93E-08 | 1.96E-10 | 1.89E-10 | 6.32E-10 | 4.82E-11 | 2.58E-11 | 1.83E-08 | 2.18E-03 | 2.18E-03 |
| | inverted | 3.93E-08 | 1.79E-10 | 1.50E-10 | 6.66E-10 | 3.17E-11 | 2.24E-11 | 1.65E-08 | 2.18E-03 | 2.18E-03 |
| $\Theta(^1\text{H})$ | No-osci | 4.52E-06 | 9.03E-09 | 1.82E-09 | 2.74E-10 | 2.20E-10 | 1.37E-10 | 7.77E-09 | 1.09E-02 | 6.96E-04 |
| | normal | 4.52E-06 | 1.13E-08 | 3.11E-09 | 4.76E-10 | 3.96E-10 | 2.47E-10 | 1.43E-08 | 1.09E-02 | 6.96E-04 |
| | inverted | 4.52E-06 | 1.03E-08 | 2.47E-09 | 5.01E-10 | 2.61E-10 | 2.15E-10 | 1.28E-08 | 1.09E-02 | 6.96E-04 |
| $\Delta M(^2\text{H})$ | No-osci | 1.83E-12 | 3.47E-12 | 9.11E-12 | 6.00E-11 | 9.58E-12 | 1.36E-11 | 5.98E-11 | 2.98E-09 | 3.14E-09 |
| | normal | 1.83E-12 | 3.97E-12 | 6.75E-12 | 6.50E-12 | 3.90E-12 | 1.26E-11 | 5.82E-11 | 2.93E-09 | 3.02E-09 |
| | inverted | 1.25E-12 | 4.17E-12 | 1.46E-11 | 1.09E-10 | 1.25E-11 | 1.42E-11 | 6.25E-11 | 6.09E-09 | 6.31E-09 |
| $\Theta(^2\text{H})$ | No-osci | 5.43E-06 | 5.14E-06 | 3.86E-06 | 1.16E-06 | 2.03E-06 | 3.37E-06 | 1.20E-06 | 3.84E-04 | 2.58E-05 |
| | normal | 5.43E-06 | 5.88E-06 | 2.86E-06 | 1.26E-07 | 8.27E-07 | 3.11E-06 | 1.16E-06 | 3.78E-04 | 2.49E-05 |
| | inverted | 3.71E-06 | 6.18E-06 | 6.19E-06 | 2.11E-06 | 2.65E-06 | 3.51E-06 | 1.25E-06 | 7.85E-04 | 5.20E-05 |
| $\Delta M(^3\text{H})$ | No-osci | 5.50E-13 | 4.42E-13 | 3.32E-13 | 3.34E-13 | 3.85E-14 | 1.07E-14 | 4.16E-13 | 1.42E-09 | 1.43E-09 |
| | normal | 5.51E-13 | 3.66E-13 | 4.17E-13 | 3.54E-12 | 3.08E-14 | 8.54E-15 | 4.32E-13 | 1.54E-09 | 1.55E-09 |
| | inverted | 9.02E-13 | 7.17E-13 | 3.53E-13 | 4.92E-13 | 5.07E-14 | 1.17E-14 | 4.34E-13 | 1.67E-09 | 1.67E-09 |
| $\Theta(^3\text{H})$ | No-osci | 5.31E-07 | 2.13E-07 | 4.58E-08 | 2.11E-09 | 2.65E-09 | 8.61E-10 | 2.71E-09 | 5.97E-05 | 3.82E-06 |
| | normal | 5.32E-07 | 1.76E-07 | 5.75E-08 | 2.24E-08 | 2.13E-09 | 6.87E-10 | 2.82E-09 | 6.48E-05 | 4.16E-06 |
| | inverted | 8.70E-07 | 3.46E-07 | 4.87E-08 | 3.10E-09 | 3.49E-09 | 9.38E-10 | 2.83E-09 | 7.02E-05 | 4.49E-06 |
| $\Delta M(^3\text{He})$ | No-osci | 4.35E-11 | 1.18E-10 | 1.77E-10 | 1.01E-09 | 5.36E-11 | 1.37E-11 | 1.45E-08 | 2.88E-07 | 3.04E-07 |
| | normal | 4.35E-11 | 1.27E-10 | 3.39E-10 | 4.42E-09 | 1.56E-10 | 2.77E-11 | 3.12E-08 | 2.91E-07 | 3.28E-07 |
| | inverted | 5.59E-11 | 1.26E-10 | 1.35E-10 | 6.14E-10 | 4.87E-11 | 2.44E-11 | 2.61E-08 | 2.89E-07 | 3.16E-07 |
| $\Theta(^3\text{He})$ | No-osci | 4.20E-05 | 5.68E-05 | 2.43E-05 | 6.36E-06 | 3.69E-06 | 1.10E-06 | 9.43E-05 | 1.21E-02 | 8.15E-04 |
| | normal | 4.20E-05 | 6.15E-05 | 4.68E-05 | 2.79E-05 | 1.08E-05 | 2.23E-06 | 2.03E-04 | 1.22E-02 | 8.79E-04 |
| | inverted | 5.39E-05 | 6.07E-05 | 1.86E-05 | 3.87E-06 | 3.36E-06 | 1.96E-06 | 1.70E-04 | 1.21E-02 | 8.47E-04 |
| $\Delta M(^4\text{He})$ | No-osci | 7.11E-08 | 6.83E-08 | 1.68E-07 | 1.81E-05 | 2.72E-04 | 5.44E-02 | 1.74E+00 | 2.68E-01 | 2.06E+00 |
| | normal | 7.11E-08 | 6.88E-08 | 1.84E-07 | 1.86E-05 | 2.72E-04 | 5.44E-02 | 1.74E+00 | 2.68E-01 | 2.06E+00 |
| | inverted | 7.05E-08 | 6.23E-08 | 1.62E-07 | 1.84E-05 | 2.73E-04 | 5.44E-02 | 1.74E+00 | 2.68E-01 | 2.06E+00 |
| $\Theta(^4\text{He})$ | No-osci | 2.11E-05 | 1.01E-05 | 7.14E-06 | 3.52E-05 | 5.78E-03 | 1.35E+00 | 3.49E+00 | 3.47E+00 | 1.70E+00 |
| | normal | 2.11E-05 | 1.02E-05 | 7.81E-06 | 3.62E-05 | 5.78E-03 | 1.35E+00 | 3.49E+00 | 3.47E+00 | 1.70E+00 |
| | inverted | 2.09E-05 | 9.25E-06 | 6.88E-06 | 3.57E-05 | 5.78E-03 | 1.35E+00 | 3.49E+00 | 3.47E+00 | 1.70E+00 |
| $\Delta M(^6\text{Li})$ | No-osci | 5.05E-16 | 5.14E-13 | 2.16E-12 | 2.24E-11 | 1.08E-12 | 1.95E-12 | 1.73E-11 | 3.96E-11 | 8.50E-11 |
| | normal | 5.05E-16 | 5.08E-13 | 2.76E-12 | 3.87E-11 | 1.54E-12 | 1.91E-12 | 1.95E-11 | 3.95E-11 | 1.04E-10 |
| | inverted | 4.82E-16 | 6.08E-13 | 3.64E-12 | 4.07E-11 | 1.97E-12 | 2.12E-12 | 2.11E-11 | 3.95E-11 | 1.10E-10 |
| $\Theta(^6\text{Li})$ | No-osci | 5.98E-05 | 3.04E-02 | 3.65E-02 | 1.73E-02 | 9.12E-03 | 1.92E-02 | 1.39E-02 | 2.04E-01 | 2.79E-02 |
| | normal | 5.98E-05 | 3.01E-02 | 4.67E-02 | 2.99E-02 | 1.30E-02 | 1.88E-02 | 1.56E-02 | 2.03E-01 | 3.43E-02 |
| | inverted | 5.70E-05 | 3.60E-02 | 6.15E-02 | 3.15E-02 | 1.67E-02 | 2.09E-02 | 1.69E-02 | 2.03E-01 | 3.60E-02 |
| $\Delta M(^7\text{Li})$ | No-osci | 7.82E-14 | 4.04E-12 | 1.69E-11 | 2.65E-10 | 1.09E-10 | 4.29E-11 | 6.70E-08 | 6.40E-09 | 7.39E-08 |
| | normal | 7.82E-14 | 4.04E-12 | 1.69E-11 | 2.80E-10 | 1.41E-10 | 4.58E-11 | 7.80E-08 | 7.04E-09 | 8.55E-08 |
| | inverted | 8.24E-14 | 3.99E-12 | 2.59E-11 | 4.67E-11 | 1.60E-10 | 5.53E-11 | 8.38E-08 | 7.46E-09 | 9.20E-08 |
| $\Theta(^7\text{Li})$ | No-osci | 6.48E-04 | 1.67E-02 | 2.00E-02 | 1.44E-02 | 6.47E-02 | 2.96E-02 | 3.75E+00 | 2.31E+00 | 1.70E+00 |
| | normal | 6.48E-04 | 1.67E-02 | 2.00E-02 | 1.52E-02 | 8.35E-02 | 3.17E-02 | 4.37E+00 | 2.54E+00 | 1.97E+00 |
| | inverted | 6.83E-04 | 1.65E-02 | 3.07E-02 | 2.53E-02 | 9.49E-02 | 3.82E-02 | 4.69E+00 | 2.69E+00 | 2.12E+00 |
| $\Delta M(^7\text{Be})$ | No-osci | 9.58E-13 | 1.30E-12 | 1.34E-11 | 2.73E-10 | 5.82E-10 | 1.28E-09 | 8.68E-08 | 1.19E-11 | 8.90E-08 |
| | normal | 9.58E-13 | 1.61E-12 | 2.36E-11 | 7.01E-10 | 1.71E-09 | 2.74E-09 | 2.40E-07 | 2.28E-11 | 2.46E-07 |
| | inverted | 2.18E-12 | 1.48E-12 | 1.85E-11 | 4.10E-10 | 5.47E-10 | 2.59E-09 | 2.05E-07 | 1.92E-11 | 2.08E-07 |
| $\Theta(^7\text{Be})$ | No-osci | 7.94E-03 | 5.40E-03 | 1.59E-02 | 1.48E-02 | 3.45E-01 | 8.81E-01 | 4.86E+00 | 4.31E-03 | 2.05E+00 |
| | normal | 7.94E-03 | 6.66E-03 | 2.79E-02 | 3.80E-02 | 1.02E+00 | 1.89E+00 | 1.35E+01 | 8.20E-03 | 5.66E+00 |
| | inverted | 1.81E-02 | 6.13E-03 | 2.19E-02 | 2.22E-02 | 3.24E-01 | 1.79E+00 | 1.15E+01 | 6.91E-03 | 4.79E+00 |
| $\Delta M(^9\text{Be})$ | No-osci | 1.28E-15 | 2.71E-13 | 3.38E-12 | 5.05E-11 | 2.73E-12 | 2.36E-13 | 4.39E-11 | 1.00E-11 | 1.11E-10 |
| | normal | 1.28E-15 | 2.17E-13 | 2.28E-12 | 3.53E-11 | 2.66E-12 | 2.39E-13 | 4.86E-11 | 1.04E-11 | 9.97E-11 |
| | inverted | 1.23E-15 | 5.88E-13 | 8.45E-12 | 1.08E-10 | 4.07E-12 | 2.88E-13 | 5.58E-11 | 1.07E-11 | 1.88E-10 |
| $\Theta(^9\text{Be})$ | No-osci | 6.96E-04 | 7.35E-02 | 2.61E-01 | 1.79E-01 | 1.06E-01 | 1.07E-02 | 1.61E-01 | 2.37E-01 | 1.67E-01 |
| | normal | 6.96E-04 | 5.88E-02 | 1.76E-01 | 1.25E-01 | 1.03E-01 | 1.08E-02 | 1.78E-01 | 2.45E-01 | 1.50E-01 |
| | inverted | 6.69E-04 | 1.59E-01 | 6.54E-01 | 3.82E-01 | 1.58E-01 | 1.30E-02 | 2.04E-01 | 2.52E-01 | 2.82E-01 |

Continued on next page

Table 1 – Continued from previous page

| shell M(r) ΔM | hierarchy | Fe/Ni | Si/S | O/Si | O/Ne | O/C | C/He | He/C | He/N | Total |
|-----------------------------|-----------|----------------|----------------|----------------|----------------|----------------|----------------|----------------|----------------|----------------|
| | | 1.600 0.012 | 1.624 0.024 | 1.710 0.086 | 3.583 1.873 | 3.767 0.184 | 3.901 0.134 | 5.713 1.812 | 6.000 0.287 | 6.000 6.000 |
| $\Delta M(^{10}\text{Be})$ | No-osci | 7.78E-31 | 2.36E-27 | 1.15E-26 | 1.73E-24 | 8.43E-24 | 3.59E-24 | 1.79E-23 | 2.73E-27 | 3.16E-23 |
| | normal | 7.91E-31 | 2.94E-29 | 3.27E-28 | 5.15E-25 | 1.95E-24 | 2.88E-23 | 1.77E-23 | 2.03E-27 | 4.90E-23 |
| | inverted | 1.07E-30 | 2.64E-28 | 2.01E-26 | 5.42E-24 | 3.01E-23 | 1.33E-23 | 2.80E-23 | 2.09E-27 | 7.68E-23 |
| $\Theta(^{10}\text{Be})$ | No-osci | 6.27E-20 | 9.51E-17 | 1.33E-16 | 9.13E-16 | 4.86E-14 | 2.41E-14 | 9.72E-15 | 9.56E-18 | 7.08E-15 |
| | normal | 6.38E-20 | 1.18E-18 | 3.77E-18 | 2.71E-16 | 1.12E-14 | 1.94E-13 | 9.63E-15 | 7.11E-18 | 1.10E-14 |
| | inverted | 8.59E-20 | 1.07E-17 | 2.32E-16 | 2.86E-15 | 1.73E-13 | 8.90E-14 | 1.52E-14 | 7.34E-18 | 1.72E-14 |
| $\Delta M(^{10}\text{B})$ | No-osci | 4.27E-14 | 7.84E-12 | 5.60E-11 | 6.91E-10 | 8.13E-11 | 3.87E-11 | 2.04E-10 | 6.64E-11 | 1.15E-09 |
| | normal | 4.27E-14 | 8.02E-12 | 6.12E-11 | 8.45E-10 | 4.18E-10 | 3.81E-10 | 3.32E-10 | 6.63E-11 | 2.11E-09 |
| | inverted | 4.06E-13 | 9.62E-12 | 1.18E-10 | 1.25E-09 | 4.61E-10 | 3.98E-10 | 3.44E-10 | 6.61E-11 | 2.64E-09 |
| $\Theta(^{10}\text{B})$ | No-osci | 3.45E-03 | 3.16E-01 | 6.45E-01 | 3.64E-01 | 4.68E-01 | 2.60E-01 | 1.11E-01 | 2.33E-01 | 2.57E-01 |
| | normal | 3.44E-03 | 3.23E-01 | 7.04E-01 | 4.45E-01 | 2.40E+00 | 2.56E+00 | 1.81E-01 | 2.33E-01 | 4.73E-01 |
| | inverted | 3.28E-02 | 3.88E-01 | 1.36E+00 | 6.57E-01 | 2.65E+00 | 2.67E+00 | 1.87E-01 | 2.32E-01 | 5.92E-01 |
| $\Delta M(^{11}\text{B})$ | No-osci | 2.54E-12 | 8.21E-10 | 7.48E-09 | 1.06E-07 | 1.16E-08 | 3.35E-09 | 2.03E-07 | 3.75E-10 | 3.32E-07 |
| | normal | 2.53E-12 | 7.56E-10 | 5.88E-09 | 7.69E-08 | 1.12E-08 | 3.52E-09 | 1.92E-07 | 3.80E-10 | 2.91E-07 |
| | inverted | 5.78E-12 | 6.69E-10 | 5.68E-09 | 7.28E-08 | 1.38E-08 | 4.04E-09 | 2.17E-07 | 3.82E-10 | 3.14E-07 |
| $\Theta(^{11}\text{B})$ | No-osci | 4.56E-02 | 7.37E+00 | 1.92E+01 | 1.24E+01 | 1.49E+01 | 5.01E+00 | 2.46E+01 | 2.93E-01 | 1.66E+01 |
| | normal | 4.55E-02 | 6.78E+00 | 1.51E+01 | 9.02E+00 | 1.44E+01 | 5.27E+00 | 2.33E+01 | 2.97E-01 | 1.45E+01 |
| | inverted | 1.04E-01 | 6.00E+00 | 1.46E+01 | 8.54E+00 | 1.76E+01 | 6.04E+00 | 2.63E+01 | 2.98E-01 | 1.57E+01 |
| $\Delta M(^{11}\text{C})$ | No-osci | 6.17E-11 | 3.58E-10 | 3.23E-09 | 5.14E-08 | 9.23E-09 | 3.32E-09 | 2.29E-08 | 1.37E-11 | 9.05E-08 |
| | normal | 6.17E-11 | 4.36E-10 | 5.71E-09 | 1.26E-07 | 4.20E-08 | 1.17E-08 | 9.53E-08 | 4.24E-11 | 2.81E-07 |
| | inverted | 2.53E-10 | 4.79E-10 | 5.78E-09 | 1.14E-07 | 3.27E-08 | 1.12E-08 | 7.74E-08 | 3.29E-11 | 2.42E-07 |
| $\Theta(^{11}\text{C})$ | No-osci | 1.11E+00 | 3.22E+00 | 8.29E+00 | 6.04E+00 | 1.18E+01 | 4.97E+00 | 2.78E+00 | 1.07E-02 | 4.52E+00 |
| | normal | 1.11E+00 | 3.92E+00 | 1.47E+01 | 1.47E+01 | 5.39E+01 | 1.76E+01 | 1.16E+01 | 3.31E-02 | 1.40E+01 |
| | inverted | 4.55E+00 | 4.30E+00 | 1.48E+01 | 1.34E+01 | 4.20E+01 | 1.68E+01 | 9.39E+00 | 2.57E-02 | 1.21E+01 |
| $\Delta M(^{12}\text{C})$ | No-osci | 1.16E-07 | 4.31E-06 | 1.30E-04 | 1.03E-02 | 3.45E-02 | 5.61E-02 | 5.74E-02 | 4.92E-04 | 1.59E-01 |
| | normal | 1.16E-07 | 4.31E-06 | 1.30E-04 | 1.03E-02 | 3.45E-02 | 5.61E-02 | 5.74E-02 | 4.92E-04 | 1.59E-01 |
| | inverted | 1.13E-07 | 3.99E-06 | 1.27E-04 | 1.03E-02 | 3.45E-02 | 5.61E-02 | 5.74E-02 | 4.92E-04 | 1.59E-01 |
| $\Theta(^{12}\text{C})$ | No-osci | 4.04E-03 | 7.54E-02 | 6.48E-01 | 2.36E+00 | 8.62E+01 | 1.63E+02 | 1.36E+01 | 7.47E-01 | 1.54E+01 |
| | normal | 4.04E-03 | 7.54E-02 | 6.49E-01 | 2.36E+00 | 8.62E+01 | 1.63E+02 | 1.36E+01 | 7.47E-01 | 1.54E+01 |
| | inverted | 3.94E-03 | 6.98E-02 | 6.36E-01 | 2.35E+00 | 8.62E+01 | 1.63E+02 | 1.36E+01 | 7.47E-01 | 1.54E+01 |
| $\Delta M(^{13}\text{C})$ | No-osci | 6.02E-10 | 5.23E-09 | 3.82E-08 | 5.22E-07 | 6.68E-08 | 4.16E-08 | 1.13E-07 | 8.73E-08 | 8.75E-07 |
| | normal | 6.00E-10 | 5.23E-09 | 3.83E-08 | 5.32E-07 | 1.19E-07 | 7.21E-08 | 9.78E-08 | 8.73E-08 | 9.53E-07 |
| | inverted | 4.19E-10 | 5.19E-09 | 3.84E-08 | 5.02E-07 | 8.52E-08 | 6.24E-08 | 1.13E-07 | 8.73E-08 | 8.93E-07 |
| $\Theta(^{13}\text{C})$ | No-osci | 1.73E-03 | 7.51E-03 | 1.57E-02 | 9.80E-03 | 1.37E-02 | 9.95E-03 | 2.20E-03 | 1.09E-02 | 6.98E-03 |
| | normal | 1.72E-03 | 7.51E-03 | 1.57E-02 | 9.99E-03 | 2.44E-02 | 1.72E-02 | 1.90E-03 | 1.09E-02 | 7.60E-03 |
| | inverted | 1.20E-03 | 7.45E-03 | 1.58E-02 | 9.41E-03 | 1.75E-02 | 1.49E-02 | 2.18E-03 | 1.09E-02 | 7.12E-03 |
| $\Delta M(^{14}\text{C})$ | No-osci | 3.03E-10 | 3.81E-08 | 3.17E-07 | 2.60E-06 | 6.50E-08 | 8.94E-08 | 4.95E-07 | 1.85E-08 | 3.63E-06 |
| | normal | 3.03E-10 | 3.81E-08 | 3.17E-07 | 2.61E-06 | 6.52E-08 | 8.06E-08 | 4.12E-07 | 2.05E-08 | 3.54E-06 |
| | inverted | 2.71E-10 | 3.38E-08 | 2.79E-07 | 2.37E-06 | 1.09E-07 | 1.06E-07 | 4.73E-07 | 2.17E-08 | 3.39E-06 |
| $\Theta(^{14}\text{C})$ | No-osci | 3.04E-05 | 1.91E-03 | 4.55E-03 | 1.71E-03 | 4.66E-04 | 7.49E-04 | 3.36E-04 | 8.09E-05 | 1.01E-03 |
| | normal | 3.04E-05 | 1.91E-03 | 4.55E-03 | 1.71E-03 | 4.68E-04 | 6.75E-04 | 2.80E-04 | 8.97E-05 | 9.88E-04 |
| | inverted | 2.72E-05 | 1.70E-03 | 4.00E-03 | 1.56E-03 | 7.84E-04 | 8.88E-04 | 3.21E-04 | 9.49E-05 | 9.48E-04 |
| $\Delta M(^{14}\text{N})$ | No-osci | 1.14E-09 | 8.51E-08 | 6.66E-07 | 4.66E-06 | 1.55E-07 | 7.48E-07 | 3.12E-04 | 8.80E-04 | 1.20E-03 |
| | normal | 1.14E-09 | 8.52E-08 | 6.70E-07 | 4.80E-06 | 3.74E-07 | 9.90E-07 | 3.12E-04 | 8.80E-04 | 1.20E-03 |
| | inverted | 1.28E-09 | 8.11E-08 | 6.36E-07 | 4.72E-06 | 2.49E-07 | 9.39E-07 | 3.12E-04 | 8.80E-04 | 1.20E-03 |
| $\Theta(^{14}\text{N})$ | No-osci | 1.15E-04 | 4.28E-03 | 9.56E-03 | 3.06E-03 | 1.11E-03 | 6.26E-03 | 2.12E-01 | 3.84E+00 | 3.34E-01 |
| | normal | 1.15E-04 | 4.28E-03 | 9.62E-03 | 3.15E-03 | 2.68E-03 | 8.29E-03 | 2.12E-01 | 3.84E+00 | 3.35E-01 |
| | inverted | 1.29E-04 | 4.07E-03 | 9.13E-03 | 3.10E-03 | 1.79E-03 | 7.86E-03 | 2.12E-01 | 3.84E+00 | 3.34E-01 |
| $\Delta M(^{15}\text{N})$ | No-osci | 1.20E-09 | 3.30E-07 | 2.39E-06 | 2.93E-05 | 1.26E-06 | 3.57E-07 | 1.63E-06 | 1.10E-08 | 3.53E-05 |
| | normal | 1.19E-09 | 3.32E-07 | 2.37E-06 | 2.82E-05 | 1.16E-06 | 3.66E-07 | 2.50E-06 | 1.11E-08 | 3.49E-05 |
| | inverted | 1.13E-09 | 2.76E-07 | 1.79E-06 | 2.01E-05 | 2.08E-06 | 5.03E-07 | 2.47E-06 | 1.10E-08 | 2.72E-05 |
| $\Theta(^{15}\text{N})$ | No-osci | 3.06E-02 | 4.22E+00 | 8.74E+00 | 4.90E+00 | 2.29E+00 | 7.60E-01 | 2.82E-01 | 1.23E-02 | 2.51E+00 |
| | normal | 3.05E-02 | 4.25E+00 | 8.65E+00 | 4.70E+00 | 2.12E+00 | 7.80E-01 | 4.31E-01 | 1.24E-02 | 2.48E+00 |
| | inverted | 2.88E-02 | 3.53E+00 | 6.53E+00 | 3.35E+00 | 3.79E+00 | 1.07E+00 | 4.26E-01 | 1.23E-02 | 1.93E+00 |
| $\Delta M(^{16}\text{O})$ | No-osci | 3.98E-06 | 5.39E-03 | 7.05E-02 | 1.37E+00 | 1.35E-01 | 3.54E-02 | 3.96E-03 | 5.46E-05 | 1.62E+00 |
| | normal | 3.98E-06 | 5.39E-03 | 7.05E-02 | 1.37E+00 | 1.35E-01 | 3.54E-02 | 3.96E-03 | 5.46E-05 | 1.62E+00 |
| | inverted | 3.99E-06 | 5.39E-03 | 7.05E-02 | 1.37E+00 | 1.35E-01 | 3.54E-02 | 3.96E-03 | 5.46E-05 | 1.62E+00 |
| $\Theta(^{16}\text{O})$ | No-osci | 4.73E-02 | 3.20E+01 | 1.20E+02 | 1.06E+02 | 1.14E+02 | 3.50E+01 | 3.18E-01 | 2.82E-02 | 5.33E+01 |
| | normal | 4.73E-02 | 3.20E+01 | 1.20E+02 | 1.06E+02 | 1.14E+02 | 3.50E+01 | 3.18E-01 | 2.82E-02 | 5.33E+01 |
| | inverted | 4.73E-02 | 3.20E+01 | 1.20E+02 | 1.06E+02 | 1.14E+02 | 3.50E+01 | 3.18E-01 | 2.82E-02 | 5.33E+01 |
| $\Delta M(^{17}\text{O})$ | No-osci | 5.20E-12 | 3.87E-09 | 2.96E-07 | 6.89E-06 | 3.31E-06 | 1.58E-06 | 5.02E-08 | 8.50E-09 | 1.21E-05 |
| | normal | 5.19E-12 | 3.87E-09 | 2.96E-07 | 6.87E-06 | 3.20E-06 | 1.43E-06 | 3.88E-08 | 8.51E-09 | 1.19E-05 |
| | inverted | 5.27E-12 | 2.83E-09 | 2.18E-07 | 7.14E-06 | 4.45E-06 | 1.79E-06 | 4.32E-08 | 8.51E-09 | 1.37E-05 |
| $\Theta(^{17}\text{O})$ | No-osci | 1.55E-04 | 5.75E-02 | 1.26E+00 | 1.34E+00 | 7.04E+00 | 3.91E+00 | 1.01E-02 | 1.10E-02 | 1.00E+00 |
| | normal | 1.54E-04 | 5.75E-02 | 1.26E+00 | 1.34E+00 | 6.80E+00 | 3.55E+00 | 7.80E-03 | 1.10E-02 | 9.79E-01 |
| | inverted | 1.57E-04 | 4.20E-02 | 9.25E-01 | 1.39E+00 | 9.44E+00 | 4.43E+00 | 8.69E-03 | 1.10E-02 | 1.13E+00 |
| $\Delta M(^{18}\text{O})$ | No-osci | 4.99E-14 | 1.40E-10 | 5.12E-09 | 1.12E-06 | 1.97E-09 | 6.28E-06 | 4.91E-04 | 5.58E-06 | 5.04E-04 |
| | normal | 4.99E-14 | 1.40E-10 | 5.12E-09 | 1.12E-06 | 1.97E-09 | 6.18E-06 | 4.90E-04 | 5.58E-06 | 5.02E-04 |

Continued on next page

Table 1 – Continued from previous page

| shell M(r) ΔM | hierarchy | Fe/Ni | Si/S | O/Si | O/Ne | O/C | C/He | He/C | He/N | Total |
|-----------------------------|-----------|----------------|----------------|----------------|----------------|----------------|----------------|----------------|----------------|----------|
| | | 1.600 0.012 | 1.624 0.024 | 1.710 0.086 | 3.583 1.873 | 3.767 0.184 | 3.901 0.134 | 5.713 1.812 | 6.000 0.287 | 6.000 |
| $\Theta(^{18}\text{O})$ | inverted | 1.16E-14 | 1.01E-10 | 1.88E-09 | 2.77E-07 | 2.45E-09 | 6.20E-06 | 4.90E-04 | 5.58E-06 | 5.02E-04 |
| | No-osci | 2.63E-07 | 3.67E-04 | 3.85E-03 | 3.84E-02 | 7.27E-04 | 2.75E+00 | 1.74E+01 | 1.28E+00 | 7.36E+00 |
| | normal | 2.63E-07 | 3.67E-04 | 3.85E-03 | 3.84E-02 | 7.38E-04 | 2.71E+00 | 1.74E+01 | 1.28E+00 | 7.34E+00 |
| $\Delta M(^{19}\text{F})$ | inverted | 6.11E-08 | 2.66E-04 | 1.41E-03 | 9.54E-03 | 9.21E-04 | 2.72E+00 | 1.74E+01 | 1.28E+00 | 7.33E+00 |
| | No-osci | 3.53E-12 | 7.75E-10 | 1.18E-07 | 2.85E-05 | 6.60E-08 | 6.20E-08 | 2.22E-07 | 2.86E-08 | 2.90E-05 |
| | normal | 3.53E-12 | 7.78E-10 | 1.19E-07 | 2.95E-05 | 6.49E-08 | 6.47E-08 | 2.41E-07 | 2.86E-08 | 3.01E-05 |
| $\Theta(^{19}\text{F})$ | inverted | 4.43E-12 | 5.59E-10 | 7.77E-08 | 1.78E-05 | 2.33E-07 | 1.61E-07 | 2.39E-07 | 2.86E-08 | 1.85E-05 |
| | No-osci | 6.90E-04 | 7.57E-02 | 3.28E+00 | 3.63E+01 | 9.21E-01 | 1.01E+00 | 2.92E-01 | 2.43E-01 | 1.57E+01 |
| | normal | 6.89E-04 | 7.60E-02 | 3.32E+00 | 3.77E+01 | 9.04E-01 | 1.05E+00 | 3.18E-01 | 2.43E-01 | 1.63E+01 |
| | inverted | 8.65E-04 | 5.45E-02 | 2.17E+00 | 2.27E+01 | 3.24E+00 | 2.62E+00 | 3.15E-01 | 2.42E-01 | 1.00E+01 |
| $\Delta M(^{20}\text{Ne})$ | No-osci | 1.80E-09 | 1.24E-06 | 1.02E-03 | 3.38E-01 | 4.04E-04 | 1.19E-04 | 7.33E-04 | 1.14E-04 | 3.40E-01 |
| | normal | 1.80E-09 | 1.24E-06 | 1.02E-03 | 3.38E-01 | 4.04E-04 | 1.19E-04 | 7.33E-04 | 1.14E-04 | 3.40E-01 |
| | inverted | 1.80E-09 | 1.13E-06 | 1.02E-03 | 3.38E-01 | 4.04E-04 | 1.19E-04 | 7.33E-04 | 1.14E-04 | 3.41E-01 |
| $\Theta(^{20}\text{Ne})$ | No-osci | 8.80E-05 | 3.02E-02 | 7.11E+00 | 1.08E+02 | 1.41E+00 | 4.84E-01 | 2.41E-01 | 2.42E-01 | 4.61E+01 |
| | normal | 8.80E-05 | 3.02E-02 | 7.11E+00 | 1.08E+02 | 1.41E+00 | 4.84E-01 | 2.41E-01 | 2.42E-01 | 4.61E+01 |
| | inverted | 8.79E-05 | 2.74E-02 | 7.11E+00 | 1.08E+02 | 1.41E+00 | 4.84E-01 | 2.41E-01 | 2.42E-01 | 4.61E+01 |
| $\Delta M(^{21}\text{Ne})$ | No-osci | 7.02E-13 | 3.59E-11 | 6.68E-08 | 6.34E-05 | 3.68E-05 | 5.80E-06 | 2.57E-06 | 2.91E-07 | 1.09E-04 |
| | normal | 7.01E-13 | 3.59E-11 | 6.68E-08 | 6.34E-05 | 3.68E-05 | 5.79E-06 | 2.56E-06 | 2.91E-07 | 1.09E-04 |
| | inverted | 7.04E-13 | 2.61E-11 | 5.82E-08 | 6.32E-05 | 3.68E-05 | 5.80E-06 | 2.56E-06 | 2.91E-07 | 1.09E-04 |
| $\Theta(^{21}\text{Ne})$ | No-osci | 1.36E-05 | 3.48E-04 | 1.85E-01 | 8.03E+00 | 5.10E+01 | 9.36E+00 | 3.36E-01 | 2.45E-01 | 5.86E+00 |
| | normal | 1.36E-05 | 3.48E-04 | 1.85E-01 | 8.03E+00 | 5.10E+01 | 9.35E+00 | 3.35E-01 | 2.45E-01 | 5.86E+00 |
| | inverted | 1.36E-05 | 2.53E-04 | 1.61E-01 | 8.00E+00 | 5.10E+01 | 9.36E+00 | 3.35E-01 | 2.45E-01 | 5.85E+00 |
| $\Delta M(^{22}\text{Ne})$ | No-osci | 1.42E-13 | 1.32E-11 | 5.64E-09 | 9.46E-05 | 6.22E-04 | 7.30E-04 | 8.78E-03 | 8.28E-05 | 1.03E-02 |
| | normal | 1.42E-13 | 1.32E-11 | 5.64E-09 | 9.46E-05 | 6.22E-04 | 7.30E-04 | 8.78E-03 | 8.28E-05 | 1.03E-02 |
| | inverted | 1.39E-13 | 7.86E-12 | 2.99E-09 | 9.41E-05 | 6.22E-04 | 7.30E-04 | 8.78E-03 | 8.28E-05 | 1.03E-02 |
| $\Theta(^{22}\text{Ne})$ | No-osci | 8.55E-08 | 3.96E-06 | 4.86E-04 | 3.72E-01 | 2.68E+01 | 3.66E+01 | 3.57E+01 | 2.17E+00 | 1.72E+01 |
| | normal | 8.55E-08 | 3.96E-06 | 4.85E-04 | 3.72E-01 | 2.68E+01 | 3.66E+01 | 3.57E+01 | 2.17E+00 | 1.72E+01 |
| | inverted | 8.37E-08 | 2.37E-06 | 2.57E-04 | 3.71E-01 | 2.68E+01 | 3.66E+01 | 3.57E+01 | 2.17E+00 | 1.72E+01 |
| $\Delta M(^{22}\text{Na})$ | No-osci | 3.30E-13 | 1.19E-11 | 2.84E-09 | 6.69E-07 | 1.05E-08 | 1.19E-09 | 1.34E-10 | 7.99E-13 | 6.84E-07 |
| | normal | 3.30E-13 | 1.19E-11 | 2.85E-09 | 6.74E-07 | 1.07E-08 | 1.25E-09 | 2.02E-10 | 8.03E-13 | 6.99E-07 |
| | inverted | 3.34E-13 | 1.09E-11 | 2.88E-09 | 7.22E-07 | 9.20E-09 | 1.27E-09 | 1.90E-10 | 6.31E-13 | 7.35E-07 |
| $\Theta(^{22}\text{Na})$ | No-osci | 1.99E-07 | 3.59E-06 | 2.45E-04 | 2.64E-03 | 4.50E-04 | 5.96E-05 | 5.47E-07 | 2.09E-08 | 1.14E-03 |
| | normal | 1.99E-07 | 3.59E-06 | 2.45E-04 | 2.65E-03 | 8.47E-04 | 1.29E-04 | 8.23E-07 | 2.10E-08 | 1.17E-03 |
| | inverted | 2.02E-07 | 3.29E-06 | 2.48E-04 | 2.84E-03 | 3.96E-04 | 6.36E-05 | 7.72E-07 | 1.65E-08 | 1.23E-03 |
| $\Delta M(^{23}\text{Na})$ | No-osci | 3.69E-10 | 2.99E-09 | 3.26E-06 | 2.96E-03 | 4.56E-06 | 2.08E-06 | 1.53E-05 | 2.36E-06 | 2.99E-03 |
| | normal | 3.69E-10 | 3.01E-09 | 3.26E-06 | 2.96E-03 | 4.57E-06 | 2.10E-06 | 1.53E-05 | 2.36E-06 | 2.98E-03 |
| | inverted | 3.69E-10 | 2.77E-09 | 3.14E-06 | 2.93E-03 | 4.57E-06 | 2.10E-06 | 1.53E-05 | 2.36E-06 | 2.96E-03 |
| $\Theta(^{23}\text{Na})$ | No-osci | 8.29E-04 | 3.37E-03 | 1.05E+00 | 4.34E+01 | 7.32E-01 | 3.90E-01 | 2.33E-01 | 2.31E-01 | 1.86E+01 |
| | normal | 8.29E-04 | 3.38E-03 | 1.05E+00 | 4.34E+01 | 7.34E-01 | 3.93E-01 | 2.32E-01 | 2.31E-01 | 1.86E+01 |
| | inverted | 8.29E-04 | 3.11E-03 | 1.01E+00 | 4.30E+01 | 7.33E-01 | 3.93E-01 | 2.32E-01 | 2.31E-01 | 1.85E+01 |
| $\Delta M(^{24}\text{Mg})$ | No-osci | 4.10E-07 | 4.76E-06 | 3.87E-03 | 8.83E-02 | 2.31E-05 | 1.87E-05 | 2.33E-04 | 3.63E-05 | 9.25E-02 |
| | normal | 4.10E-07 | 4.76E-06 | 3.87E-03 | 8.83E-02 | 2.31E-05 | 1.88E-05 | 2.33E-04 | 3.63E-05 | 9.25E-02 |
| | inverted | 4.10E-07 | 4.70E-06 | 3.89E-03 | 8.83E-02 | 2.30E-05 | 1.87E-05 | 2.33E-04 | 3.63E-05 | 9.25E-02 |
| $\Theta(^{24}\text{Mg})$ | No-osci | 6.28E-02 | 3.65E-01 | 8.49E+01 | 8.85E+01 | 2.53E-01 | 2.40E-01 | 2.42E-01 | 2.42E-01 | 3.94E+01 |
| | normal | 6.28E-02 | 3.65E-01 | 8.49E+01 | 8.85E+01 | 2.53E-01 | 2.40E-01 | 2.42E-01 | 2.42E-01 | 3.94E+01 |
| | inverted | 6.28E-02 | 3.60E-01 | 8.52E+01 | 8.85E+01 | 2.53E-01 | 2.40E-01 | 2.42E-01 | 2.42E-01 | 3.94E+01 |
| $\Delta M(^{25}\text{Mg})$ | No-osci | 1.49E-08 | 3.23E-09 | 3.81E-05 | 9.29E-03 | 1.12E-04 | 2.37E-05 | 3.18E-05 | 4.78E-06 | 9.50E-03 |
| | normal | 1.49E-08 | 3.24E-09 | 3.81E-05 | 9.30E-03 | 1.12E-04 | 2.37E-05 | 3.18E-05 | 4.78E-06 | 9.51E-03 |
| | inverted | 1.49E-08 | 2.98E-09 | 3.64E-05 | 9.29E-03 | 1.11E-04 | 2.37E-05 | 3.18E-05 | 4.78E-06 | 9.50E-03 |
| $\Theta(^{25}\text{Mg})$ | No-osci | 1.72E-02 | 1.87E-03 | 6.30E+00 | 7.04E+01 | 9.23E+00 | 2.29E+00 | 2.49E-01 | 2.41E-01 | 3.06E+01 |
| | normal | 1.72E-02 | 1.87E-03 | 6.31E+00 | 7.04E+01 | 9.23E+00 | 2.29E+00 | 2.49E-01 | 2.41E-01 | 3.06E+01 |
| | inverted | 1.72E-02 | 1.73E-03 | 6.02E+00 | 7.03E+01 | 9.22E+00 | 2.29E+00 | 2.49E-01 | 2.41E-01 | 3.06E+01 |
| $\Delta M(^{26}\text{Mg})$ | No-osci | 1.49E-09 | 1.41E-09 | 1.57E-05 | 9.43E-03 | 2.58E-04 | 5.34E-05 | 3.93E-05 | 5.51E-06 | 9.80E-03 |
| | normal | 1.49E-09 | 1.41E-09 | 1.57E-05 | 9.43E-03 | 2.58E-04 | 5.34E-05 | 3.92E-05 | 5.51E-06 | 9.80E-03 |
| | inverted | 1.49E-09 | 1.36E-09 | 1.54E-05 | 9.41E-03 | 2.59E-04 | 5.35E-05 | 3.92E-05 | 5.51E-06 | 9.78E-03 |
| $\Theta(^{26}\text{Mg})$ | No-osci | 1.52E-03 | 7.17E-04 | 2.28E+00 | 6.25E+01 | 1.87E+01 | 4.52E+00 | 2.69E-01 | 2.43E-01 | 2.76E+01 |
| | normal | 1.52E-03 | 7.17E-04 | 2.28E+00 | 6.25E+01 | 1.87E+01 | 4.52E+00 | 2.69E-01 | 2.43E-01 | 2.76E+01 |
| | inverted | 1.52E-03 | 6.91E-04 | 2.24E+00 | 6.24E+01 | 1.88E+01 | 4.52E+00 | 2.69E-01 | 2.43E-01 | 2.76E+01 |
| $\Delta M(^{26}\text{Al})$ | No-osci | 9.37E-10 | 4.95E-10 | 3.89E-06 | 5.83E-05 | 5.10E-09 | 1.32E-09 | 1.73E-10 | 5.81E-14 | 6.22E-05 |
| | normal | 9.37E-10 | 4.95E-10 | 3.89E-06 | 5.84E-05 | 5.79E-09 | 2.96E-09 | 2.97E-10 | 5.81E-14 | 6.23E-05 |
| | inverted | 9.37E-10 | 4.92E-10 | 3.99E-06 | 6.34E-05 | 4.86E-09 | 1.78E-09 | 2.81E-10 | 5.78E-14 | 6.74E-05 |
| $\Theta(^{26}\text{Al})$ | No-osci | 9.51E-04 | 2.51E-04 | 5.64E-01 | 3.87E-01 | 3.70E-04 | 1.11E-04 | 1.19E-06 | 2.56E-09 | 1.75E-01 |
| | normal | 9.51E-04 | 2.51E-04 | 5.64E-01 | 3.88E-01 | 7.10E-04 | 2.51E-04 | 2.04E-06 | 2.56E-09 | 1.76E-01 |
| | inverted | 9.51E-04 | 2.49E-04 | 5.79E-01 | 4.20E-01 | 3.52E-04 | 1.50E-04 | 1.92E-06 | 2.55E-09 | 1.90E-01 |
| $\Delta M(^{27}\text{Al})$ | No-osci | 1.91E-06 | 6.15E-07 | 2.72E-04 | 9.18E-03 | 2.92E-06 | 2.21E-06 | 2.76E-05 | 4.30E-06 | 9.49E-03 |
| | normal | 1.91E-06 | 6.15E-07 | 2.72E-04 | 9.18E-03 | 2.95E-06 | 2.22E-06 | 2.76E-05 | 4.30E-06 | 9.49E-03 |
| | inverted | 1.91E-06 | 6.12E-07 | 2.71E-04 | 9.19E-03 | 2.91E-06 | 2.21E-06 | 2.76E-05 | 4.30E-06 | 9.50E-03 |
| $\Theta(^{27}\text{Al})$ | No-osci | 2.49E+00 | 4.02E-01 | 5.08E+01 | 7.83E+01 | 2.72E-01 | 2.40E-01 | 2.43E-01 | 2.44E-01 | 3.44E+01 |

Continued on next page

Table 1 – Continued from previous page

| shell M(r) ΔM | hierarchy | Fe/Ni | Si/S | O/Si | O/Ne | O/C | C/He | He/C | He/N | Total |
|-----------------------------|-----------|----------------|----------------|----------------|----------------|----------------|----------------|----------------|----------------|----------|
| | | 1.600 0.012 | 1.624 0.024 | 1.710 0.086 | 3.583 1.873 | 3.767 0.184 | 3.901 0.134 | 5.713 1.812 | 6.000 0.287 | 6.000 |
| $\Theta(^{27}\text{Al})$ | normal | 2.49E+00 | 4.02E-01 | 5.08E+01 | 7.83E+01 | 2.75E-01 | 2.42E-01 | 2.44E-01 | 2.44E-01 | 3.44E+01 |
| | inverted | 2.49E+00 | 3.99E-01 | 5.05E+01 | 7.84E+01 | 2.72E-01 | 2.41E-01 | 2.44E-01 | 2.44E-01 | 3.44E+01 |
| $\Delta M(^{28}\text{Si})$ | No-osci | 2.08E-03 | 6.87E-03 | 6.99E-03 | 2.74E-02 | 2.72E-05 | 2.38E-05 | 2.96E-04 | 4.61E-05 | 4.38E-02 |
| | normal | 2.08E-03 | 6.87E-03 | 6.99E-03 | 2.74E-02 | 2.72E-05 | 2.38E-05 | 2.96E-04 | 4.61E-05 | 4.38E-02 |
| | inverted | 2.08E-03 | 6.87E-03 | 6.99E-03 | 2.74E-02 | 2.72E-05 | 2.38E-05 | 2.96E-04 | 4.61E-05 | 4.38E-02 |
| $\Theta(^{28}\text{Si})$ | No-osci | 2.41E+02 | 3.97E+02 | 1.15E+02 | 2.07E+01 | 2.25E-01 | 2.29E-01 | 2.31E-01 | 2.32E-01 | 1.40E+01 |
| | normal | 2.41E+02 | 3.97E+02 | 1.15E+02 | 2.07E+01 | 2.25E-01 | 2.29E-01 | 2.31E-01 | 2.32E-01 | 1.40E+01 |
| | inverted | 2.41E+02 | 3.97E+02 | 1.15E+02 | 2.07E+01 | 2.25E-01 | 2.29E-01 | 2.31E-01 | 2.32E-01 | 1.40E+01 |
| $\Delta M(^{29}\text{Si})$ | No-osci | 1.61E-06 | 1.15E-05 | 3.16E-04 | 4.31E-03 | 2.26E-06 | 1.48E-06 | 1.56E-05 | 2.42E-06 | 4.66E-03 |
| | normal | 1.61E-06 | 1.15E-05 | 3.16E-04 | 4.31E-03 | 2.26E-06 | 1.48E-06 | 1.56E-05 | 2.42E-06 | 4.66E-03 |
| | inverted | 1.61E-06 | 1.13E-05 | 3.12E-04 | 4.30E-03 | 2.26E-06 | 1.49E-06 | 1.56E-05 | 2.42E-06 | 4.65E-03 |
| $\Theta(^{29}\text{Si})$ | No-osci | 3.53E+00 | 1.26E+01 | 9.91E+01 | 6.19E+01 | 3.54E-01 | 2.72E-01 | 2.31E-01 | 2.31E-01 | 2.84E+01 |
| | normal | 3.53E+00 | 1.26E+01 | 9.91E+01 | 6.19E+01 | 3.54E-01 | 2.71E-01 | 2.31E-01 | 2.31E-01 | 2.84E+01 |
| | inverted | 3.54E+00 | 1.24E+01 | 9.78E+01 | 6.18E+01 | 3.55E-01 | 2.72E-01 | 2.31E-01 | 2.31E-01 | 2.84E+01 |
| $\Delta M(^{30}\text{Si})$ | No-osci | 1.07E-08 | 2.87E-05 | 6.41E-04 | 2.82E-03 | 4.64E-06 | 1.68E-06 | 1.08E-05 | 1.66E-06 | 3.51E-03 |
| | normal | 1.06E-08 | 2.87E-05 | 6.41E-04 | 2.82E-03 | 4.64E-06 | 1.67E-06 | 1.08E-05 | 1.66E-06 | 3.51E-03 |
| | inverted | 1.07E-08 | 2.86E-05 | 6.36E-04 | 2.82E-03 | 4.66E-06 | 1.69E-06 | 1.08E-05 | 1.66E-06 | 3.51E-03 |
| $\Theta(^{30}\text{Si})$ | No-osci | 3.43E-02 | 4.61E+01 | 2.95E+02 | 5.94E+01 | 1.07E+00 | 4.51E-01 | 2.35E-01 | 2.33E-01 | 3.14E+01 |
| | normal | 3.42E-02 | 4.61E+01 | 2.95E+02 | 5.94E+01 | 1.07E+00 | 4.49E-01 | 2.34E-01 | 2.33E-01 | 3.14E+01 |
| | inverted | 3.43E-02 | 4.59E+01 | 2.92E+02 | 5.93E+01 | 1.07E+00 | 4.52E-01 | 2.35E-01 | 2.33E-01 | 3.13E+01 |
| $\Delta M(^{31}\text{P})$ | No-osci | 3.39E-06 | 2.87E-05 | 1.85E-04 | 1.18E-03 | 7.03E-07 | 3.58E-07 | 3.69E-06 | 5.71E-07 | 1.40E-03 |
| | normal | 3.39E-06 | 2.87E-05 | 1.85E-04 | 1.18E-03 | 7.03E-07 | 3.58E-07 | 3.69E-06 | 5.71E-07 | 1.40E-03 |
| | inverted | 3.39E-06 | 2.84E-05 | 1.84E-04 | 1.18E-03 | 7.03E-07 | 3.58E-07 | 3.69E-06 | 5.71E-07 | 1.40E-03 |
| $\Theta(^{31}\text{P})$ | No-osci | 3.93E+01 | 1.66E+02 | 3.07E+02 | 8.92E+01 | 5.82E-01 | 3.46E-01 | 2.89E-01 | 2.88E-01 | 4.51E+01 |
| | normal | 3.93E+01 | 1.66E+02 | 3.07E+02 | 8.92E+01 | 5.82E-01 | 3.46E-01 | 2.89E-01 | 2.88E-01 | 4.51E+01 |
| | inverted | 3.93E+01 | 1.64E+02 | 3.04E+02 | 8.92E+01 | 5.82E-01 | 3.46E-01 | 2.89E-01 | 2.88E-01 | 4.50E+01 |
| $\Delta M(^{32}\text{P})$ | No-osci | 2.33E-07 | 6.79E-08 | 3.28E-07 | 1.34E-05 | 4.04E-10 | 1.19E-09 | 2.22E-09 | 5.09E-12 | 1.40E-05 |
| | normal | 2.33E-07 | 6.79E-08 | 3.28E-07 | 1.34E-05 | 3.75E-10 | 1.05E-09 | 1.64E-09 | 5.60E-12 | 1.40E-05 |
| | inverted | 2.33E-07 | 6.59E-08 | 2.86E-07 | 1.33E-05 | 7.26E-10 | 1.26E-09 | 1.88E-09 | 5.91E-12 | 1.39E-05 |
| $\Theta(^{32}\text{P})$ | No-osci | 5.43E-02 | 7.90E-03 | 1.09E-02 | 2.04E-02 | 6.71E-06 | 2.32E-05 | 3.50E-06 | 5.15E-08 | 9.06E-03 |
| | normal | 5.43E-02 | 7.90E-03 | 1.09E-02 | 2.04E-02 | 6.24E-06 | 2.03E-05 | 2.58E-06 | 5.66E-08 | 9.06E-03 |
| | inverted | 5.43E-02 | 7.67E-03 | 9.53E-03 | 2.03E-02 | 1.21E-05 | 2.44E-05 | 2.96E-06 | 5.98E-08 | 9.01E-03 |
| $\Delta M(^{33}\text{P})$ | No-osci | 7.93E-11 | 1.89E-08 | 1.94E-07 | 1.22E-06 | 4.58E-11 | 2.45E-10 | 1.83E-10 | 1.33E-13 | 1.43E-06 |
| | normal | 7.93E-11 | 1.88E-08 | 1.94E-07 | 1.22E-06 | 4.31E-11 | 2.11E-10 | 1.30E-10 | 1.45E-13 | 1.43E-06 |
| | inverted | 7.93E-11 | 1.66E-08 | 1.65E-07 | 1.21E-06 | 7.26E-11 | 2.51E-10 | 1.47E-10 | 1.53E-13 | 1.39E-06 |
| $\Theta(^{33}\text{P})$ | No-osci | 2.27E-03 | 2.70E-01 | 7.92E-01 | 2.27E-01 | 9.37E-05 | 5.84E-04 | 3.53E-05 | 1.65E-07 | 1.14E-01 |
| | normal | 2.27E-03 | 2.70E-01 | 7.92E-01 | 2.27E-01 | 8.80E-05 | 5.03E-04 | 2.51E-05 | 1.81E-07 | 1.14E-01 |
| | inverted | 2.27E-03 | 2.38E-01 | 6.74E-01 | 2.26E-01 | 1.48E-04 | 5.99E-04 | 2.84E-05 | 1.90E-07 | 1.11E-01 |
| $\Delta M(^{32}\text{S})$ | No-osci | 1.70E-03 | 4.98E-03 | 1.21E-03 | 1.25E-03 | 1.32E-05 | 1.36E-05 | 1.79E-04 | 2.77E-05 | 9.37E-03 |
| | normal | 1.70E-03 | 4.98E-03 | 1.21E-03 | 1.25E-03 | 1.32E-05 | 1.36E-05 | 1.79E-04 | 2.77E-05 | 9.37E-03 |
| | inverted | 1.70E-03 | 4.98E-03 | 1.21E-03 | 1.25E-03 | 1.32E-05 | 1.36E-05 | 1.79E-04 | 2.77E-05 | 9.37E-03 |
| $\Theta(^{32}\text{S})$ | No-osci | 3.95E+02 | 5.80E+02 | 4.03E+01 | 1.90E+00 | 2.20E-01 | 2.63E-01 | 2.82E-01 | 2.81E-01 | 6.06E+00 |
| | normal | 3.95E+02 | 5.80E+02 | 4.03E+01 | 1.90E+00 | 2.20E-01 | 2.64E-01 | 2.82E-01 | 2.81E-01 | 6.06E+00 |
| | inverted | 3.95E+02 | 5.80E+02 | 4.02E+01 | 1.90E+00 | 2.20E-01 | 2.63E-01 | 2.82E-01 | 2.81E-01 | 6.06E+00 |
| $\Delta M(^{33}\text{S})$ | No-osci | 2.11E-06 | 2.86E-05 | 4.66E-05 | 4.64E-05 | 3.58E-07 | 3.09E-07 | 1.59E-06 | 2.26E-07 | 1.26E-04 |
| | normal | 2.11E-06 | 2.86E-05 | 4.66E-05 | 4.64E-05 | 3.58E-07 | 3.05E-07 | 1.56E-06 | 2.26E-07 | 1.26E-04 |
| | inverted | 2.11E-06 | 2.84E-05 | 4.66E-05 | 4.64E-05 | 3.56E-07 | 3.08E-07 | 1.57E-06 | 2.26E-07 | 1.26E-04 |
| $\Theta(^{33}\text{S})$ | No-osci | 6.02E+01 | 4.09E+02 | 1.90E+02 | 8.67E+00 | 7.32E-01 | 7.37E-01 | 3.08E-01 | 2.81E-01 | 1.00E+01 |
| | normal | 6.02E+01 | 4.09E+02 | 1.90E+02 | 8.67E+00 | 7.32E-01 | 7.26E-01 | 3.02E-01 | 2.81E-01 | 1.00E+01 |
| | inverted | 6.02E+01 | 4.06E+02 | 1.90E+02 | 8.67E+00 | 7.28E-01 | 7.35E-01 | 3.04E-01 | 2.81E-01 | 1.00E+01 |
| $\Delta M(^{34}\text{S})$ | No-osci | 6.60E-09 | 6.42E-04 | 2.67E-04 | 9.98E-05 | 9.89E-07 | 7.78E-07 | 8.49E-06 | 1.31E-06 | 1.02E-03 |
| | normal | 6.60E-09 | 6.42E-04 | 2.67E-04 | 9.98E-05 | 9.89E-07 | 7.74E-07 | 8.48E-06 | 1.31E-06 | 1.02E-03 |
| | inverted | 6.60E-09 | 6.42E-04 | 2.66E-04 | 9.97E-05 | 9.91E-07 | 7.78E-07 | 8.49E-06 | 1.31E-06 | 1.02E-03 |
| $\Theta(^{34}\text{S})$ | No-osci | 3.25E-02 | 1.58E+03 | 1.88E+02 | 3.22E+00 | 3.48E-01 | 3.19E-01 | 2.83E-01 | 2.80E-01 | 1.40E+01 |
| | normal | 3.25E-02 | 1.58E+03 | 1.88E+02 | 3.22E+00 | 3.48E-01 | 3.18E-01 | 2.82E-01 | 2.80E-01 | 1.40E+01 |
| | inverted | 3.25E-02 | 1.58E+03 | 1.87E+02 | 3.21E+00 | 3.49E-01 | 3.20E-01 | 2.83E-01 | 2.80E-01 | 1.39E+01 |
| $\Delta M(^{35}\text{S})$ | No-osci | 3.09E-09 | 2.68E-08 | 3.80E-07 | 3.44E-06 | 1.36E-10 | 5.98E-10 | 1.09E-09 | 2.87E-12 | 3.85E-06 |
| | normal | 3.09E-09 | 2.68E-08 | 3.80E-07 | 3.44E-06 | 1.30E-10 | 5.29E-10 | 8.15E-10 | 3.16E-12 | 3.85E-06 |
| | inverted | 3.09E-09 | 2.00E-08 | 3.33E-07 | 3.43E-06 | 2.07E-09 | 6.15E-10 | 9.36E-10 | 3.35E-12 | 3.79E-06 |
| $\Theta(^{35}\text{S})$ | No-osci | 6.71E-02 | 2.92E-01 | 1.18E+00 | 4.89E-01 | 2.12E-04 | 1.08E-03 | 1.60E-04 | 2.71E-06 | 2.33E-01 |
| | normal | 6.71E-02 | 2.91E-01 | 1.18E+00 | 4.89E-01 | 2.02E-04 | 9.59E-04 | 1.20E-04 | 2.99E-06 | 2.33E-01 |
| | inverted | 6.71E-02 | 2.18E-01 | 1.03E+00 | 4.87E-01 | 3.22E-04 | 1.11E-03 | 1.37E-04 | 3.16E-06 | 2.29E-01 |
| $\Delta M(^{36}\text{S})$ | No-osci | 6.03E-12 | 7.47E-10 | 1.05E-07 | 3.05E-06 | 5.13E-08 | 1.38E-08 | 4.29E-08 | 6.53E-09 | 3.27E-06 |
| | normal | 6.03E-12 | 7.47E-10 | 1.05E-07 | 3.05E-06 | 5.13E-08 | 1.37E-08 | 4.27E-08 | 6.53E-09 | 3.27E-06 |
| | inverted | 6.01E-12 | 5.87E-10 | 9.77E-08 | 3.04E-06 | 5.15E-08 | 1.39E-08 | 4.28E-08 | 6.53E-09 | 3.26E-06 |
| $\Theta(^{36}\text{S})$ | No-osci | 6.94E-03 | 4.30E-01 | 1.72E+01 | 2.29E+01 | 4.22E+00 | 1.33E+00 | 3.34E-01 | 3.27E-01 | 1.04E+01 |
| | normal | 6.94E-03 | 4.30E-01 | 1.72E+01 | 2.29E+01 | 4.22E+00 | 1.31E+00 | 3.32E-01 | 3.27E-01 | 1.04E+01 |
| | inverted | 6.92E-03 | 3.38E-01 | 1.61E+01 | 2.29E+01 | 4.23E+00 | 1.33E+00 | 3.33E-01 | 3.27E-01 | 1.04E+01 |

Continued on next page

Table 1 – Continued from previous page

| shell M(r) ΔM | hierarchy | Fe/Ni | Si/S | O/Si | O/Ne | O/C | C/He | He/C | He/N | Total |
|-----------------------------|-----------|----------------|----------------|----------------|----------------|----------------|----------------|----------------|----------------|----------|
| | | 1.600 0.012 | 1.624 0.024 | 1.710 0.086 | 3.583 1.873 | 3.767 0.184 | 3.901 0.134 | 5.713 1.812 | 6.000 0.287 | 6.000 |
| $\Delta M(^{35}\text{Cl})$ | No-osci | 3.42E-07 | 2.44E-05 | 3.24E-05 | 4.14E-05 | 5.86E-08 | 7.83E-08 | 1.14E-06 | 1.82E-07 | 1.00E-04 |
| | normal | 3.42E-07 | 2.44E-05 | 3.24E-05 | 4.14E-05 | 5.86E-08 | 7.85E-08 | 1.14E-06 | 1.82E-07 | 1.00E-04 |
| | inverted | 3.42E-07 | 2.44E-05 | 3.25E-05 | 4.15E-05 | 5.84E-08 | 7.83E-08 | 1.14E-06 | 1.82E-07 | 1.00E-04 |
| $\Theta(^{35}\text{Cl})$ | No-osci | 7.43E+00 | 2.66E+02 | 1.01E+02 | 5.89E+00 | 9.10E-02 | 1.42E-01 | 1.67E-01 | 1.72E-01 | 6.05E+00 |
| | normal | 7.43E+00 | 2.66E+02 | 1.01E+02 | 5.89E+00 | 9.10E-02 | 1.42E-01 | 1.68E-01 | 1.72E-01 | 6.05E+00 |
| | inverted | 7.42E+00 | 2.66E+02 | 1.01E+02 | 5.90E+00 | 9.07E-02 | 1.42E-01 | 1.68E-01 | 1.72E-01 | 6.05E+00 |
| $\Delta M(^{36}\text{Cl})$ | No-osci | 2.31E-08 | 7.03E-08 | 3.20E-07 | 1.31E-06 | 5.90E-09 | 5.35E-09 | 6.41E-09 | 3.47E-11 | 1.74E-06 |
| | normal | 2.31E-08 | 7.03E-08 | 3.20E-07 | 1.31E-06 | 5.90E-09 | 5.29E-09 | 5.27E-09 | 3.71E-11 | 1.74E-06 |
| | inverted | 2.31E-08 | 6.02E-08 | 3.03E-07 | 1.31E-06 | 5.90E-09 | 5.32E-09 | 5.95E-09 | 3.86E-11 | 1.71E-06 |
| $\Theta(^{36}\text{Cl})$ | No-osci | 2.44E-02 | 3.72E-02 | 4.84E-02 | 9.04E-03 | 4.45E-04 | 4.71E-04 | 4.58E-05 | 1.59E-06 | 5.11E-03 |
| | normal | 2.44E-02 | 3.72E-02 | 4.84E-02 | 9.04E-03 | 4.45E-04 | 4.66E-04 | 3.76E-05 | 1.71E-06 | 5.10E-03 |
| | inverted | 2.44E-02 | 3.18E-02 | 4.58E-02 | 9.04E-03 | 4.45E-04 | 4.69E-04 | 4.25E-05 | 1.77E-06 | 5.03E-03 |
| $\Delta M(^{37}\text{Cl})$ | No-osci | 5.15E-11 | 1.28E-07 | 2.29E-07 | 9.73E-06 | 1.68E-06 | 4.31E-07 | 4.32E-07 | 6.17E-08 | 1.27E-05 |
| | normal | 5.15E-11 | 1.28E-07 | 2.29E-07 | 9.73E-06 | 1.68E-06 | 4.30E-07 | 4.28E-07 | 6.17E-08 | 1.27E-05 |
| | inverted | 5.14E-11 | 1.05E-07 | 2.13E-07 | 9.72E-06 | 1.68E-06 | 4.31E-07 | 4.30E-07 | 6.17E-08 | 1.26E-05 |
| $\Theta(^{37}\text{Cl})$ | No-osci | 3.32E-03 | 4.12E+00 | 2.11E+00 | 4.10E+00 | 7.73E+00 | 2.32E+00 | 1.88E-01 | 1.73E-01 | 2.27E+00 |
| | normal | 3.32E-03 | 4.12E+00 | 2.11E+00 | 4.10E+00 | 7.73E+00 | 2.31E+00 | 1.86E-01 | 1.73E-01 | 2.27E+00 |
| | inverted | 3.31E-03 | 3.40E+00 | 1.96E+00 | 4.10E+00 | 7.73E+00 | 2.32E+00 | 1.87E-01 | 1.73E-01 | 2.26E+00 |
| $\Delta M(^{36}\text{Ar})$ | No-osci | 3.67E-04 | 9.60E-04 | 3.54E-05 | 1.86E-05 | 1.61E-06 | 2.37E-06 | 3.49E-05 | 5.45E-06 | 1.43E-03 |
| | normal | 3.67E-04 | 9.60E-04 | 3.54E-05 | 1.86E-05 | 1.61E-06 | 2.37E-06 | 3.49E-05 | 5.45E-06 | 1.43E-03 |
| | inverted | 3.67E-04 | 9.60E-04 | 3.55E-05 | 1.87E-05 | 1.61E-06 | 2.37E-06 | 3.49E-05 | 5.45E-06 | 1.43E-03 |
| $\Theta(^{36}\text{Ar})$ | No-osci | 3.87E+02 | 5.07E+02 | 5.34E+00 | 1.29E-01 | 1.22E-01 | 2.08E-01 | 2.49E-01 | 2.50E-01 | 4.18E+00 |
| | normal | 3.87E+02 | 5.07E+02 | 5.34E+00 | 1.29E-01 | 1.22E-01 | 2.09E-01 | 2.49E-01 | 2.50E-01 | 4.18E+00 |
| | inverted | 3.87E+02 | 5.07E+02 | 5.36E+00 | 1.29E-01 | 1.21E-01 | 2.08E-01 | 2.49E-01 | 2.50E-01 | 4.18E+00 |
| $\Delta M(^{37}\text{Ar})$ | No-osci | 1.58E-07 | 6.80E-06 | 4.23E-07 | 1.86E-07 | 6.88E-09 | 1.90E-08 | 1.03E-07 | 6.48E-10 | 7.70E-06 |
| | normal | 1.58E-07 | 6.80E-06 | 4.23E-07 | 1.86E-07 | 6.68E-09 | 1.86E-08 | 8.76E-08 | 7.11E-10 | 7.68E-06 |
| | inverted | 1.58E-07 | 6.81E-06 | 4.32E-07 | 1.87E-07 | 9.11E-09 | 1.94E-08 | 9.89E-08 | 7.50E-10 | 7.72E-06 |
| $\Theta(^{37}\text{Ar})$ | No-osci | 1.02E+01 | 2.19E+02 | 3.90E+00 | 7.83E-02 | 3.17E-02 | 1.02E-01 | 4.51E-02 | 1.82E-03 | 1.38E+00 |
| | normal | 1.02E+01 | 2.19E+02 | 3.90E+00 | 7.83E-02 | 3.08E-02 | 9.98E-02 | 3.82E-02 | 1.99E-03 | 1.38E+00 |
| | inverted | 1.02E+01 | 2.20E+02 | 3.98E+00 | 7.87E-02 | 4.20E-02 | 1.04E-01 | 4.31E-02 | 2.10E-03 | 1.38E+00 |
| $\Delta M(^{38}\text{Ar})$ | No-osci | 7.24E-09 | 8.49E-04 | 1.45E-05 | 1.88E-05 | 1.37E-06 | 7.32E-07 | 6.97E-06 | 1.08E-06 | 8.93E-04 |
| | normal | 7.24E-09 | 8.49E-04 | 1.45E-05 | 1.88E-05 | 1.37E-06 | 7.30E-07 | 6.97E-06 | 1.08E-06 | 8.93E-04 |
| | inverted | 7.24E-09 | 8.49E-04 | 1.44E-05 | 1.88E-05 | 1.37E-06 | 7.32E-07 | 6.97E-06 | 1.08E-06 | 8.93E-04 |
| $\Theta(^{38}\text{Ar})$ | No-osci | 3.97E-02 | 2.33E+03 | 1.14E+01 | 6.74E-01 | 5.36E-01 | 3.35E-01 | 2.58E-01 | 2.58E-01 | 1.36E+01 |
| | normal | 3.97E-02 | 2.33E+03 | 1.14E+01 | 6.74E-01 | 5.36E-01 | 3.34E-01 | 2.58E-01 | 2.58E-01 | 1.36E+01 |
| | inverted | 3.97E-02 | 2.33E+03 | 1.13E+01 | 6.74E-01 | 5.37E-01 | 3.35E-01 | 2.58E-01 | 2.58E-01 | 1.36E+01 |
| $\Delta M(^{39}\text{Ar})$ | No-osci | 1.60E-09 | 5.83E-08 | 1.11E-08 | 8.43E-07 | 1.02E-08 | 1.20E-08 | 1.16E-08 | 5.25E-11 | 9.48E-07 |
| | normal | 1.60E-09 | 5.83E-08 | 1.11E-08 | 8.43E-07 | 1.01E-08 | 1.15E-08 | 9.03E-09 | 5.74E-11 | 9.45E-07 |
| | inverted | 1.60E-09 | 4.19E-09 | 8.84E-09 | 8.43E-07 | 1.15E-08 | 1.22E-08 | 1.05E-08 | 6.05E-11 | 9.29E-07 |
| $\Theta(^{39}\text{Ar})$ | No-osci | 3.51E-02 | 6.37E-01 | 3.47E-02 | 1.20E-01 | 1.59E-02 | 2.18E-02 | 1.71E-03 | 4.99E-05 | 5.75E-02 |
| | normal | 3.51E-02 | 6.36E-01 | 3.47E-02 | 1.20E-01 | 1.57E-02 | 2.10E-02 | 1.33E-03 | 5.46E-05 | 5.74E-02 |
| | inverted | 3.51E-02 | 4.57E-01 | 2.76E-02 | 1.20E-01 | 1.79E-02 | 2.22E-02 | 1.55E-03 | 5.75E-05 | 5.64E-02 |
| $\Delta M(^{40}\text{Ar})$ | No-osci | 4.75E-13 | 8.05E-11 | 2.39E-09 | 3.23E-07 | 1.42E-08 | 3.72E-09 | 1.20E-08 | 1.85E-09 | 3.57E-07 |
| | normal | 4.75E-13 | 8.05E-11 | 2.39E-09 | 3.23E-07 | 1.42E-08 | 3.68E-09 | 1.20E-08 | 1.85E-09 | 3.57E-07 |
| | inverted | 4.75E-13 | 7.33E-11 | 2.29E-09 | 3.23E-07 | 1.43E-08 | 3.74E-09 | 1.20E-08 | 1.85E-09 | 3.57E-07 |
| $\Theta(^{40}\text{Ar})$ | No-osci | 1.61E-03 | 1.36E-01 | 1.16E+00 | 7.15E+00 | 3.45E+00 | 1.05E+00 | 2.75E-01 | 2.72E-01 | 3.36E+00 |
| | normal | 1.61E-03 | 1.36E-01 | 1.16E+00 | 7.15E+00 | 3.44E+00 | 1.04E+00 | 2.74E-01 | 2.72E-01 | 3.36E+00 |
| | inverted | 1.61E-03 | 1.24E-01 | 1.11E+00 | 7.15E+00 | 3.47E+00 | 1.06E+00 | 2.75E-01 | 2.72E-01 | 3.36E+00 |
| $\Delta M(^{39}\text{K})$ | No-osci | 2.38E-07 | 3.77E-05 | 1.53E-06 | 5.93E-06 | 2.31E-07 | 1.32E-07 | 1.56E-06 | 2.45E-07 | 4.76E-05 |
| | normal | 2.38E-07 | 3.77E-05 | 1.53E-06 | 5.93E-06 | 2.31E-07 | 1.33E-07 | 1.56E-06 | 2.45E-07 | 4.76E-05 |
| | inverted | 2.38E-07 | 3.77E-05 | 1.53E-06 | 5.94E-06 | 2.30E-07 | 1.32E-07 | 1.56E-06 | 2.45E-07 | 4.76E-05 |
| $\Theta(^{39}\text{K})$ | No-osci | 5.20E+00 | 4.12E+02 | 4.77E+00 | 8.48E-01 | 3.60E-01 | 2.41E-01 | 2.31E-01 | 2.33E-01 | 2.89E+00 |
| | normal | 5.20E+00 | 4.12E+02 | 4.77E+00 | 8.48E-01 | 3.61E-01 | 2.41E-01 | 2.31E-01 | 2.33E-01 | 2.89E+00 |
| | inverted | 5.20E+00 | 4.12E+02 | 4.78E+00 | 8.48E-01 | 3.59E-01 | 2.41E-01 | 2.31E-01 | 2.33E-01 | 2.89E+00 |
| $\Delta M(^{40}\text{K})$ | No-osci | 3.18E-11 | 1.45E-08 | 2.58E-08 | 4.81E-07 | 3.11E-08 | 1.26E-08 | 9.81E-09 | 9.74E-11 | 5.75E-07 |
| | normal | 3.18E-11 | 1.45E-08 | 2.58E-08 | 4.81E-07 | 3.11E-08 | 1.25E-08 | 8.05E-09 | 1.01E-10 | 5.73E-07 |
| | inverted | 3.18E-11 | 1.17E-08 | 2.49E-08 | 4.81E-07 | 3.11E-08 | 1.26E-08 | 9.03E-09 | 1.03E-10 | 5.70E-07 |
| $\Theta(^{40}\text{K})$ | No-osci | 3.95E-01 | 9.03E+01 | 4.58E+01 | 3.91E+01 | 2.76E+01 | 1.31E+01 | 8.23E-01 | 5.26E-02 | 1.98E+01 |
| | normal | 3.95E-01 | 9.03E+01 | 4.58E+01 | 3.91E+01 | 2.76E+01 | 1.29E+01 | 6.76E-01 | 5.45E-02 | 1.98E+01 |
| | inverted | 3.95E-01 | 7.30E+01 | 4.42E+01 | 3.91E+01 | 2.76E+01 | 1.30E+01 | 7.59E-01 | 5.56E-02 | 1.97E+01 |
| $\Delta M(^{41}\text{K})$ | No-osci | 5.52E-13 | 2.09E-09 | 1.77E-09 | 3.85E-07 | 3.69E-08 | 1.45E-08 | 1.18E-07 | 1.86E-08 | 5.77E-07 |
| | normal | 5.52E-13 | 2.09E-09 | 1.77E-09 | 3.85E-07 | 3.69E-08 | 1.45E-08 | 1.18E-07 | 1.86E-08 | 5.77E-07 |
| | inverted | 5.51E-13 | 1.71E-09 | 1.66E-09 | 3.85E-07 | 3.70E-08 | 1.45E-08 | 1.18E-07 | 1.86E-08 | 5.76E-07 |
| $\Theta(^{41}\text{K})$ | No-osci | 1.59E-04 | 3.01E-01 | 7.25E-02 | 7.23E-01 | 7.57E-01 | 3.48E-01 | 2.29E-01 | 2.32E-01 | 4.61E-01 |
| | normal | 1.59E-04 | 3.01E-01 | 7.25E-02 | 7.23E-01 | 7.57E-01 | 3.46E-01 | 2.30E-01 | 2.32E-01 | 4.61E-01 |
| | inverted | 1.58E-04 | 2.47E-01 | 6.83E-02 | 7.23E-01 | 7.59E-01 | 3.48E-01 | 2.29E-01 | 2.32E-01 | 4.60E-01 |
| $\Delta M(^{40}\text{Ca})$ | No-osci | 3.48E-04 | 8.16E-04 | 7.50E-07 | 1.11E-05 | 1.35E-06 | 1.71E-06 | 2.42E-05 | 3.80E-06 | 1.21E-03 |
| | normal | 3.48E-04 | 8.16E-04 | 7.50E-07 | 1.11E-05 | 1.35E-06 | 1.72E-06 | 2.42E-05 | 3.80E-06 | 1.21E-03 |

Continued on next page

Table 1 – Continued from previous page

| shell M(r) ΔM | hierarchy | Fe/Ni | Si/S | O/Si | O/Ne | O/C | C/He | He/C | He/N | Total |
|-----------------------------|-----------|----------------|----------------|----------------|----------------|----------------|----------------|----------------|----------------|----------|
| | | 1.600 0.012 | 1.624 0.024 | 1.710 0.086 | 3.583 1.873 | 3.767 0.184 | 3.901 0.134 | 5.713 1.812 | 6.000 0.287 | 6.000 |
| | inverted | 3.48E-04 | 8.16E-04 | 7.54E-07 | 1.11E-05 | 1.35E-06 | 1.71E-06 | 2.42E-05 | 3.80E-06 | 1.21E-03 |
| $\Theta(^{40}\text{Ca})$ | No-osci | 4.43E+02 | 5.20E+02 | 1.37E-01 | 9.23E-02 | 1.23E-01 | 1.82E-01 | 2.08E-01 | 2.11E-01 | 4.27E+00 |
| | normal | 4.43E+02 | 5.20E+02 | 1.37E-01 | 9.23E-02 | 1.23E-01 | 1.82E-01 | 2.08E-01 | 2.11E-01 | 4.27E+00 |
| | inverted | 4.43E+02 | 5.20E+02 | 1.37E-01 | 9.23E-02 | 1.23E-01 | 1.82E-01 | 2.08E-01 | 2.11E-01 | 4.27E+00 |
| $\Delta M(^{41}\text{Ca})$ | No-osci | 2.23E-08 | 2.08E-06 | 2.61E-08 | 3.08E-07 | 2.51E-08 | 3.13E-08 | 7.11E-08 | 3.84E-10 | 2.57E-06 |
| | normal | 2.23E-08 | 2.08E-06 | 2.61E-08 | 3.08E-07 | 2.52E-08 | 3.07E-08 | 5.93E-08 | 4.11E-10 | 2.55E-06 |
| | inverted | 2.23E-08 | 2.05E-06 | 2.62E-08 | 3.08E-07 | 2.49E-08 | 3.11E-08 | 6.58E-08 | 4.27E-10 | 2.52E-06 |
| $\Theta(^{41}\text{Ca})$ | No-osci | 6.41E+00 | 2.99E+02 | 1.07E+00 | 5.79E-01 | 5.16E-01 | 7.49E-01 | 1.38E-01 | 4.81E-03 | 2.05E+00 |
| | normal | 6.41E+00 | 2.99E+02 | 1.07E+00 | 5.79E-01 | 5.17E-01 | 7.36E-01 | 1.15E-01 | 5.14E-03 | 2.04E+00 |
| | inverted | 6.40E+00 | 2.94E+02 | 1.08E+00 | 5.79E-01 | 5.12E-01 | 7.45E-01 | 1.28E-01 | 5.34E-03 | 2.02E+00 |
| $\Delta M(^{42}\text{Ca})$ | No-osci | 7.86E-10 | 2.85E-05 | 1.44E-07 | 9.54E-07 | 7.65E-08 | 3.04E-08 | 1.90E-07 | 2.96E-08 | 2.99E-05 |
| | normal | 7.86E-10 | 2.85E-05 | 1.44E-07 | 9.54E-07 | 7.65E-08 | 3.03E-08 | 1.90E-07 | 2.96E-08 | 2.99E-05 |
| | inverted | 7.85E-10 | 2.85E-05 | 1.43E-07 | 9.54E-07 | 7.64E-08 | 3.04E-08 | 1.90E-07 | 2.96E-08 | 2.99E-05 |
| $\Theta(^{42}\text{Ca})$ | No-osci | 1.43E-01 | 2.59E+03 | 3.73E+00 | 1.13E+00 | 9.93E-01 | 4.61E-01 | 2.34E-01 | 2.34E-01 | 1.51E+01 |
| | normal | 1.43E-01 | 2.59E+03 | 3.73E+00 | 1.13E+00 | 9.93E-01 | 4.59E-01 | 2.33E-01 | 2.34E-01 | 1.51E+01 |
| | inverted | 1.43E-01 | 2.59E+03 | 3.72E+00 | 1.13E+00 | 9.91E-01 | 4.61E-01 | 2.33E-01 | 2.34E-01 | 1.51E+01 |
| $\Delta M(^{43}\text{Ca})$ | No-osci | 3.79E-12 | 4.00E-08 | 1.02E-08 | 3.31E-07 | 1.98E-08 | 6.53E-09 | 4.10E-08 | 6.34E-09 | 4.55E-07 |
| | normal | 3.78E-12 | 4.00E-08 | 1.02E-08 | 3.31E-07 | 1.98E-08 | 6.50E-09 | 4.09E-08 | 6.34E-09 | 4.55E-07 |
| | inverted | 3.78E-12 | 3.53E-08 | 9.98E-09 | 3.31E-07 | 1.99E-08 | 6.55E-09 | 4.10E-08 | 6.34E-09 | 4.50E-07 |
| $\Theta(^{43}\text{Ca})$ | No-osci | 3.20E-03 | 1.69E+01 | 1.23E+00 | 1.83E+00 | 1.20E+00 | 4.60E-01 | 2.34E-01 | 2.33E-01 | 1.07E+00 |
| | normal | 3.20E-03 | 1.69E+01 | 1.23E+00 | 1.83E+00 | 1.20E+00 | 4.58E-01 | 2.34E-01 | 2.33E-01 | 1.07E+00 |
| | inverted | 3.20E-03 | 1.49E+01 | 1.21E+00 | 1.83E+00 | 1.20E+00 | 4.61E-01 | 2.34E-01 | 2.33E-01 | 1.06E+00 |
| $\Delta M(^{44}\text{Ca})$ | No-osci | 4.28E-13 | 1.06E-08 | 1.31E-08 | 8.89E-07 | 6.90E-08 | 5.09E-08 | 6.41E-07 | 1.00E-07 | 1.77E-06 |
| | normal | 4.28E-13 | 1.06E-08 | 1.31E-08 | 8.89E-07 | 6.90E-08 | 5.09E-08 | 6.42E-07 | 1.00E-07 | 1.77E-06 |
| | inverted | 4.28E-13 | 1.05E-08 | 1.29E-08 | 8.89E-07 | 6.92E-08 | 5.09E-08 | 6.41E-07 | 1.00E-07 | 1.77E-06 |
| $\Theta(^{44}\text{Ca})$ | No-osci | 2.30E-05 | 2.85E-01 | 1.00E-01 | 3.13E-01 | 2.65E-01 | 2.28E-01 | 2.33E-01 | 2.34E-01 | 2.65E-01 |
| | normal | 2.30E-05 | 2.85E-01 | 1.00E-01 | 3.13E-01 | 2.65E-01 | 2.28E-01 | 2.33E-01 | 2.34E-01 | 2.65E-01 |
| | inverted | 2.30E-05 | 2.82E-01 | 9.89E-02 | 3.13E-01 | 2.66E-01 | 2.28E-01 | 2.33E-01 | 2.34E-01 | 2.65E-01 |
| $\Delta M(^{45}\text{Ca})$ | No-osci | 1.32E-13 | 4.93E-12 | 2.55E-10 | 1.03E-07 | 3.58E-10 | 8.60E-10 | 2.13E-09 | 7.49E-12 | 1.07E-07 |
| | normal | 1.32E-13 | 4.93E-12 | 2.55E-10 | 1.03E-07 | 3.45E-10 | 7.68E-10 | 1.61E-09 | 8.25E-12 | 1.06E-07 |
| | inverted | 1.32E-13 | 3.95E-12 | 2.42E-10 | 1.03E-07 | 5.17E-10 | 8.91E-10 | 1.87E-09 | 8.72E-12 | 1.07E-07 |
| $\Theta(^{45}\text{Ca})$ | No-osci | 2.55E-04 | 4.75E-03 | 7.02E-02 | 1.30E+00 | 4.93E-02 | 1.38E-01 | 2.77E-02 | 6.27E-04 | 5.72E-01 |
| | normal | 2.55E-04 | 4.75E-03 | 7.02E-02 | 1.30E+00 | 4.74E-02 | 1.23E-01 | 2.09E-02 | 6.91E-04 | 5.68E-01 |
| | inverted | 2.55E-04 | 3.80E-03 | 6.66E-02 | 1.30E+00 | 7.11E-02 | 1.43E-01 | 2.44E-02 | 7.31E-04 | 5.71E-01 |
| $\Delta M(^{46}\text{Ca})$ | No-osci | 1.44E-15 | 2.10E-13 | 3.51E-10 | 3.35E-08 | 9.90E-11 | 1.33E-10 | 1.28E-09 | 1.97E-10 | 3.55E-08 |
| | normal | 1.44E-15 | 2.10E-13 | 3.51E-10 | 3.35E-08 | 9.88E-11 | 1.29E-10 | 1.28E-09 | 1.97E-10 | 3.55E-08 |
| | inverted | 1.44E-15 | 1.93E-13 | 3.37E-10 | 3.34E-08 | 1.01E-10 | 1.33E-10 | 1.28E-09 | 1.97E-10 | 3.55E-08 |
| $\Theta(^{46}\text{Ca})$ | No-osci | 4.67E-05 | 3.40E-03 | 1.62E+00 | 7.09E+00 | 2.29E-01 | 3.59E-01 | 2.81E-01 | 2.78E-01 | 3.20E+00 |
| | normal | 4.67E-05 | 3.40E-03 | 1.62E+00 | 7.09E+00 | 2.29E-01 | 3.48E-01 | 2.79E-01 | 2.78E-01 | 3.20E+00 |
| | inverted | 4.67E-05 | 3.12E-03 | 1.56E+00 | 7.09E+00 | 2.34E-01 | 3.58E-01 | 2.80E-01 | 2.78E-01 | 3.20E+00 |
| $\Delta M(^{47}\text{Ca})$ | No-osci | 5.40E-19 | 5.77E-17 | 4.47E-12 | 3.70E-10 | 1.19E-13 | 9.14E-13 | 2.70E-12 | 1.00E-14 | 3.78E-10 |
| | normal | 5.40E-19 | 5.77E-17 | 4.47E-12 | 3.70E-10 | 1.07E-13 | 7.61E-13 | 2.02E-12 | 1.10E-14 | 3.77E-10 |
| | inverted | 5.39E-19 | 4.99E-17 | 4.20E-12 | 3.69E-10 | 2.55E-13 | 9.47E-13 | 2.37E-12 | 1.16E-14 | 3.77E-10 |
| $\Theta(^{47}\text{Ca})$ | No-osci | 1.86E-10 | 9.95E-09 | 2.20E-04 | 8.34E-04 | 2.92E-06 | 2.63E-05 | 6.29E-06 | 1.50E-07 | 3.62E-04 |
| | normal | 1.86E-10 | 9.94E-09 | 2.20E-04 | 8.34E-04 | 2.64E-06 | 2.19E-05 | 4.71E-06 | 1.65E-07 | 3.61E-04 |
| | inverted | 1.86E-10 | 8.60E-09 | 2.07E-04 | 8.32E-04 | 6.29E-06 | 2.72E-05 | 5.52E-06 | 1.74E-07 | 3.61E-04 |
| $\Delta M(^{48}\text{Ca})$ | No-osci | 2.37E-19 | 2.95E-18 | 1.81E-13 | 4.13E-08 | 5.56E-09 | 4.99E-09 | 6.27E-08 | 9.77E-09 | 1.24E-07 |
| | normal | 2.37E-19 | 2.95E-18 | 1.81E-13 | 4.13E-08 | 5.56E-09 | 4.99E-09 | 6.27E-08 | 9.77E-09 | 1.24E-07 |
| | inverted | 2.37E-19 | 2.70E-18 | 1.69E-13 | 4.13E-08 | 5.56E-09 | 4.99E-09 | 6.27E-08 | 9.77E-09 | 1.24E-07 |
| $\Theta(^{48}\text{Ca})$ | No-osci | 1.30E-10 | 8.11E-10 | 1.42E-05 | 1.49E-01 | 2.18E-01 | 2.29E-01 | 2.33E-01 | 2.34E-01 | 1.90E-01 |
| | normal | 1.30E-10 | 8.11E-10 | 1.42E-05 | 1.49E-01 | 2.18E-01 | 2.29E-01 | 2.33E-01 | 2.34E-01 | 1.90E-01 |
| | inverted | 1.30E-10 | 7.42E-10 | 1.33E-05 | 1.49E-01 | 2.18E-01 | 2.29E-01 | 2.33E-01 | 2.34E-01 | 1.90E-01 |
| $\Delta M(^{45}\text{Sc})$ | No-osci | 5.24E-11 | 1.14E-08 | 1.22E-08 | 1.22E-07 | 8.13E-09 | 3.73E-09 | 1.75E-08 | 2.75E-09 | 1.77E-07 |
| | normal | 5.23E-11 | 1.14E-08 | 1.22E-08 | 1.22E-07 | 8.14E-09 | 3.77E-09 | 1.76E-08 | 2.75E-09 | 1.78E-07 |
| | inverted | 5.23E-11 | 1.11E-08 | 1.22E-08 | 1.22E-07 | 7.98E-09 | 3.69E-09 | 1.75E-08 | 2.75E-09 | 1.77E-07 |
| $\Theta(^{45}\text{Sc})$ | No-osci | 1.01E-01 | 1.10E+01 | 3.37E+00 | 1.53E+00 | 1.12E+00 | 5.99E-01 | 2.28E-01 | 2.31E-01 | 9.49E-01 |
| | normal | 1.01E-01 | 1.10E+01 | 3.37E+00 | 1.53E+00 | 1.12E+00 | 6.05E-01 | 2.29E-01 | 2.31E-01 | 9.50E-01 |
| | inverted | 1.01E-01 | 1.07E+01 | 3.36E+00 | 1.53E+00 | 1.10E+00 | 5.93E-01 | 2.28E-01 | 2.31E-01 | 9.47E-01 |
| $\Delta M(^{46}\text{Sc})$ | No-osci | 1.65E-11 | 1.25E-10 | 2.09E-09 | 3.55E-08 | 2.52E-10 | 3.35E-10 | 5.36E-10 | 2.47E-12 | 3.89E-08 |
| | normal | 1.65E-11 | 1.25E-10 | 2.09E-09 | 3.55E-08 | 2.40E-10 | 3.04E-10 | 4.20E-10 | 2.72E-12 | 3.87E-08 |
| | inverted | 1.65E-11 | 1.19E-10 | 2.02E-09 | 3.55E-08 | 3.98E-10 | 3.70E-10 | 4.89E-10 | 2.88E-12 | 3.90E-08 |
| $\Theta(^{46}\text{Sc})$ | No-osci | 5.23E-03 | 1.99E-02 | 9.47E-02 | 7.38E-02 | 5.73E-03 | 8.87E-03 | 1.15E-03 | 3.41E-05 | 3.43E-02 |
| | normal | 5.23E-03 | 1.99E-02 | 9.47E-02 | 7.38E-02 | 5.45E-03 | 8.05E-03 | 9.02E-04 | 3.76E-05 | 3.42E-02 |
| | inverted | 5.23E-03 | 1.89E-02 | 9.18E-02 | 7.38E-02 | 9.05E-03 | 9.81E-03 | 1.05E-03 | 3.98E-05 | 3.44E-02 |
| $\Delta M(^{47}\text{Sc})$ | No-osci | 1.75E-14 | 1.01E-11 | 6.36E-10 | 4.05E-09 | 3.60E-12 | 1.96E-11 | 2.26E-11 | 2.56E-15 | 4.75E-09 |
| | normal | 1.75E-14 | 1.01E-11 | 6.36E-10 | 4.05E-09 | 3.16E-12 | 1.52E-11 | 1.30E-11 | 3.00E-15 | 4.73E-09 |
| | inverted | 1.75E-14 | 9.63E-12 | 6.16E-10 | 4.05E-09 | 1.08E-11 | 2.20E-11 | 1.72E-11 | 3.31E-15 | 4.73E-09 |
| | No-osci | 6.04E-06 | 1.75E-03 | 3.14E-02 | 9.14E-03 | 8.88E-05 | 5.63E-04 | 5.26E-05 | 3.84E-08 | 4.55E-03 |

Continued on next page

Table 1 – Continued from previous page

| shell M(r) ΔM | hierarchy | Fe/Ni | Si/S | O/Si | O/Ne | O/C | C/He | He/C | He/N | Total |
|-----------------------------|-------------------------------|----------------------------------|----------------------------------|----------------------------------|----------------------------------|----------------------------------|----------------------------------|----------------------------------|----------------------------------|----------------------------------|
| | | 1.600 0.012 | 1.624 0.024 | 1.710 0.086 | 3.583 1.873 | 3.767 0.184 | 3.901 0.134 | 5.713 1.812 | 6.000 0.287 | 6.000 |
| $\Theta(^{47}\text{Sc})$ | normal inverted | 6.04E-06 6.03E-06 | 1.75E-03 1.66E-03 | 3.13E-02 3.03E-02 | 9.14E-03 9.14E-03 | 7.77E-05 2.66E-04 | 4.38E-04 6.32E-04 | 3.02E-05 4.02E-05 | 4.49E-08 4.96E-08 | 4.53E-03 4.53E-03 |
| $\Delta M(^{44}\text{Ti})$ | No-osci normal inverted | 1.69E-07 1.69E-07 1.69E-07 | 3.67E-07 3.67E-07 3.67E-07 | 4.15E-10 4.15E-10 4.29E-10 | 6.40E-11 6.40E-11 6.52E-11 | 1.19E-15 1.19E-15 1.17E-15 | 4.27E-16 4.31E-16 4.23E-16 | 3.82E-16 3.88E-16 3.85E-16 | 5.11E-18 5.11E-18 5.11E-18 | 5.37E-07 5.37E-07 5.37E-07 |
| $\Theta(^{44}\text{Ti})$ | No-osci normal inverted | 9.12E+00 9.12E+00 9.12E+00 | 9.86E+00 9.86E+00 9.87E+00 | 3.19E-03 3.19E-03 3.30E-03 | 2.25E-05 2.25E-05 2.29E-05 | 4.58E-09 4.58E-09 4.50E-09 | 1.92E-09 1.93E-09 1.89E-09 | 1.39E-10 1.41E-10 1.40E-10 | 1.20E-11 1.20E-11 1.20E-11 | 8.02E-02 8.02E-02 8.02E-02 |
| $\Delta M(^{46}\text{Ti})$ | No-osci normal inverted | 1.49E-07 1.49E-07 1.49E-07 | 1.01E-05 1.01E-05 1.01E-05 | 4.41E-08 4.41E-08 4.44E-08 | 1.71E-07 1.71E-07 1.71E-07 | 1.70E-08 1.70E-08 1.69E-08 | 8.81E-09 8.86E-09 8.79E-09 | 1.00E-07 1.00E-07 1.00E-07 | 1.58E-08 1.58E-08 1.58E-08 | 1.06E-05 1.06E-05 1.06E-05 |
| $\Theta(^{46}\text{Ti})$ | No-osci normal inverted | 4.74E+01 4.74E+01 4.74E+01 | 1.60E+03 1.60E+03 1.60E+03 | 2.00E+00 2.00E+00 2.02E+00 | 3.56E-01 3.56E-01 3.56E-01 | 3.86E-01 3.86E-01 3.83E-01 | 2.33E-01 2.35E-01 2.33E-01 | 2.15E-01 2.16E-01 2.15E-01 | 2.19E-01 2.19E-01 2.19E-01 | 9.32E+00 9.32E+00 9.32E+00 |
| $\Delta M(^{47}\text{Ti})$ | No-osci normal inverted | 5.09E-10 5.08E-10 5.08E-10 | 2.56E-07 2.56E-07 2.53E-07 | 1.59E-08 1.59E-08 1.58E-08 | 1.16E-07 1.16E-07 1.16E-07 | 6.43E-09 6.43E-09 6.43E-09 | 5.45E-09 5.49E-09 5.46E-09 | 9.18E-08 9.22E-08 9.20E-08 | 1.47E-08 1.47E-08 1.47E-08 | 5.07E-07 5.08E-07 5.04E-07 |
| $\Theta(^{47}\text{Ti})$ | No-osci normal inverted | 1.75E-01 1.75E-01 1.75E-01 | 4.42E+01 4.42E+01 4.37E+01 | 7.84E-01 7.84E-01 7.79E-01 | 2.62E-01 2.62E-01 2.62E-01 | 1.58E-01 1.58E-01 1.58E-01 | 1.57E-01 1.58E-01 1.57E-01 | 2.14E-01 2.15E-01 2.14E-01 | 2.21E-01 2.21E-01 2.21E-01 | 4.86E-01 4.87E-01 4.83E-01 |
| $\Delta M(^{48}\text{Ti})$ | No-osci normal inverted | 1.10E-10 1.10E-10 1.10E-10 | 1.13E-07 1.13E-07 1.12E-07 | 3.17E-08 3.17E-08 3.16E-08 | 2.29E-07 2.29E-07 2.29E-07 | 2.11E-08 2.11E-08 2.10E-08 | 5.38E-08 5.41E-08 5.38E-08 | 9.63E-07 9.65E-07 9.64E-07 | 1.52E-07 1.52E-07 1.52E-07 | 1.56E-06 1.57E-06 1.56E-06 |
| $\Theta(^{48}\text{Ti})$ | No-osci normal inverted | 3.74E-03 3.74E-03 3.74E-03 | 1.92E+00 1.92E+00 1.91E+00 | 1.55E-01 1.55E-01 1.54E-01 | 5.10E-02 5.10E-02 5.10E-02 | 5.14E-02 5.15E-02 5.13E-02 | 1.53E-01 1.54E-01 1.53E-01 | 2.22E-01 2.23E-01 2.22E-01 | 2.26E-01 2.26E-01 2.26E-01 | 1.48E-01 1.48E-01 1.48E-01 |
| $\Delta M(^{49}\text{Ti})$ | No-osci normal inverted | 5.19E-11 5.19E-11 5.19E-11 | 3.29E-10 3.29E-10 3.28E-10 | 3.31E-09 3.31E-09 3.20E-09 | 3.52E-07 3.52E-07 3.52E-07 | 4.38E-08 4.38E-08 4.37E-08 | 2.73E-08 2.70E-08 2.72E-08 | 8.80E-08 8.54E-08 8.68E-08 | 1.16E-08 1.16E-08 1.16E-08 | 5.26E-07 5.23E-07 5.24E-07 |
| $\Theta(^{49}\text{Ti})$ | No-osci normal inverted | 2.36E-02 2.36E-02 2.36E-02 | 7.47E-02 7.47E-02 7.47E-02 | 2.15E-01 2.15E-01 2.07E-01 | 1.04E+00 1.04E+00 1.04E+00 | 1.42E+00 1.42E+00 1.42E+00 | 1.03E+00 1.02E+00 1.03E+00 | 2.70E-01 2.62E-01 2.66E-01 | 2.30E-01 2.30E-01 2.30E-01 | 6.64E-01 6.60E-01 6.62E-01 |
| $\Delta M(^{50}\text{Ti})$ | No-osci normal inverted | 2.26E-12 2.26E-12 2.25E-12 | 6.61E-11 6.61E-11 6.52E-11 | 7.19E-09 7.19E-09 7.07E-09 | 8.92E-07 8.92E-07 8.92E-07 | 6.64E-08 6.64E-08 6.66E-08 | 1.75E-08 1.74E-08 1.76E-08 | 7.55E-08 7.53E-08 7.54E-08 | 1.16E-08 1.16E-08 1.16E-08 | 1.07E-06 1.07E-06 1.07E-06 |
| $\Theta(^{50}\text{Ti})$ | No-osci normal inverted | 1.05E-03 1.05E-03 1.05E-03 | 1.54E-02 1.54E-02 1.52E-02 | 4.79E-01 4.79E-01 4.71E-01 | 2.72E+00 2.72E+00 2.72E+00 | 2.21E+00 2.21E+00 2.22E+00 | 6.81E-01 6.78E-01 6.84E-01 | 2.38E-01 2.37E-01 2.37E-01 | 2.35E-01 2.35E-01 2.35E-01 | 1.39E+00 1.39E+00 1.39E+00 |
| $\Delta M(^{48}\text{V})$ | No-osci normal inverted | 6.54E-09 6.54E-09 6.53E-09 | 2.28E-08 2.28E-08 2.30E-08 | 3.15E-10 3.15E-10 3.47E-10 | 7.72E-11 7.72E-11 8.02E-11 | 1.04E-14 1.09E-14 8.20E-15 | 5.17E-15 6.11E-15 4.53E-15 | 3.87E-14 4.67E-14 4.33E-14 | 1.01E-15 1.01E-15 1.01E-15 | 2.98E-08 2.98E-08 2.99E-08 |
| $\Theta(^{48}\text{V})$ | No-osci normal inverted | 2.23E-01 2.23E-01 2.23E-01 | 3.90E-01 3.90E-01 3.92E-01 | 1.53E-03 1.53E-03 1.69E-03 | 1.72E-05 1.72E-05 1.79E-05 | 2.53E-08 2.65E-08 2.00E-08 | 1.47E-08 1.74E-08 1.29E-08 | 8.92E-09 1.08E-08 9.98E-09 | 1.50E-09 1.50E-09 1.50E-09 | 2.82E-03 2.82E-03 2.84E-03 |
| $\Delta M(^{49}\text{V})$ | No-osci normal inverted | 3.63E-08 3.63E-08 3.63E-08 | 7.39E-08 7.39E-08 7.31E-08 | 1.20E-08 1.20E-08 1.21E-08 | 9.08E-09 9.08E-09 9.13E-09 | 4.15E-14 4.20E-14 4.12E-14 | 3.25E-14 3.36E-14 3.30E-14 | 9.23E-14 8.80E-14 9.04E-14 | 6.85E-16 6.88E-16 6.90E-16 | 1.31E-07 1.31E-07 1.31E-07 |
| $\Theta(^{49}\text{V})$ | No-osci normal inverted | 1.65E+01 1.65E+01 1.65E+01 | 1.68E+01 1.68E+01 1.66E+01 | 7.78E-01 7.78E-01 7.84E-01 | 2.70E-02 2.70E-02 2.71E-02 | 1.35E-06 1.36E-06 1.34E-06 | 1.23E-06 1.27E-06 1.25E-06 | 2.83E-07 2.70E-07 2.78E-07 | 1.35E-08 1.36E-08 1.36E-08 | 1.66E-01 1.66E-01 1.65E-01 |
| $\Delta M(^{50}\text{V})$ | No-osci normal inverted | 9.71E-09 9.71E-09 9.71E-09 | 1.76E-09 1.76E-09 1.71E-09 | 3.25E-09 3.25E-09 3.21E-09 | 9.64E-09 9.64E-09 9.66E-09 | 7.92E-13 7.94E-13 7.81E-13 | 1.62E-11 1.64E-11 1.62E-11 | 4.07E-10 4.09E-10 4.08E-10 | 6.53E-11 6.53E-11 6.53E-11 | 2.49E-08 2.49E-08 2.48E-08 |
| $\Theta(^{50}\text{V})$ | No-osci normal inverted | 8.28E+02 8.28E+02 8.28E+02 | 7.49E+01 7.49E+01 7.28E+01 | 3.96E+01 3.96E+01 3.91E+01 | 5.37E+00 5.37E+00 5.38E+00 | 4.82E-03 4.83E-03 4.75E-03 | 1.15E-01 1.16E-01 1.15E-01 | 2.34E-01 2.35E-01 2.35E-01 | 2.42E-01 2.42E-01 2.42E-01 | 5.88E+00 5.88E+00 5.87E+00 |
| $\Delta M(^{51}\text{V})$ | No-osci normal inverted | 1.40E-11 1.40E-11 1.40E-11 | 8.71E-09 8.71E-09 8.08E-09 | 1.14E-08 1.14E-08 1.13E-08 | 1.22E-07 1.22E-07 1.22E-07 | 8.08E-09 8.08E-09 7.99E-09 | 1.43E-08 1.44E-08 1.42E-08 | 1.69E-07 1.69E-07 1.69E-07 | 2.66E-08 2.66E-08 2.66E-08 | 3.60E-07 3.60E-07 3.59E-07 |
| $\Theta(^{51}\text{V})$ | No-osci normal inverted | 2.86E-03 2.86E-03 2.86E-03 | 8.91E-01 8.91E-01 8.27E-01 | 3.35E-01 3.35E-01 3.30E-01 | 1.63E-01 1.63E-01 1.63E-01 | 1.18E-01 1.18E-01 1.17E-01 | 2.43E-01 2.45E-01 2.43E-01 | 2.33E-01 2.34E-01 2.34E-01 | 2.37E-01 2.37E-01 2.37E-01 | 2.04E-01 2.05E-01 2.04E-01 |
| $\Delta M(^{50}\text{Cr})$ | No-osci normal inverted | 5.11E-05 5.11E-05 5.11E-05 | 4.48E-05 4.48E-05 4.48E-05 | 1.45E-08 1.45E-08 1.47E-08 | 3.60E-09 3.60E-09 3.61E-09 | 5.22E-10 5.22E-10 5.13E-10 | 1.28E-08 1.28E-08 1.28E-08 | 3.25E-07 3.27E-07 3.26E-07 | 5.23E-08 5.23E-08 5.23E-08 | 9.63E-05 9.63E-05 9.64E-05 |
| $\Theta(^{50}\text{Cr})$ | No-osci normal inverted | 5.36E+03 5.36E+03 5.36E+03 | 2.35E+03 2.35E+03 2.35E+03 | 2.18E-01 2.18E-01 2.20E-01 | 2.47E-03 2.47E-03 2.47E-03 | 3.91E-03 3.91E-03 3.84E-03 | 1.12E-01 1.13E-01 1.12E-01 | 2.30E-01 2.32E-01 2.31E-01 | 2.38E-01 2.38E-01 2.38E-01 | 2.81E+01 2.81E+01 2.81E+01 |

Continued on next page

Table 1 – Continued from previous page

| shell M(r) ΔM | hierarchy | Fe/Ni | Si/S | O/Si | O/Ne | O/C | C/He | He/C | He/N | Total |
|-----------------------------|-----------|----------------|----------------|----------------|----------------|----------------|----------------|----------------|----------------|----------------|
| | | 1.600 0.012 | 1.624 0.024 | 1.710 0.086 | 3.583 1.873 | 3.767 0.184 | 3.901 0.134 | 5.713 1.812 | 6.000 0.287 | 6.000 6.000 |
| $\Delta M(^{51}\text{Cr})$ | No-osci | 1.23E-07 | 1.78E-06 | 9.38E-09 | 1.66E-09 | 2.29E-11 | 1.87E-09 | 9.16E-09 | 4.84E-11 | 1.93E-06 |
| | normal | 1.23E-07 | 1.78E-06 | 9.38E-09 | 1.66E-09 | 2.23E-11 | 1.74E-09 | 7.30E-09 | 5.32E-11 | 1.93E-06 |
| | inverted | 1.23E-07 | 1.78E-06 | 9.49E-09 | 1.68E-09 | 3.06E-11 | 1.86E-09 | 8.49E-09 | 5.61E-11 | 1.92E-06 |
| $\Theta(^{51}\text{Cr})$ | No-osci | 2.52E+01 | 1.83E+02 | 2.74E-01 | 2.22E-03 | 3.35E-04 | 3.18E-02 | 1.27E-02 | 4.30E-04 | 1.10E+00 |
| | normal | 2.52E+01 | 1.83E+02 | 2.74E-01 | 2.22E-03 | 3.26E-04 | 2.97E-02 | 1.01E-02 | 4.73E-04 | 1.10E+00 |
| | inverted | 2.52E+01 | 1.82E+02 | 2.77E-01 | 2.25E-03 | 4.47E-04 | 3.18E-02 | 1.17E-02 | 4.99E-04 | 1.09E+00 |
| $\Delta M(^{52}\text{Cr})$ | No-osci | 1.26E-08 | 3.11E-05 | 1.36E-07 | 3.03E-06 | 4.04E-07 | 4.84E-07 | 6.71E-06 | 1.05E-06 | 4.30E-05 |
| | normal | 1.26E-08 | 3.11E-05 | 1.36E-07 | 3.03E-06 | 4.04E-07 | 4.85E-07 | 6.72E-06 | 1.05E-06 | 4.30E-05 |
| | inverted | 1.26E-08 | 3.11E-05 | 1.36E-07 | 3.03E-06 | 4.03E-07 | 4.84E-07 | 6.72E-06 | 1.05E-06 | 4.29E-05 |
| $\Theta(^{52}\text{Cr})$ | No-osci | 6.58E-02 | 8.11E+01 | 1.01E-01 | 1.03E-01 | 1.50E-01 | 2.10E-01 | 2.37E-01 | 2.38E-01 | 6.22E-01 |
| | normal | 6.58E-02 | 8.11E+01 | 1.01E-01 | 1.03E-01 | 1.50E-01 | 2.11E-01 | 2.37E-01 | 2.38E-01 | 6.22E-01 |
| | inverted | 6.57E-02 | 8.11E+01 | 1.01E-01 | 1.03E-01 | 1.50E-01 | 2.10E-01 | 2.37E-01 | 2.38E-01 | 6.22E-01 |
| $\Delta M(^{53}\text{Cr})$ | No-osci | 3.32E-09 | 8.00E-09 | 9.24E-09 | 8.58E-07 | 5.84E-08 | 6.33E-08 | 7.76E-07 | 1.21E-07 | 1.90E-06 |
| | normal | 3.32E-09 | 8.00E-09 | 9.24E-09 | 8.58E-07 | 5.84E-08 | 6.31E-08 | 7.76E-07 | 1.21E-07 | 1.90E-06 |
| | inverted | 3.32E-09 | 6.88E-09 | 9.05E-09 | 8.58E-07 | 5.83E-08 | 6.32E-08 | 7.75E-07 | 1.21E-07 | 1.90E-06 |
| $\Theta(^{53}\text{Cr})$ | No-osci | 1.51E-01 | 1.82E-01 | 5.99E-02 | 2.55E-01 | 1.89E-01 | 2.39E-01 | 2.38E-01 | 2.39E-01 | 2.39E-01 |
| | normal | 1.51E-01 | 1.81E-01 | 5.99E-02 | 2.55E-01 | 1.89E-01 | 2.39E-01 | 2.38E-01 | 2.39E-01 | 2.39E-01 |
| | inverted | 1.51E-01 | 1.56E-01 | 5.87E-02 | 2.54E-01 | 1.89E-01 | 2.39E-01 | 2.38E-01 | 2.39E-01 | 2.39E-01 |
| $\Delta M(^{54}\text{Cr})$ | No-osci | 2.69E-10 | 2.30E-10 | 3.37E-08 | 3.08E-06 | 2.48E-07 | 8.14E-08 | 2.25E-07 | 3.09E-08 | 3.70E-06 |
| | normal | 2.69E-10 | 2.30E-10 | 3.37E-08 | 3.08E-06 | 2.48E-07 | 8.07E-08 | 2.20E-07 | 3.09E-08 | 3.70E-06 |
| | inverted | 2.69E-10 | 2.21E-10 | 3.32E-08 | 3.08E-06 | 2.49E-07 | 8.15E-08 | 2.23E-07 | 3.09E-08 | 3.70E-06 |
| $\Theta(^{54}\text{Cr})$ | No-osci | 4.82E-02 | 2.05E-02 | 8.62E-01 | 3.60E+00 | 3.17E+00 | 1.21E+00 | 2.72E-01 | 2.40E-01 | 1.84E+00 |
| | normal | 4.82E-02 | 2.05E-02 | 8.62E-01 | 3.60E+00 | 3.17E+00 | 1.20E+00 | 2.66E-01 | 2.40E-01 | 1.84E+00 |
| | inverted | 4.81E-02 | 1.97E-02 | 8.49E-01 | 3.60E+00 | 3.18E+00 | 1.21E+00 | 2.70E-01 | 2.40E-01 | 1.84E+00 |
| $\Delta M(^{52}\text{Mn})$ | No-osci | 3.85E-07 | 1.86E-07 | 9.80E-11 | 1.03E-11 | 1.87E-13 | 9.02E-14 | 3.72E-13 | 6.75E-15 | 5.71E-07 |
| | normal | 3.84E-07 | 1.86E-07 | 9.80E-11 | 1.03E-11 | 1.89E-13 | 9.82E-14 | 4.10E-13 | 6.75E-15 | 5.71E-07 |
| | inverted | 3.84E-07 | 1.87E-07 | 1.08E-10 | 1.05E-11 | 1.69E-13 | 8.47E-14 | 3.96E-13 | 6.74E-15 | 5.71E-07 |
| $\Theta(^{52}\text{Mn})$ | No-osci | 2.01E+00 | 4.86E-01 | 7.30E-05 | 3.50E-07 | 6.97E-08 | 3.92E-08 | 1.31E-08 | 1.53E-09 | 8.27E-03 |
| | normal | 2.00E+00 | 4.86E-01 | 7.30E-05 | 3.50E-07 | 7.05E-08 | 4.27E-08 | 1.44E-08 | 1.53E-09 | 8.27E-03 |
| | inverted | 2.00E+00 | 4.87E-01 | 8.01E-05 | 3.59E-07 | 6.30E-08 | 3.68E-08 | 1.39E-08 | 1.53E-09 | 8.27E-03 |
| $\Delta M(^{53}\text{Mn})$ | No-osci | 4.53E-06 | 2.02E-05 | 2.11E-08 | 2.37E-08 | 4.03E-13 | 1.76E-12 | 7.12E-12 | 7.18E-14 | 2.48E-05 |
| | normal | 4.53E-06 | 2.02E-05 | 2.11E-08 | 2.37E-08 | 4.00E-13 | 1.78E-12 | 7.01E-12 | 7.19E-14 | 2.48E-05 |
| | inverted | 4.53E-06 | 2.02E-05 | 2.14E-08 | 2.38E-08 | 4.32E-13 | 1.77E-12 | 7.08E-12 | 7.20E-14 | 2.48E-05 |
| $\Theta(^{53}\text{Mn})$ | No-osci | 2.06E+02 | 4.59E+02 | 1.37E-01 | 7.02E-03 | 1.31E-06 | 6.65E-06 | 2.18E-06 | 1.42E-07 | 3.13E+00 |
| | normal | 2.05E+02 | 4.59E+02 | 1.37E-01 | 7.02E-03 | 1.30E-06 | 6.73E-06 | 2.15E-06 | 1.42E-07 | 3.13E+00 |
| | inverted | 2.06E+02 | 4.59E+02 | 1.39E-01 | 7.05E-03 | 1.40E-06 | 6.68E-06 | 2.17E-06 | 1.42E-07 | 3.13E+00 |
| $\Delta M(^{54}\text{Mn})$ | No-osci | 1.46E-06 | 1.50E-07 | 1.75E-08 | 1.86E-08 | 8.40E-13 | 1.28E-12 | 4.26E-12 | 5.66E-14 | 1.64E-06 |
| | normal | 1.46E-06 | 1.50E-07 | 1.75E-08 | 1.86E-08 | 8.42E-13 | 1.29E-12 | 4.29E-12 | 5.65E-14 | 1.64E-06 |
| | inverted | 1.46E-06 | 1.46E-07 | 1.75E-08 | 1.87E-08 | 8.22E-13 | 1.28E-12 | 4.28E-12 | 5.65E-14 | 1.64E-06 |
| $\Theta(^{54}\text{Mn})$ | No-osci | 2.61E+02 | 1.34E+01 | 4.47E-01 | 2.17E-02 | 1.07E-05 | 1.91E-05 | 5.15E-06 | 4.40E-07 | 8.16E-01 |
| | normal | 2.61E+02 | 1.34E+01 | 4.47E-01 | 2.17E-02 | 1.08E-05 | 1.92E-05 | 5.18E-06 | 4.39E-07 | 8.16E-01 |
| | inverted | 2.61E+02 | 1.31E+01 | 4.48E-01 | 2.18E-02 | 1.05E-05 | 1.90E-05 | 5.17E-06 | 4.39E-07 | 8.14E-01 |
| $\Delta M(^{55}\text{Mn})$ | No-osci | 1.80E-09 | 2.93E-08 | 4.21E-08 | 2.67E-06 | 4.98E-07 | 5.80E-07 | 5.94E-06 | 9.37E-07 | 1.07E-05 |
| | normal | 1.80E-09 | 2.93E-08 | 4.21E-08 | 2.67E-06 | 4.98E-07 | 5.85E-07 | 5.97E-06 | 9.37E-07 | 1.07E-05 |
| | inverted | 1.80E-09 | 2.76E-08 | 4.16E-08 | 2.67E-06 | 4.92E-07 | 5.78E-07 | 5.95E-06 | 9.37E-07 | 1.07E-05 |
| $\Theta(^{55}\text{Mn})$ | No-osci | 1.06E-02 | 8.63E-02 | 3.54E-02 | 1.03E-01 | 2.09E-01 | 2.85E-01 | 2.36E-01 | 2.40E-01 | 1.75E-01 |
| | normal | 1.06E-02 | 8.63E-02 | 3.54E-02 | 1.03E-01 | 2.09E-01 | 2.87E-01 | 2.37E-01 | 2.40E-01 | 1.75E-01 |
| | inverted | 1.06E-02 | 8.10E-02 | 3.50E-02 | 1.03E-01 | 2.07E-01 | 2.83E-01 | 2.37E-01 | 2.40E-01 | 1.75E-01 |
| $\Delta M(^{54}\text{Fe})$ | No-osci | 5.59E-03 | 2.97E-03 | 8.10E-08 | 9.31E-07 | 2.40E-07 | 1.54E-06 | 3.16E-05 | 5.02E-06 | 8.60E-03 |
| | normal | 5.59E-03 | 2.97E-03 | 8.10E-08 | 9.31E-07 | 2.40E-07 | 1.55E-06 | 3.18E-05 | 5.02E-06 | 8.60E-03 |
| | inverted | 5.59E-03 | 2.97E-03 | 8.23E-08 | 9.31E-07 | 2.37E-07 | 1.54E-06 | 3.17E-05 | 5.02E-06 | 8.60E-03 |
| $\Theta(^{54}\text{Fe})$ | No-osci | 6.22E+03 | 1.65E+03 | 1.29E-02 | 6.77E-03 | 1.91E-02 | 1.43E-01 | 2.38E-01 | 2.43E-01 | 2.66E+01 |
| | normal | 6.22E+03 | 1.65E+03 | 1.29E-02 | 6.77E-03 | 1.91E-02 | 1.44E-01 | 2.39E-01 | 2.43E-01 | 2.66E+01 |
| | inverted | 6.22E+03 | 1.65E+03 | 1.31E-02 | 6.77E-03 | 1.89E-02 | 1.43E-01 | 2.38E-01 | 2.43E-01 | 2.66E+01 |
| $\Delta M(^{55}\text{Fe})$ | No-osci | 5.93E-06 | 1.09E-04 | 9.01E-08 | 3.90E-07 | 1.39E-08 | 2.33E-07 | 5.63E-07 | 2.86E-09 | 1.17E-04 |
| | normal | 5.93E-06 | 1.09E-04 | 9.01E-08 | 3.90E-07 | 1.38E-08 | 2.23E-07 | 4.49E-07 | 3.12E-09 | 1.16E-04 |
| | inverted | 5.93E-06 | 1.09E-04 | 9.11E-08 | 3.90E-07 | 1.60E-08 | 2.32E-07 | 5.18E-07 | 3.27E-09 | 1.16E-04 |
| $\Theta(^{55}\text{Fe})$ | No-osci | 3.49E+01 | 3.21E+02 | 7.57E-02 | 1.50E-02 | 5.85E-03 | 1.14E-01 | 2.24E-02 | 7.31E-04 | 1.90E+00 |
| | normal | 3.49E+01 | 3.21E+02 | 7.57E-02 | 1.50E-02 | 5.78E-03 | 1.09E-01 | 1.79E-02 | 7.97E-04 | 1.90E+00 |
| | inverted | 3.49E+01 | 3.20E+02 | 7.66E-02 | 1.50E-02 | 6.71E-03 | 1.14E-01 | 2.06E-02 | 8.37E-04 | 1.90E+00 |
| $\Delta M(^{56}\text{Fe})$ | No-osci | 2.40E-07 | 3.26E-04 | 6.56E-06 | 1.86E-04 | 2.67E-05 | 3.64E-05 | 5.27E-04 | 8.23E-05 | 1.19E-03 |
| | normal | 2.40E-07 | 3.26E-04 | 6.56E-06 | 1.86E-04 | 2.67E-05 | 3.65E-05 | 5.27E-04 | 8.23E-05 | 1.19E-03 |
| | inverted | 2.40E-07 | 3.26E-04 | 6.58E-06 | 1.86E-04 | 2.66E-05 | 3.64E-05 | 5.27E-04 | 8.23E-05 | 1.19E-03 |
| $\Theta(^{56}\text{Fe})$ | No-osci | 1.65E-02 | 1.12E+01 | 6.42E-02 | 8.34E-02 | 1.31E-01 | 2.08E-01 | 2.44E-01 | 2.45E-01 | 2.27E-01 |
| | normal | 1.65E-02 | 1.12E+01 | 6.42E-02 | 8.34E-02 | 1.31E-01 | 2.08E-01 | 2.44E-01 | 2.45E-01 | 2.27E-01 |
| | inverted | 1.64E-02 | 1.12E+01 | 6.44E-02 | 8.34E-02 | 1.30E-01 | 2.08E-01 | 2.44E-01 | 2.45E-01 | 2.27E-01 |
| $\Delta M(^{57}\text{Fe})$ | No-osci | 5.64E-10 | 5.23E-08 | 7.20E-07 | 7.08E-05 | 7.04E-06 | 4.46E-06 | 1.50E-05 | 2.02E-06 | 1.00E-04 |
| | normal | 5.64E-10 | 5.23E-08 | 7.20E-07 | 7.08E-05 | 7.04E-06 | 4.40E-06 | 1.46E-05 | 2.02E-06 | 9.96E-05 |

Continued on next page

Table 1 – Continued from previous page

| shell M(r) ΔM | hierarchy | Fe/Ni | Si/S | O/Si | O/Ne | O/C | C/He | He/C | He/N | Total |
|-----------------------------|-----------|----------------|----------------|----------------|----------------|----------------|----------------|----------------|----------------|----------|
| | | 1.600 0.012 | 1.624 0.024 | 1.710 0.086 | 3.583 1.873 | 3.767 0.184 | 3.901 0.134 | 5.713 1.812 | 6.000 0.287 | 6.000 |
| | inverted | 5.63E-10 | 4.33E-08 | 7.14E-07 | 7.08E-05 | 7.02E-06 | 4.45E-06 | 1.48E-05 | 2.02E-06 | 9.98E-05 |
| $\Theta(^{57}\text{Fe})$ | No-osci | 1.64E-03 | 7.60E-02 | 2.99E-01 | 1.34E+00 | 1.46E+00 | 1.08E+00 | 2.95E-01 | 2.55E-01 | 8.08E-01 |
| | normal | 1.64E-03 | 7.60E-02 | 2.99E-01 | 1.34E+00 | 1.46E+00 | 1.07E+00 | 2.87E-01 | 2.55E-01 | 8.04E-01 |
| | inverted | 1.64E-03 | 6.30E-02 | 2.97E-01 | 1.34E+00 | 1.46E+00 | 1.08E+00 | 2.90E-01 | 2.55E-01 | 8.06E-01 |
| $\Delta M(^{58}\text{Fe})$ | No-osci | 2.60E-11 | 6.79E-10 | 5.25E-06 | 1.93E-04 | 1.49E-05 | 3.32E-06 | 2.05E-06 | 2.62E-07 | 2.19E-04 |
| | normal | 2.60E-11 | 6.79E-10 | 5.25E-06 | 1.93E-04 | 1.49E-05 | 3.29E-06 | 1.97E-06 | 2.62E-07 | 2.19E-04 |
| | inverted | 2.60E-11 | 6.58E-10 | 5.21E-06 | 1.93E-04 | 1.49E-05 | 3.33E-06 | 2.01E-06 | 2.62E-07 | 2.19E-04 |
| $\Theta(^{58}\text{Fe})$ | No-osci | 5.60E-04 | 7.31E-03 | 1.61E+01 | 2.72E+01 | 2.29E+01 | 5.94E+00 | 2.98E-01 | 2.45E-01 | 1.31E+01 |
| | normal | 5.60E-04 | 7.31E-03 | 1.61E+01 | 2.72E+01 | 2.29E+01 | 5.89E+00 | 2.86E-01 | 2.45E-01 | 1.31E+01 |
| | inverted | 5.59E-04 | 7.08E-03 | 1.60E+01 | 2.72E+01 | 2.29E+01 | 5.97E+00 | 2.92E-01 | 2.45E-01 | 1.31E+01 |
| $\Delta M(^{59}\text{Fe})$ | No-osci | 1.71E-14 | 1.86E-13 | 2.29E-08 | 1.56E-05 | 7.72E-08 | 3.79E-08 | 1.17E-08 | 3.58E-11 | 1.57E-05 |
| | normal | 1.71E-14 | 1.86E-13 | 2.29E-08 | 1.56E-05 | 7.30E-08 | 3.37E-08 | 8.44E-09 | 3.95E-11 | 1.57E-05 |
| | inverted | 1.71E-14 | 1.57E-13 | 2.02E-08 | 1.56E-05 | 1.28E-07 | 4.66E-08 | 1.00E-08 | 4.18E-11 | 1.58E-05 |
| $\Theta(^{59}\text{Fe})$ | No-osci | 3.69E-07 | 2.00E-06 | 7.04E-02 | 2.19E+00 | 1.19E-01 | 6.79E-02 | 1.70E-03 | 3.35E-05 | 9.41E-01 |
| | normal | 3.69E-07 | 2.00E-06 | 7.04E-02 | 2.19E+00 | 1.12E-01 | 6.05E-02 | 1.23E-03 | 3.69E-05 | 9.40E-01 |
| | inverted | 3.68E-07 | 1.69E-06 | 6.22E-02 | 2.19E+00 | 1.96E-01 | 8.36E-02 | 1.45E-03 | 3.91E-05 | 9.44E-01 |
| $\Delta M(^{60}\text{Fe})$ | No-osci | 2.84E-19 | 2.05E-17 | 3.80E-08 | 4.85E-06 | 3.20E-09 | 1.52E-09 | 1.63E-10 | 8.04E-15 | 4.90E-06 |
| | normal | 2.84E-19 | 2.05E-17 | 3.80E-08 | 4.85E-06 | 3.16E-09 | 1.40E-09 | 9.02E-11 | 9.71E-15 | 4.90E-06 |
| | inverted | 2.83E-19 | 1.31E-17 | 3.71E-08 | 4.85E-06 | 3.84E-09 | 1.67E-09 | 1.18E-10 | 1.09E-14 | 4.90E-06 |
| $\Theta(^{60}\text{Fe})$ | No-osci | 1.09E-12 | 3.96E-11 | 2.09E-02 | 1.22E-01 | 8.80E-04 | 4.89E-04 | 4.24E-06 | 1.35E-09 | 5.24E-02 |
| | normal | 1.09E-12 | 3.95E-11 | 2.09E-02 | 1.22E-01 | 8.70E-04 | 4.51E-04 | 2.35E-06 | 1.63E-09 | 5.24E-02 |
| | inverted | 1.09E-12 | 2.53E-11 | 2.04E-02 | 1.22E-01 | 1.06E-03 | 5.36E-04 | 3.06E-06 | 1.83E-09 | 5.24E-02 |
| $\Delta M(^{56}\text{Co})$ | No-osci | 3.89E-06 | 8.95E-07 | 2.84E-10 | 2.00E-09 | 4.92E-11 | 1.31E-11 | 8.00E-11 | 2.59E-12 | 4.79E-06 |
| | normal | 3.89E-06 | 8.95E-07 | 2.84E-10 | 2.00E-09 | 5.12E-11 | 1.53E-11 | 1.01E-10 | 2.59E-12 | 4.79E-06 |
| | inverted | 3.89E-06 | 8.96E-07 | 3.08E-10 | 2.00E-09 | 3.53E-11 | 1.06E-11 | 9.13E-11 | 2.58E-12 | 4.79E-06 |
| $\Theta(^{56}\text{Co})$ | No-osci | 2.67E-01 | 3.06E-02 | 2.77E-06 | 8.96E-07 | 2.41E-07 | 7.48E-08 | 3.70E-08 | 7.72E-09 | 9.11E-04 |
| | normal | 2.67E-01 | 3.06E-02 | 2.77E-06 | 8.96E-07 | 2.50E-07 | 8.76E-08 | 4.68E-08 | 7.70E-09 | 9.11E-04 |
| | inverted | 2.66E-01 | 3.07E-02 | 3.02E-06 | 8.94E-07 | 1.73E-07 | 6.07E-08 | 4.22E-08 | 7.69E-09 | 9.11E-04 |
| $\Delta M(^{57}\text{Co})$ | No-osci | 1.14E-06 | 1.58E-05 | 3.20E-07 | 4.22E-07 | 1.00E-11 | 6.16E-12 | 1.20E-11 | 8.28E-14 | 1.77E-05 |
| | normal | 1.14E-06 | 1.58E-05 | 3.20E-07 | 4.22E-07 | 9.98E-12 | 6.14E-12 | 1.11E-11 | 8.31E-14 | 1.77E-05 |
| | inverted | 1.13E-06 | 1.58E-05 | 3.28E-07 | 4.25E-07 | 1.04E-11 | 6.25E-12 | 1.15E-11 | 8.33E-14 | 1.77E-05 |
| $\Theta(^{57}\text{Co})$ | No-osci | 3.30E+00 | 2.30E+01 | 1.33E-01 | 8.01E-03 | 2.08E-06 | 1.49E-06 | 2.35E-07 | 1.05E-08 | 1.43E-01 |
| | normal | 3.30E+00 | 2.30E+01 | 1.33E-01 | 8.01E-03 | 2.07E-06 | 1.49E-06 | 2.17E-07 | 1.05E-08 | 1.43E-01 |
| | inverted | 3.30E+00 | 2.30E+01 | 1.36E-01 | 8.07E-03 | 2.16E-06 | 1.51E-06 | 2.26E-07 | 1.05E-08 | 1.43E-01 |
| $\Delta M(^{58}\text{Co})$ | No-osci | 1.34E-07 | 4.16E-08 | 2.18E-07 | 2.19E-07 | 1.34E-11 | 2.76E-12 | 2.89E-12 | 3.85E-14 | 6.13E-07 |
| | normal | 1.34E-07 | 4.16E-08 | 2.18E-07 | 2.19E-07 | 1.35E-11 | 2.78E-12 | 2.90E-12 | 3.85E-14 | 6.13E-07 |
| | inverted | 1.34E-07 | 3.89E-08 | 2.22E-07 | 2.20E-07 | 1.27E-11 | 2.68E-12 | 2.89E-12 | 3.85E-14 | 6.15E-07 |
| $\Theta(^{58}\text{Co})$ | No-osci | 2.88E+00 | 4.47E-01 | 6.71E-01 | 3.08E-02 | 2.06E-05 | 4.95E-06 | 4.20E-07 | 3.60E-08 | 3.66E-02 |
| | normal | 2.88E+00 | 4.47E-01 | 6.71E-01 | 3.08E-02 | 2.07E-05 | 4.98E-06 | 4.22E-07 | 3.60E-08 | 3.66E-02 |
| | inverted | 2.88E+00 | 4.19E-01 | 6.84E-01 | 3.10E-02 | 1.95E-05 | 4.81E-06 | 4.20E-07 | 3.60E-08 | 3.68E-02 |
| $\Delta M(^{59}\text{Co})$ | No-osci | 1.57E-10 | 1.01E-08 | 4.27E-06 | 6.52E-05 | 3.26E-06 | 5.66E-07 | 1.49E-06 | 2.38E-07 | 7.51E-05 |
| | normal | 1.57E-10 | 1.01E-08 | 4.27E-06 | 6.52E-05 | 3.26E-06 | 5.67E-07 | 1.50E-06 | 2.38E-07 | 7.51E-05 |
| | inverted | 1.57E-10 | 9.63E-09 | 4.27E-06 | 6.52E-05 | 3.22E-06 | 5.61E-07 | 1.49E-06 | 2.38E-07 | 7.50E-05 |
| $\Theta(^{59}\text{Co})$ | No-osci | 3.38E-03 | 1.09E-01 | 1.31E+01 | 9.17E+00 | 5.01E+00 | 1.02E+00 | 2.17E-01 | 2.22E-01 | 4.48E+00 |
| | normal | 3.38E-03 | 1.09E-01 | 1.31E+01 | 9.17E+00 | 5.01E+00 | 1.02E+00 | 2.18E-01 | 2.22E-01 | 4.49E+00 |
| | inverted | 3.37E-03 | 1.04E-01 | 1.31E+01 | 9.17E+00 | 4.95E+00 | 1.01E+00 | 2.17E-01 | 2.22E-01 | 4.48E+00 |
| $\Delta M(^{60}\text{Co})$ | No-osci | 1.45E-11 | 1.72E-10 | 2.57E-07 | 2.90E-06 | 5.45E-08 | 1.57E-08 | 2.81E-08 | 1.40E-10 | 3.26E-06 |
| | normal | 1.45E-11 | 1.72E-10 | 2.57E-07 | 2.90E-06 | 5.16E-08 | 1.43E-08 | 2.20E-08 | 1.55E-10 | 3.25E-06 |
| | inverted | 1.45E-11 | 1.72E-10 | 2.53E-07 | 2.92E-06 | 8.99E-08 | 2.05E-08 | 2.58E-08 | 1.63E-10 | 3.31E-06 |
| $\Theta(^{60}\text{Co})$ | No-osci | 5.58E-05 | 3.32E-04 | 1.42E-01 | 7.32E-02 | 1.50E-02 | 5.06E-03 | 7.30E-04 | 2.35E-05 | 3.49E-02 |
| | normal | 5.58E-05 | 3.32E-04 | 1.42E-01 | 7.31E-02 | 1.42E-02 | 4.58E-03 | 5.74E-04 | 2.59E-05 | 3.48E-02 |
| | inverted | 5.58E-05 | 3.31E-04 | 1.39E-01 | 7.35E-02 | 2.48E-02 | 6.58E-03 | 6.72E-04 | 2.74E-05 | 3.54E-02 |
| $\Delta M(^{56}\text{Ni})$ | No-osci | 1.21E-03 | 7.68E-07 | 5.45E-13 | 3.00E-13 | 1.80E-17 | 9.46E-18 | 9.29E-18 | 1.18E-20 | 1.21E-03 |
| | normal | 1.21E-03 | 7.68E-07 | 5.45E-13 | 3.00E-13 | 1.84E-17 | 1.03E-17 | 1.13E-17 | 1.18E-20 | 1.21E-03 |
| | inverted | 1.21E-03 | 7.69E-07 | 5.66E-13 | 3.05E-13 | 1.42E-17 | 8.60E-18 | 1.03E-17 | 1.18E-20 | 1.21E-03 |
| $\Theta(^{56}\text{Ni})$ | No-osci | 8.25E+01 | 2.63E-02 | 5.33E-09 | 1.34E-10 | 8.80E-14 | 5.40E-14 | 4.30E-15 | 3.51E-17 | 2.29E-01 |
| | normal | 8.25E+01 | 2.63E-02 | 5.33E-09 | 1.34E-10 | 9.00E-14 | 5.86E-14 | 5.23E-15 | 3.51E-17 | 2.29E-01 |
| | inverted | 8.25E+01 | 2.63E-02 | 5.54E-09 | 1.36E-10 | 6.94E-14 | 4.91E-14 | 4.78E-15 | 3.51E-17 | 2.29E-01 |
| $\Delta M(^{57}\text{Ni})$ | No-osci | 7.88E-05 | 9.38E-07 | 6.02E-12 | 3.25E-12 | 1.17E-13 | 1.62E-13 | 1.62E-12 | 4.29E-14 | 7.98E-05 |
| | normal | 7.88E-05 | 9.38E-07 | 6.02E-12 | 3.25E-12 | 1.20E-13 | 1.94E-13 | 1.96E-12 | 4.28E-14 | 7.98E-05 |
| | inverted | 7.88E-05 | 9.42E-07 | 6.58E-12 | 3.27E-12 | 9.12E-14 | 1.45E-13 | 1.81E-12 | 4.28E-14 | 7.98E-05 |
| $\Theta(^{57}\text{Ni})$ | No-osci | 2.29E+02 | 1.36E+00 | 2.50E-06 | 6.17E-08 | 2.42E-08 | 3.94E-08 | 3.18E-08 | 5.42E-09 | 6.44E-01 |
| | normal | 2.29E+02 | 1.36E+00 | 2.50E-06 | 6.17E-08 | 2.49E-08 | 4.70E-08 | 3.85E-08 | 5.41E-09 | 6.44E-01 |
| | inverted | 2.29E+02 | 1.37E+00 | 2.73E-06 | 6.22E-08 | 1.89E-08 | 3.51E-08 | 3.56E-08 | 5.41E-09 | 6.44E-01 |
| $\Delta M(^{58}\text{Ni})$ | No-osci | 4.85E-04 | 2.08E-04 | 1.85E-07 | 4.05E-07 | 1.49E-07 | 1.04E-06 | 2.20E-05 | 3.49E-06 | 7.21E-04 |
| | normal | 4.85E-04 | 2.08E-04 | 1.85E-07 | 4.05E-07 | 1.49E-07 | 1.05E-06 | 2.21E-05 | 3.49E-06 | 7.21E-04 |
| | inverted | 4.85E-04 | 2.08E-04 | 1.89E-07 | 4.05E-07 | 1.47E-07 | 1.04E-06 | 2.21E-05 | 3.49E-06 | 7.21E-04 |
| | No-osci | 7.46E+02 | 1.60E+02 | 4.06E-02 | 4.08E-03 | 1.64E-02 | 1.34E-01 | 2.29E-01 | 2.34E-01 | 3.08E+00 |

Continued on next page

Table 1 – Continued from previous page

| shell M(r) ΔM | hierarchy | Fe/Ni | Si/S | O/Si | O/Ne | O/C | C/He | He/C | He/N | Total |
|-----------------------------|-------------------------------|----------------------------------|----------------------------------|----------------------------------|----------------------------------|----------------------------------|----------------------------------|----------------------------------|----------------------------------|----------------------------------|
| | | 1.600 0.012 | 1.624 0.024 | 1.710 0.086 | 3.583 1.873 | 3.767 0.184 | 3.901 0.134 | 5.713 1.812 | 6.000 0.287 | 6.000 |
| $\Theta(^{58}\text{Ni})$ | normal inverted | 7.46E+02 7.46E+02 | 1.60E+02 1.60E+02 | 4.06E-02 4.15E-02 | 4.08E-03 4.08E-03 | 1.64E-02 1.62E-02 | 1.35E-01 1.34E-01 | 2.30E-01 2.29E-01 | 2.34E-01 2.34E-01 | 3.08E+00 3.08E+00 |
| $\Delta M(^{59}\text{Ni})$ | No-osci normal inverted | 3.26E-07 3.26E-07 3.26E-07 | 3.02E-06 3.02E-06 3.00E-06 | 4.80E-07 4.80E-07 4.92E-07 | 2.11E-07 2.11E-07 2.11E-07 | 6.83E-08 6.83E-08 6.75E-08 | 2.62E-07 2.57E-07 2.60E-07 | 3.58E-07 2.91E-07 3.24E-07 | 1.64E-09 1.74E-09 1.80E-09 | 4.73E-06 4.66E-06 4.68E-06 |
| $\Theta(^{59}\text{Ni})$ | No-osci normal inverted | 7.02E+00 7.02E+00 7.02E+00 | 3.25E+01 3.25E+01 3.22E+01 | 1.48E+00 1.48E+00 1.51E+00 | 2.96E-02 2.96E-02 2.97E-02 | 1.05E-01 1.05E-01 1.04E-01 | 4.69E-01 4.60E-01 4.66E-01 | 5.20E-02 4.22E-02 4.71E-02 | 1.53E-03 1.63E-03 1.68E-03 | 2.82E-01 2.78E-01 2.80E-01 |
| $\Delta M(^{60}\text{Ni})$ | No-osci normal inverted | 7.07E-08 7.07E-08 7.07E-08 | 1.20E-05 1.20E-05 1.20E-05 | 6.05E-06 6.05E-06 6.09E-06 | 2.58E-05 2.58E-05 2.58E-05 | 2.62E-06 2.62E-06 2.60E-06 | 9.58E-07 9.59E-07 9.56E-07 | 8.73E-06 8.75E-06 8.74E-06 | 1.38E-06 1.38E-06 1.38E-06 | 5.76E-05 5.76E-05 5.76E-05 |
| $\Theta(^{60}\text{Ni})$ | No-osci normal inverted | 2.73E-01 2.73E-01 2.73E-01 | 2.30E+01 2.30E+01 2.30E+01 | 3.33E+00 3.33E+00 3.35E+00 | 6.50E-01 6.50E-01 6.50E-01 | 7.22E-01 7.22E-01 7.15E-01 | 3.08E-01 3.08E-01 3.07E-01 | 2.27E-01 2.28E-01 2.27E-01 | 2.32E-01 2.32E-01 2.32E-01 | 6.16E-01 6.17E-01 6.16E-01 |
| $\Delta M(^{61}\text{Ni})$ | No-osci normal inverted | 7.83E-12 7.83E-12 7.81E-12 | 5.58E-09 5.58E-09 4.56E-09 | 6.97E-07 6.97E-07 6.83E-07 | 1.67E-05 1.67E-05 1.67E-05 | 9.70E-07 9.69E-07 9.74E-07 | 2.85E-07 2.82E-07 2.85E-07 | 5.37E-07 5.10E-07 5.25E-07 | 6.15E-08 6.16E-08 6.16E-08 | 1.93E-05 1.93E-05 1.93E-05 |
| $\Theta(^{61}\text{Ni})$ | No-osci normal inverted | 6.85E-04 6.85E-04 6.83E-04 | 2.44E-01 2.44E-01 1.99E-01 | 8.71E+00 8.71E+00 8.54E+00 | 9.58E+00 9.58E+00 9.57E+00 | 6.06E+00 6.06E+00 6.08E+00 | 2.08E+00 2.06E+00 2.08E+00 | 3.17E-01 3.01E-01 3.10E-01 | 2.34E-01 2.34E-01 2.34E-01 | 4.69E+00 4.68E+00 4.68E+00 |
| $\Delta M(^{62}\text{Ni})$ | No-osci normal inverted | 4.35E-14 4.33E-14 4.34E-14 | 9.41E-10 9.41E-10 9.37E-10 | 3.57E-06 3.57E-06 3.55E-06 | 4.67E-05 4.67E-05 4.67E-05 | 2.14E-06 2.14E-06 2.16E-06 | 4.42E-07 4.40E-07 4.45E-07 | 1.27E-06 1.27E-06 1.27E-06 | 1.96E-07 1.96E-07 1.96E-07 | 5.43E-05 5.43E-05 5.43E-05 |
| $\Theta(^{62}\text{Ni})$ | No-osci normal inverted | 1.17E-06 1.17E-06 1.17E-06 | 1.27E-02 1.27E-02 1.27E-02 | 1.38E+01 1.38E+01 1.37E+01 | 8.25E+00 8.25E+00 8.25E+00 | 4.14E+00 4.13E+00 4.16E+00 | 9.96E-01 9.91E-01 1.00E+00 | 2.32E-01 2.32E-01 2.32E-01 | 2.31E-01 2.31E-01 2.31E-01 | 4.08E+00 4.08E+00 4.08E+00 |
| $\Delta M(^{63}\text{Ni})$ | No-osci normal inverted | 5.78E-19 5.78E-19 5.78E-19 | 2.05E-13 2.05E-13 1.47E-13 | 4.53E-08 4.53E-08 4.28E-08 | 9.31E-06 9.31E-06 9.31E-06 | 5.94E-08 5.87E-08 6.79E-08 | 1.51E-08 1.45E-08 1.64E-08 | 9.42E-09 7.32E-09 8.54E-09 | 4.36E-11 4.79E-11 5.05E-11 | 9.44E-06 9.44E-06 9.44E-06 |
| $\Theta(^{63}\text{Ni})$ | No-osci normal inverted | 7.32E-11 7.32E-11 7.31E-11 | 1.30E-05 1.30E-05 9.29E-06 | 8.18E-01 8.18E-01 7.74E-01 | 7.70E+00 7.70E+00 7.70E+00 | 5.37E-01 5.31E-01 6.14E-01 | 1.60E-01 1.53E-01 1.73E-01 | 8.06E-03 6.26E-03 7.31E-03 | 2.40E-04 2.63E-04 2.78E-04 | 3.32E+00 3.32E+00 3.32E+00 |
| $\Delta M(^{64}\text{Ni})$ | No-osci normal inverted | 2.40E-20 2.39E-20 2.40E-20 | 6.74E-15 6.74E-15 6.71E-15 | 3.52E-07 3.52E-07 3.48E-07 | 7.11E-06 7.11E-06 7.11E-06 | 2.11E-07 2.11E-07 2.11E-07 | 5.11E-08 5.10E-08 5.11E-08 | 3.30E-07 3.29E-07 3.30E-07 | 5.14E-08 5.14E-08 5.14E-08 | 8.10E-06 8.10E-06 8.10E-06 |
| $\Theta(^{64}\text{Ni})$ | No-osci normal inverted | 2.44E-12 2.45E-12 2.44E-12 | 3.46E-07 3.46E-07 5.10E+00 | 5.16E+00 4.77E+00 4.77E+00 | 4.77E+00 4.77E+00 1.55E+00 | 1.55E+00 1.55E+00 1.55E+00 | 4.37E-01 4.36E-01 4.37E-01 | 2.29E-01 2.29E-01 2.29E-01 | 2.29E-01 2.29E-01 2.29E-01 | 2.31E+00 2.31E+00 2.31E+00 |
| $\Delta M(^{63}\text{Cu})$ | No-osci normal inverted | 7.12E-15 7.11E-15 7.11E-15 | 2.02E-11 2.02E-11 2.01E-11 | 2.54E-07 2.54E-07 2.58E-07 | 6.33E-07 6.33E-07 6.33E-07 | 2.04E-07 2.05E-07 1.99E-07 | 3.93E-08 3.97E-08 3.85E-08 | 2.48E-07 2.51E-07 2.49E-07 | 4.06E-08 4.06E-08 4.06E-08 | 1.42E-06 1.42E-06 1.42E-06 |
| $\Theta(^{63}\text{Cu})$ | No-osci normal inverted | 9.02E-07 9.00E-07 9.00E-07 | 1.28E-03 1.28E-03 1.27E-03 | 4.60E+00 4.60E+00 4.66E+00 | 5.23E-01 5.23E-01 5.24E-01 | 1.85E+00 1.85E+00 1.80E+00 | 4.15E-01 4.19E-01 4.06E-01 | 2.12E-01 2.14E-01 2.13E-01 | 2.24E-01 2.24E-01 2.24E-01 | 4.99E-01 5.00E-01 4.99E-01 |
| $\Delta M(^{65}\text{Cu})$ | No-osci normal inverted | 1.17E-20 1.17E-20 1.16E-20 | 5.32E-14 5.32E-14 5.32E-14 | 3.90E-07 3.90E-07 3.89E-07 | 2.74E-06 2.74E-06 2.74E-06 | 1.86E-07 1.86E-07 1.84E-07 | 3.93E-08 3.93E-08 3.91E-08 | 1.22E-07 1.21E-07 1.21E-07 | 1.87E-08 1.87E-08 1.87E-08 | 3.50E-06 3.50E-06 3.50E-06 |
| $\Theta(^{65}\text{Cu})$ | No-osci normal inverted | 3.21E-12 3.21E-12 3.20E-12 | 7.31E-06 7.31E-06 7.30E-06 | 1.53E+01 1.53E+01 1.53E+01 | 4.93E+00 4.93E+00 4.93E+00 | 3.65E+00 3.65E+00 3.62E+00 | 9.00E-01 9.00E-01 8.94E-01 | 2.26E-01 2.25E-01 2.25E-01 | 2.24E-01 2.24E-01 2.24E-01 | 2.67E+00 2.67E+00 2.67E+00 |
| $\Delta M(^{64}\text{Zn})$ | No-osci normal inverted | 2.18E-13 2.18E-13 2.18E-13 | 4.90E-11 4.90E-11 4.90E-11 | 8.18E-08 8.18E-08 8.35E-08 | 1.01E-06 1.02E-06 1.01E-06 | 1.85E-07 1.86E-07 1.82E-07 | 4.43E-08 4.47E-08 4.39E-08 | 4.37E-07 4.39E-07 4.38E-07 | 7.01E-08 7.01E-08 7.01E-08 | 1.83E-06 1.84E-06 1.83E-06 |
| $\Theta(^{64}\text{Zn})$ | No-osci normal inverted | 1.62E-05 1.62E-05 1.62E-05 | 1.81E-03 1.81E-03 1.81E-03 | 8.64E-01 8.64E-01 8.82E-01 | 4.91E-01 4.91E-01 4.91E-01 | 9.80E-01 9.81E-01 9.62E-01 | 2.73E-01 2.76E-01 2.70E-01 | 2.18E-01 2.20E-01 2.19E-01 | 2.26E-01 2.26E-01 2.26E-01 | 3.77E-01 3.77E-01 3.76E-01 |
| $\Delta M(^{66}\text{Zn})$ | No-osci normal inverted | 4.72E-20 4.72E-20 4.71E-20 | 2.26E-11 2.26E-11 2.26E-11 | 2.71E-07 2.71E-07 2.72E-07 | 3.05E-06 3.05E-06 3.05E-06 | 1.29E-07 1.29E-07 1.28E-07 | 3.40E-08 3.41E-08 3.39E-08 | 2.62E-07 2.63E-07 2.63E-07 | 4.16E-08 4.16E-08 4.16E-08 | 3.78E-06 3.78E-06 3.78E-06 |
| $\Theta(^{66}\text{Zn})$ | No-osci normal inverted | 5.89E-12 5.89E-12 5.88E-12 | 1.41E-03 1.41E-03 1.41E-03 | 4.83E+00 4.83E+00 4.85E+00 | 2.49E+00 2.49E+00 2.49E+00 | 1.15E+00 1.15E+00 1.14E+00 | 3.54E-01 3.55E-01 3.53E-01 | 2.21E-01 2.22E-01 2.22E-01 | 2.26E-01 2.26E-01 2.26E-01 | 1.31E+00 1.31E+00 1.31E+00 |
| $\Delta M(^{67}\text{Zn})$ | No-osci normal inverted | 5.21E-24 5.21E-24 5.20E-24 | 2.37E-14 2.36E-14 1.69E-14 | 6.86E-09 6.86E-09 6.39E-09 | 9.37E-07 9.37E-07 9.37E-07 | 2.80E-08 2.80E-08 2.82E-08 | 7.67E-09 7.63E-09 7.69E-09 | 4.14E-08 4.11E-08 4.13E-08 | 6.21E-09 6.21E-09 6.21E-09 | 1.03E-06 1.03E-06 1.03E-06 |
| $\Theta(^{67}\text{Zn})$ | No-osci normal inverted | 4.38E-15 4.38E-15 4.37E-15 | 9.93E-06 9.93E-06 7.11E-06 | 8.24E-01 8.24E-01 7.67E-01 | 5.15E+00 5.15E+00 5.15E+00 | 1.68E+00 1.68E+00 1.69E+00 | 5.37E-01 5.34E-01 5.38E-01 | 2.35E-01 2.33E-01 2.34E-01 | 2.27E-01 2.27E-01 2.27E-01 | 2.40E+00 2.40E+00 2.40E+00 |

Continued on next page

Table 1 – Continued from previous page

| shell M(r) ΔM | hierarchy | Fe/Ni | Si/S | O/Si | O/Ne | O/C | C/He | He/C | He/N | Total |
|-----------------------------|-----------|----------------|----------------|----------------|----------------|----------------|----------------|----------------|----------------|----------|
| | | 1.600 0.012 | 1.624 0.024 | 1.710 0.086 | 3.583 1.873 | 3.767 0.184 | 3.901 0.134 | 5.713 1.812 | 6.000 0.287 | 6.000 |
| $\Delta M(^{68}\text{Zn})$ | No-osci | 1.67E-26 | 4.76E-13 | 1.49E-07 | 2.92E-06 | 8.63E-08 | 2.61E-08 | 1.85E-07 | 2.87E-08 | 3.40E-06 |
| | normal | 1.63E-26 | 4.76E-13 | 1.49E-07 | 2.92E-06 | 8.62E-08 | 2.60E-08 | 1.85E-07 | 2.87E-08 | 3.40E-06 |
| | inverted | 1.63E-26 | 4.76E-13 | 1.48E-07 | 2.92E-06 | 8.69E-08 | 2.62E-08 | 1.85E-07 | 2.87E-08 | 3.40E-06 |
| $\Theta(^{68}\text{Zn})$ | No-osci | 3.01E-18 | 4.29E-05 | 3.85E+00 | 3.45E+00 | 1.11E+00 | 3.93E-01 | 2.26E-01 | 2.25E-01 | 1.70E+00 |
| | normal | 2.95E-18 | 4.29E-05 | 3.85E+00 | 3.45E+00 | 1.11E+00 | 3.92E-01 | 2.25E-01 | 2.25E-01 | 1.70E+00 |
| | inverted | 2.95E-18 | 4.29E-05 | 3.82E+00 | 3.45E+00 | 1.12E+00 | 3.94E-01 | 2.26E-01 | 2.25E-01 | 1.70E+00 |
| $\Delta M(^{70}\text{Zn})$ | No-osci | 1.45E-29 | 2.71E-19 | 4.68E-09 | 6.79E-08 | 1.35E-10 | 3.95E-10 | 6.26E-09 | 9.77E-10 | 8.03E-08 |
| | normal | 1.12E-32 | 2.71E-19 | 4.68E-09 | 6.79E-08 | 1.34E-10 | 3.84E-10 | 6.24E-09 | 9.77E-10 | 8.03E-08 |
| | inverted | 1.66E-33 | 2.06E-19 | 4.57E-09 | 6.78E-08 | 1.50E-10 | 3.95E-10 | 6.25E-09 | 9.77E-10 | 8.01E-08 |
| $\Theta(^{70}\text{Zn})$ | No-osci | 7.74E-20 | 7.22E-10 | 3.56E+00 | 2.36E+00 | 5.14E-02 | 1.75E-01 | 2.25E-01 | 2.26E-01 | 1.19E+00 |
| | normal | 5.96E-23 | 7.23E-10 | 3.56E+00 | 2.36E+00 | 5.12E-02 | 1.71E-01 | 2.25E-01 | 2.26E-01 | 1.19E+00 |
| | inverted | 8.86E-24 | 5.49E-10 | 3.48E+00 | 2.36E+00 | 5.70E-02 | 1.75E-01 | 2.25E-01 | 2.26E-01 | 1.19E+00 |
| $\Delta M(^{138}\text{La})$ | No-osci | 8.19E-32 | 8.11E-33 | 6.75E-12 | 1.25E-10 | 1.57E-12 | 4.86E-13 | 8.82E-13 | 7.41E-14 | 1.35E-10 |
| | normal | 7.19E-34 | 3.40E-35 | 2.39E-10 | 5.20E-09 | 1.37E-10 | 5.52E-11 | 1.02E-10 | 1.02E-11 | 5.75E-09 |
| | inverted | 5.76E-33 | 6.11E-34 | 8.39E-10 | 1.75E-08 | 2.25E-10 | 6.85E-11 | 1.17E-10 | 9.97E-12 | 1.87E-08 |
| $\Theta(^{138}\text{La})$ | No-osci | 4.33E-18 | 2.14E-19 | 5.10E+01 | 4.32E+01 | 5.93E+00 | 2.14E+00 | 3.15E-01 | 1.70E-01 | 1.98E+01 |
| | normal | 3.80E-20 | 8.99E-22 | 1.81E+03 | 1.80E+03 | 5.16E+02 | 2.43E+02 | 3.64E+01 | 2.34E+01 | 8.44E+02 |
| | inverted | 3.05E-19 | 1.62E-20 | 6.33E+03 | 6.04E+03 | 8.48E+02 | 3.02E+02 | 4.19E+01 | 2.29E+01 | 2.75E+03 |

REFERENCES

- Acero, M. A., Adamson, P., Aliaga, L., Alion, T., & NOvA Collaboration. 2019, Phys. Rev. Lett., 123, 151803, doi: [10.1103/PhysRevLett.123.151803](https://doi.org/10.1103/PhysRevLett.123.151803)
- Acero, M. A., Adamson, P., Aliaga, L., et al. 2022, Physical Review D, 106, 032004, doi: [10.1103/PhysRevD.106.032004](https://doi.org/10.1103/PhysRevD.106.032004)
- Amari, S., Hoppe, P., Zinner, E., & Lewis, R. S. 1992, The Astrophysical Journal, 394, L43, doi: [10.1086/186468](https://doi.org/10.1086/186468)
- Austin, S. M., Heger, A., & Tur, C. 2011, Phys. Rev. Lett., 106, 152501, doi: [10.1103/PhysRevLett.106.152501](https://doi.org/10.1103/PhysRevLett.106.152501)
- Balantekin, A. B., Cervia, M. J., Patwardhan, A. V., Surman, R., & Wang, X. 2024, ApJ, 967, 146, doi: [10.3847/1538-4357/ad393d](https://doi.org/10.3847/1538-4357/ad393d)
- Bisterzo, S., Travaglio, C., Gallino, R., Wiescher, M., & Käppeler, F. 2014, ApJ, 787, 10, doi: [10.1103/PhysRevC.82.035504](https://doi.org/10.1103/PhysRevC.82.035504)
- Bodmann, B. E., et al. 1994, Phys. Lett. B, 332, 251, doi: [10.1016/0370-2693\(94\)91250-5](https://doi.org/10.1016/0370-2693(94)91250-5)
- Cheoun, M.-K., Ha, E., Hayakawa, T., Kajino, T., & Chiba, S. 2010a, Phys. Rev. C, 82, 035504, doi: [10.1103/PhysRevC.82.035504](https://doi.org/10.1103/PhysRevC.82.035504)
- Cheoun, M.-K., Ha, E., Kim, K. S., & Kajino, T. 2010b, Journal of Physics G: Nuclear and Particle Physics, 37, 055101, doi: [10.1088/0954-3899/37/5/055101](https://doi.org/10.1088/0954-3899/37/5/055101)
- den Hartogh, J., Petö, M. K., Lawson, T., et al. 2022, ApJ, 927, 220, doi: [10.3847/1538-4357/ac4965](https://doi.org/10.3847/1538-4357/ac4965)
- Fujiya, W., Hoppe, P., & Ott, U. 2011, The Astrophysical Journal Letters, 730, L7, doi: [10.1088/2041-8205/730/1/L7](https://doi.org/10.1088/2041-8205/730/1/L7)
- Gyngard, F., Amari, S., Zinner, E., & Ott, U. 2009, The Astrophysical Journal, 694, 359, doi: [10.1088/0004-637X/694/1/359](https://doi.org/10.1088/0004-637X/694/1/359)
- Haenecour, P., Howe, J. Y., Zega, T. J., et al. 2019, Nature Astronomy, 3, 626, doi: [10.1038/s41550-019-0757-4](https://doi.org/10.1038/s41550-019-0757-4)
- Hauser, W., & Feshbach, H. 1952, Physical Review, 87, 366, doi: [10.1103/PhysRev.87.366](https://doi.org/10.1103/PhysRev.87.366)
- Hayakawa, T., Mohr, P., Kajino, T., Chiba, S., & Mathews, G. J. 2010, Phys. Rev. C, 82, 058801, doi: [10.1103/PhysRevC.82.058801](https://doi.org/10.1103/PhysRevC.82.058801)
- Hayakawa, T., Nakamura, K., Kajino, T., et al. 2013, The Astrophysical Journal Letters, 779, L9, doi: [10.1088/2041-8205/779/1/L9](https://doi.org/10.1088/2041-8205/779/1/L9)
- Hayakawa, T., Shizuma, T., Kajino, T., Ogawa, K., & Nakada, H. 2008, PhRvC, 77, 065802, doi: [10.1103/PhysRevC.77.065802](https://doi.org/10.1103/PhysRevC.77.065802)
- Hayakawa, T., et al. 2018, Phys. Rev. Lett., 121, 102701, doi: [10.1103/PhysRevLett.121.102701](https://doi.org/10.1103/PhysRevLett.121.102701)
- Heger, A., Kolbe, E., Haxton, W. C., et al. 2005, Physics Letters B, 606, 258, doi: [10.1016/j.physletb.2004.12.017](https://doi.org/10.1016/j.physletb.2004.12.017)
- Hirata, K., et al. 1987, Phys. Rev. Lett., 58, 1490, doi: [10.1103/PhysRevLett.58.1490](https://doi.org/10.1103/PhysRevLett.58.1490)
- Hoffmann, R. D., & Woosley, S. 1992, Stellar Nucleosynthesis Data. http://dbserv.pnpi.spb.ru/elbib/talisot/toi98/www/astro/hw92_1.htm
- Hoppe, P., Lodders, K., Strelbel, R., Amari, S., & Lewis, R. S. 2001, ApJ, 551, 478, doi: [10.1086/320075](https://doi.org/10.1086/320075)
- Hoppe, P., Pignatari, M., Kodolányi, J., Gröner, E., & Amari, S. 2018, GeoCoA, 221, 182, doi: [10.1016/j.gca.2017.01.051](https://doi.org/10.1016/j.gca.2017.01.051)

- Hoppe, P., Strelbel, R., Eberhardt, P., Amari, S., & Lewis, R. S. 1996, *Science*, 272, 1314, doi: [10.1126/science.272.5266.1314](https://doi.org/10.1126/science.272.5266.1314)
- . 2000, *M&PS*, 35, 1157, doi: [10.1111/j.1945-5100.2000.tb01505.x](https://doi.org/10.1111/j.1945-5100.2000.tb01505.x)
- Jimenez, R., Pena-Garay, C., Short, K., Simpson, F., & Verde, L. 2022, *Journal of Cosmology and Astroparticle Physics*, 2022, 006, doi: [10.1088/1475-7516/2022/09/006](https://doi.org/10.1088/1475-7516/2022/09/006)
- Kikuchi, Y., Hashimoto, M.-a., Ono, M., & Fukuda, R. 2015, *PTEP*, 2015, 063E01, doi: [10.1093/ptep/ptv072](https://doi.org/10.1093/ptep/ptv072)
- Ko, H., et al. 2020, *Astrophys. J. Lett.*, 891, L24, doi: [10.3847/2041-8213/ab775b](https://doi.org/10.3847/2041-8213/ab775b)
- . 2022, *Astrophys. J.*, 937, 116, doi: [10.3847/1538-4357/ac88cd](https://doi.org/10.3847/1538-4357/ac88cd)
- Kobayashi, C., Izutani, N., Karakas, A. I., et al. 2011, *The Astrophysical Journal*, 739, L57, doi: [10.1088/2041-8205/739/2/L57](https://doi.org/10.1088/2041-8205/739/2/L57)
- Kusakabe, M., Cheoun, M.-K., Kim, K. S., et al. 2019, *Astrophys. J.*, 872, 164, doi: [10.3847/1538-4357/aafc35](https://doi.org/10.3847/1538-4357/aafc35)
- Lahkar, N., Kalita, S., Duorah, H. L., & Duorah, K. 2017, *Journal of Astrophysics and Astronomy*, 38, 8, doi: [10.1007/s12036-017-9428-y](https://doi.org/10.1007/s12036-017-9428-y)
- Liu, N., Barosch, J., Nittler, L. R., et al. 2021, *ApJL*, 920, L26, doi: [10.3847/2041-8213/ac260b](https://doi.org/10.3847/2041-8213/ac260b)
- Liu, N., Lugaro, M., Leitner, J., Meyer, B. S., & Schönbächler, M. 2024, *SSRv*, 220, 88, doi: [10.1007/s11214-024-01122-w](https://doi.org/10.1007/s11214-024-01122-w)
- Liu, N., Nittler, L. R., Alexander, C. M. O., & Wang, J. 2018, *Science Advances*, 4, eaao1054, doi: [10.1126/sciadv.aao1054](https://doi.org/10.1126/sciadv.aao1054)
- Lodders, K., & Fegley, Jr., B. 1995, *Meteoritics*, 30, 661, doi: [10.1111/j.1945-5100.1995.tb01164.x](https://doi.org/10.1111/j.1945-5100.1995.tb01164.x)
- Lodders, K., Palme, H., & Gail, H. P. 2009, *Landolt-Börnstein*, 4B, 712, doi: [10.1007/978-3-540-88055-4_34](https://doi.org/10.1007/978-3-540-88055-4_34)
- Mathews, G. J., Kajino, T., Aoki, W., Fujiya, W., & Pitts, J. B. 2012, *Phys. Rev. D*, 85, 105023, doi: [10.1103/PhysRevD.85.105023](https://doi.org/10.1103/PhysRevD.85.105023)
- Meyer, B. S., Weaver, T. A., & Woosley, S. E. 1995, *Meteoritics*, 30, 325, doi: [10.1111/j.1945-5100.1995.tb01131.x](https://doi.org/10.1111/j.1945-5100.1995.tb01131.x)
- Mikheyev, S. P., & Smirnov, A. Y. 1985, *Sov. J. Nucl. Phys.*, 42, 913
- Nagakura, H., & Zaizen, M. 2022, *PhRvL*, 129, 261101, doi: [10.1103/PhysRevLett.129.261101](https://doi.org/10.1103/PhysRevLett.129.261101)
- Niculescu-Duvaz, M., Barlow, M. J., Bevan, A., et al. 2022, *MNRAS*, 515, 4302, doi: [10.1093/mnras/stac1626](https://doi.org/10.1093/mnras/stac1626)
- Nittler, L. R., Amari, S., Zinner, E., Woosley, S. E., & Lewis, R. S. 1996, *The Astrophysical Journal*, 462, doi: [10.1086/310021](https://doi.org/10.1086/310021)
- Ott, U., Stephan, T., Hoppe, P., & Savina, M. R. 2019, *ApJ*, 885, 128, doi: [10.3847/1538-4357/ab41f3](https://doi.org/10.3847/1538-4357/ab41f3)
- Pehlivan, Y., Balantekin, A. B., Kajino, T., & Yoshida, T. 2011, *Phys. Rev. D*, 84, 065008, doi: [10.1103/PhysRevD.84.065008](https://doi.org/10.1103/PhysRevD.84.065008)
- Prantzos, N. 2012, *A&A*, 542, A67, doi: [10.1051/0004-6361/201219043](https://doi.org/10.1051/0004-6361/201219043)
- Rauscher, T., Heger, A., Hoffman, R. D., & Woosley, S. E. 2002, *The Astrophysical Journal*, 576, 323, doi: [10.1086/341728](https://doi.org/10.1086/341728)
- Reeves, H. 1994, *Rev. Mod. Phys.*, 66, 193, doi: [10.1103/RevModPhys.66.193](https://doi.org/10.1103/RevModPhys.66.193)
- Sasaki, H., Kajino, T., Takiwaki, T., et al. 2017, 96, 043013, doi: [10.1103/PhysRevD.96.043013](https://doi.org/10.1103/PhysRevD.96.043013)
- Sieverding, A., Martínez-Pinedo, G., Huther, L., Langanke, K., & Heger, A. 2018, *Astrophys. J.*, 865, 143, doi: [10.3847/1538-4357/aadd48](https://doi.org/10.3847/1538-4357/aadd48)
- Sigl, G., & Raffelt, G. 1993, *Nucl. Phys. B*, 406, 423, doi: [10.1016/0550-3213\(93\)90175-O](https://doi.org/10.1016/0550-3213(93)90175-O)
- Suzuki, T., Chiba, S., Yoshida, T., Kajino, T., & Otsuka, T. 2006, *Physical Review C*, 74, 034307, doi: [10.1103/PhysRevC.74.034307](https://doi.org/10.1103/PhysRevC.74.034307)
- Suzuki, T., Chiba, S., Yoshida, T., Takahashi, K., & Umeda, H. 2018, *Phys. Rev. C*, 98, 034613, doi: [10.1103/PhysRevC.98.034613](https://doi.org/10.1103/PhysRevC.98.034613)
- Weinberg, S. 2005, *The Quantum theory of fields. Vol. 1: Foundations* (Cambridge University Press), doi: [10.1017/CBO9781139644167](https://doi.org/10.1017/CBO9781139644167)
- Wolfenstein, L. 1978, *Phys. Rev. D*, 17, 2369, doi: [10.1103/PhysRevD.17.2369](https://doi.org/10.1103/PhysRevD.17.2369)
- Woosley, S. E., Hartmann, D. H., Hoffman, R. D., & Haxton, W. C. 1990, *Astrophys. J.*, 356, 272, doi: [10.1086/168839](https://doi.org/10.1086/168839)
- Woosley, S. E., & Weaver, T. A. 1995, *ApJS*, 101, 181, doi: [10.1086/192237](https://doi.org/10.1086/192237)
- Wu, M.-R., George, M., Lin, C.-Y., & Xiong, Z. 2021, *Phys. Rev. D*, 104, 103003, doi: [10.1103/PhysRevD.104.103003](https://doi.org/10.1103/PhysRevD.104.103003)
- Xiong, Z., Sieverding, A., Sen, M., & Qian, Y.-Z. 2020, *The Astrophysical Journal*, 900, 144, doi: [10.3847/1538-4357/abac5e](https://doi.org/10.3847/1538-4357/abac5e)
- Yoshida, T., Kajino, T., & Hartmann, D. H. 2005, *Physical Review Letters*, 94, 231101, doi: [10.1103/PhysRevLett.94.231101](https://doi.org/10.1103/PhysRevLett.94.231101)
- Yoshida, T., Kajino, T., Yokomakura, H., et al. 2006a, *Astrophys. J.*, 649, 319, doi: [10.1086/506374](https://doi.org/10.1086/506374)
- . 2006b, *Phys. Rev. Lett.*, 96, 091101, doi: [10.1103/PhysRevLett.96.091101](https://doi.org/10.1103/PhysRevLett.96.091101)
- Yoshida, T., Suzuki, T., Chiba, S., et al. 2008, *Astrophys. J.*, 686, 448, doi: [10.1086/591266](https://doi.org/10.1086/591266)

Zhai, M., Nakamura, E., Shaw, D. M., & Nakano, T. 1996,
Geochimica et Cosmochimica Acta, 60, 4877,
doi: [10.1016/S0016-7037\(96\)00338-9](https://doi.org/10.1016/S0016-7037(96)00338-9)